Cluster shape analysis and strangeness tracking for the ALICE upgrade

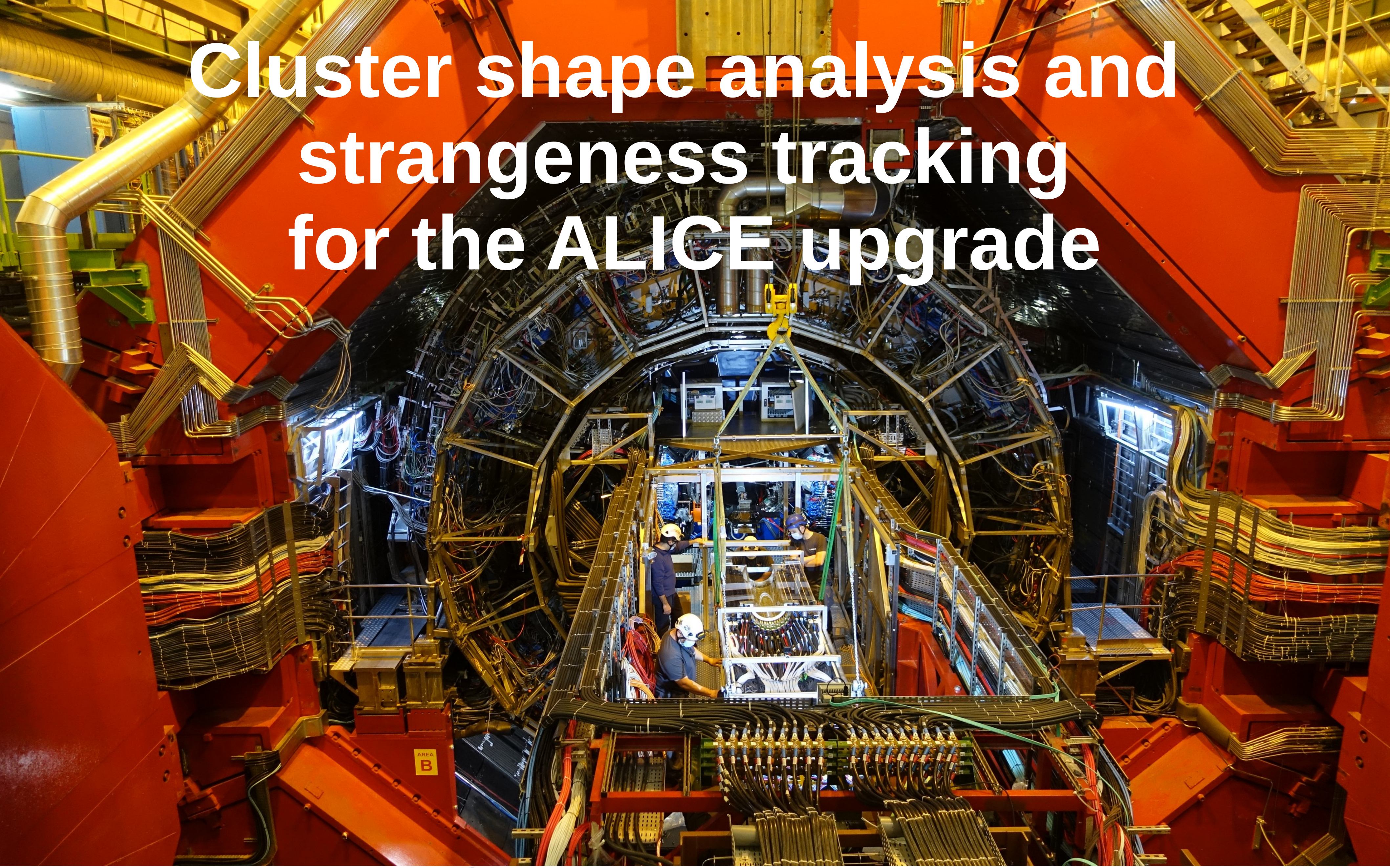

Université de Strasbourg
IPHC Institut Pluridisciplinaire Hubert CURIEN STRASBOURG
CERN
cnrs advancing the frontiers

Alexandre BIGOT, 1st year PhD student

QGP France 2022, May the 4th (be with you)

ALICE

Motivations

Decay channel studied:

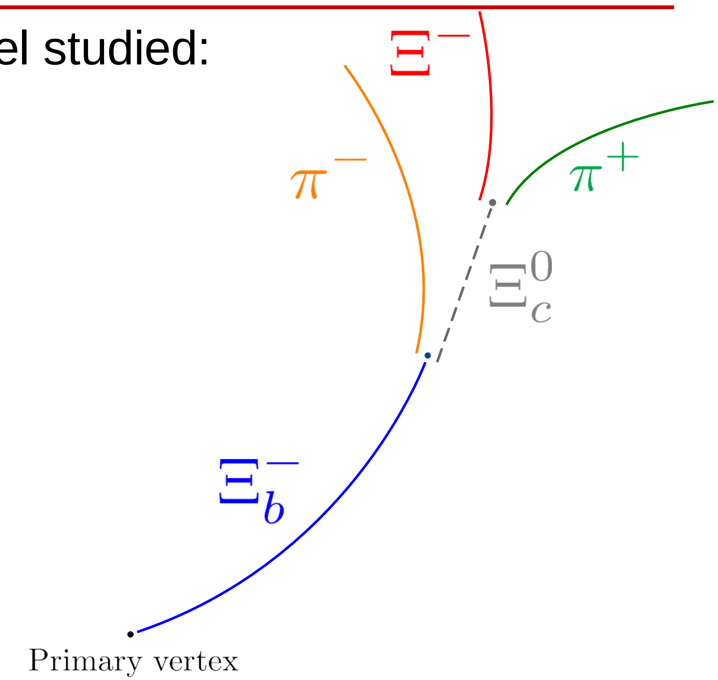

Study Ξ_b^- (d s b)

→ production cross section in pp and Pb-Pb collisions to constrain theoretical models

ALICE 1 unable to efficiently reconstruct this channel

upgrades needed

ALICE Run 3 (2022) **Cluster shape analysis**	ALICE 3 (~ 2030) **Strangeness tracking**
Ξ_c^0	Ξ_b^-
(Master 2 project)	(CERN Summer School project)

Motivations

Decay channel studied:

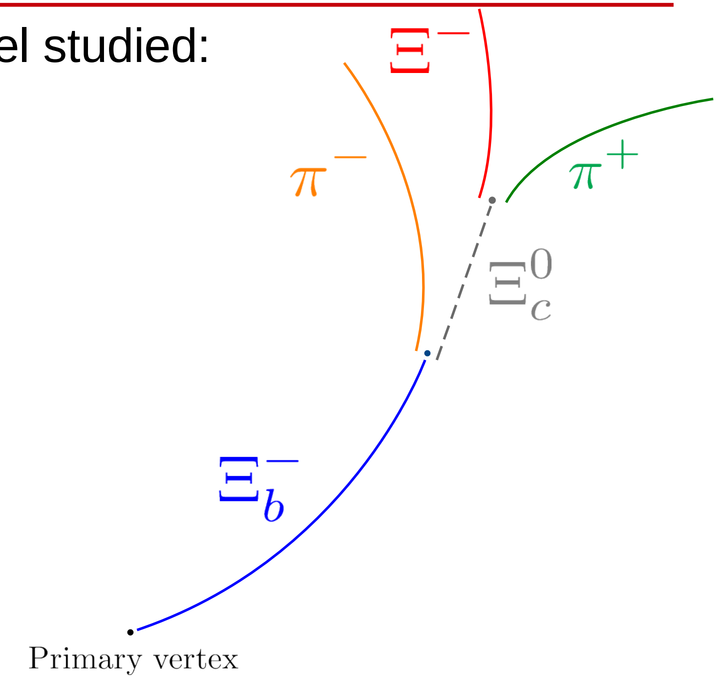

Study Ξ_b^- (d s b)

→ production cross section in pp and Pb-Pb collisions to constrain theoretical models

ALICE 1 unable to efficiently reconstruct this channel

upgrades needed

ALICE Run 3 (2022)
Cluster shape analysis

(Master 2 project)

ALICE 3
(~ 2030)
Strangeness tracking

(CERN Summer School project)

A Large Ion Collider Experiment

ALICE

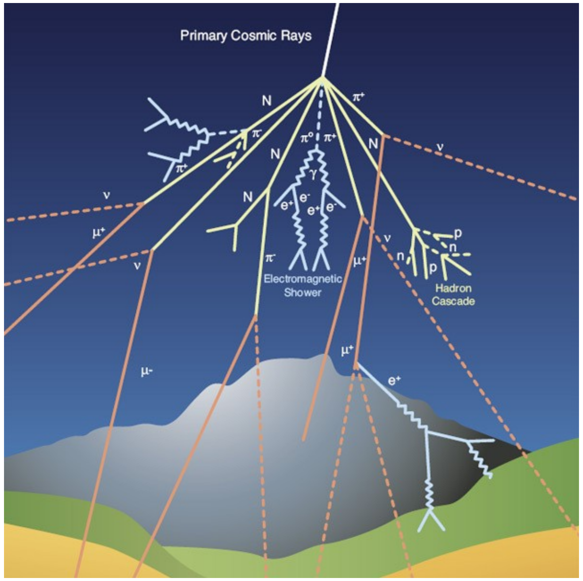

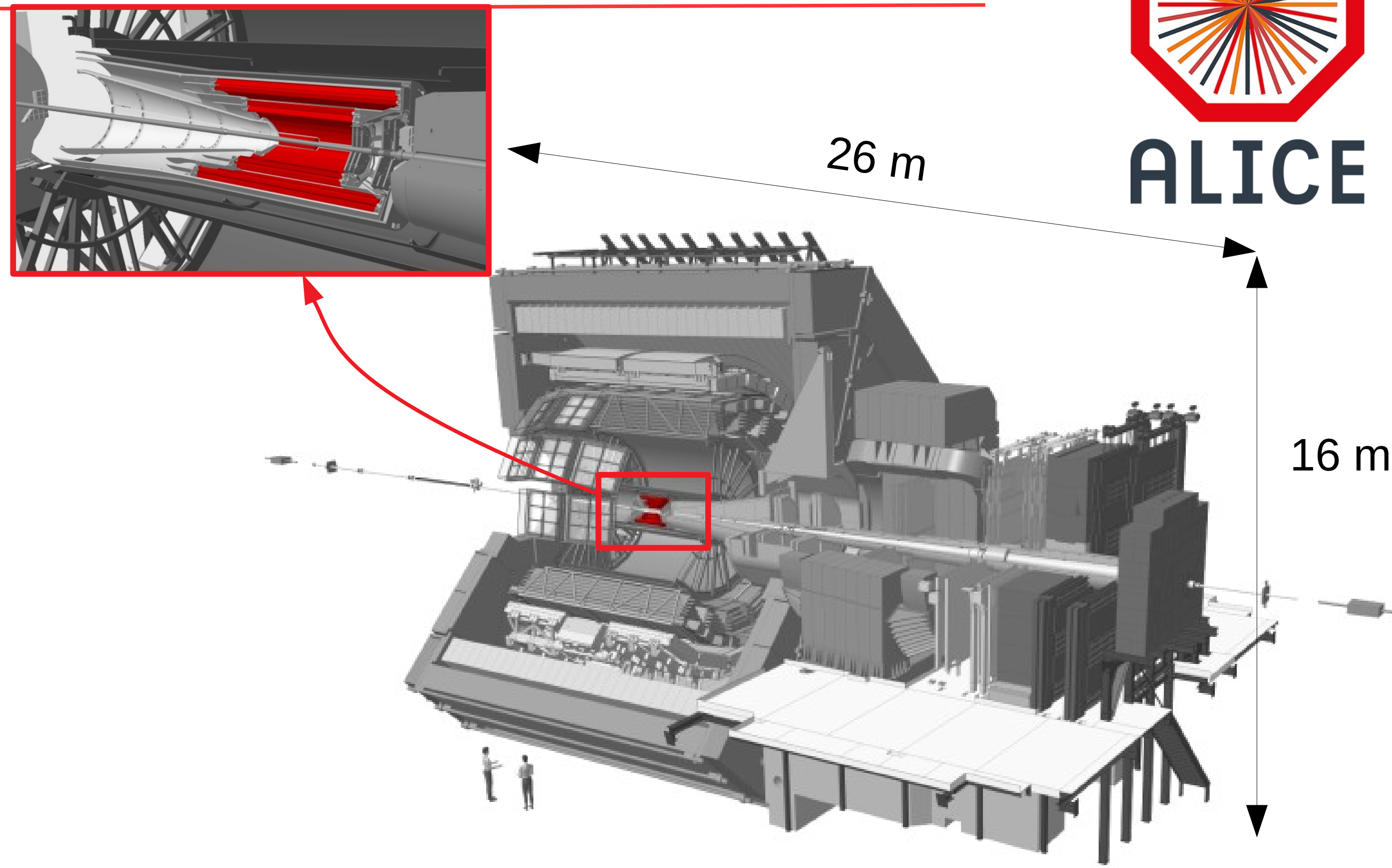

Cluster shape analysis of the cosmic-ray data collected during surface commissioning of the ALICE Inner Tracking System (ITS2)

under the supervision of Iouri BELIKOV

Inner Tracking System

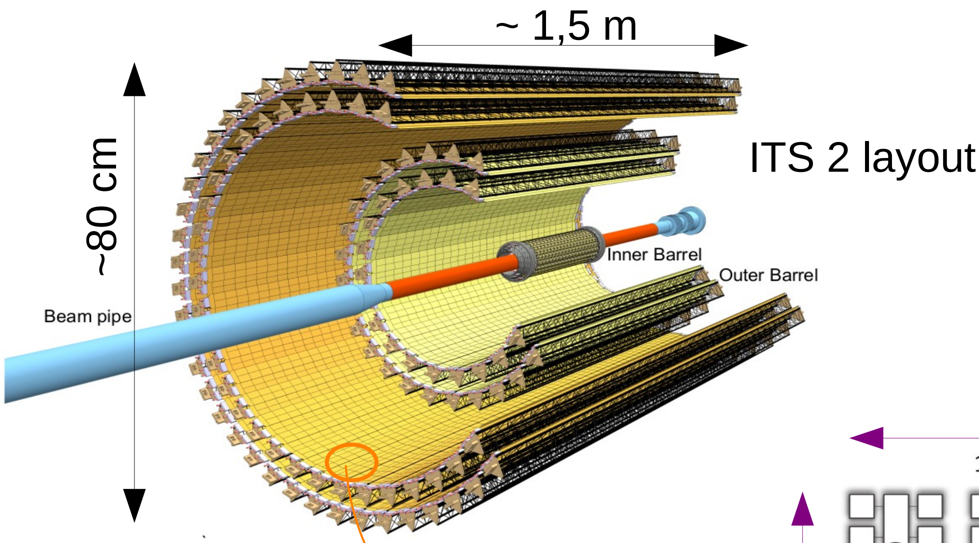

- ~ 500k pixels per chip
- ~ 24k chips on the detector
- ~ 12G pixels on the detector

Zoom on a chip

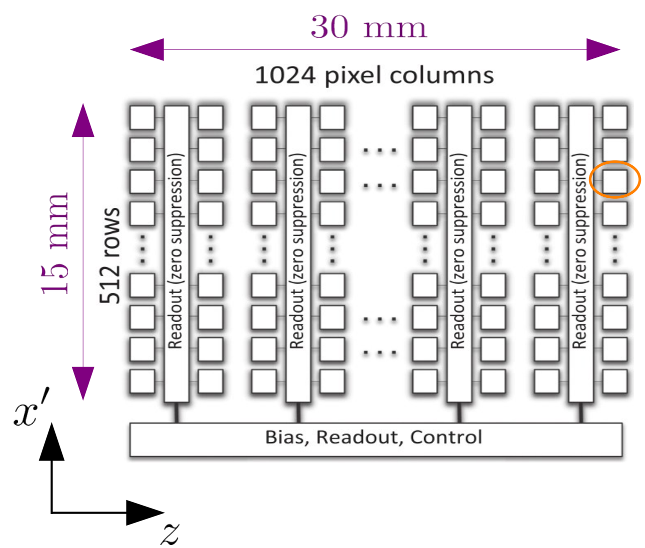

Architecture of an ALPIDE chip in the (zx') plane

Zoom on a pixel

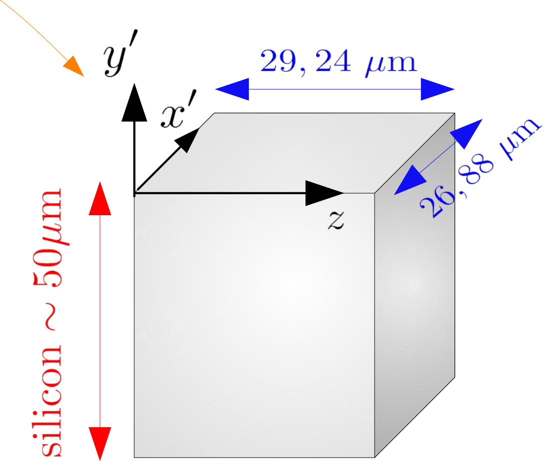

Inner Tracking System

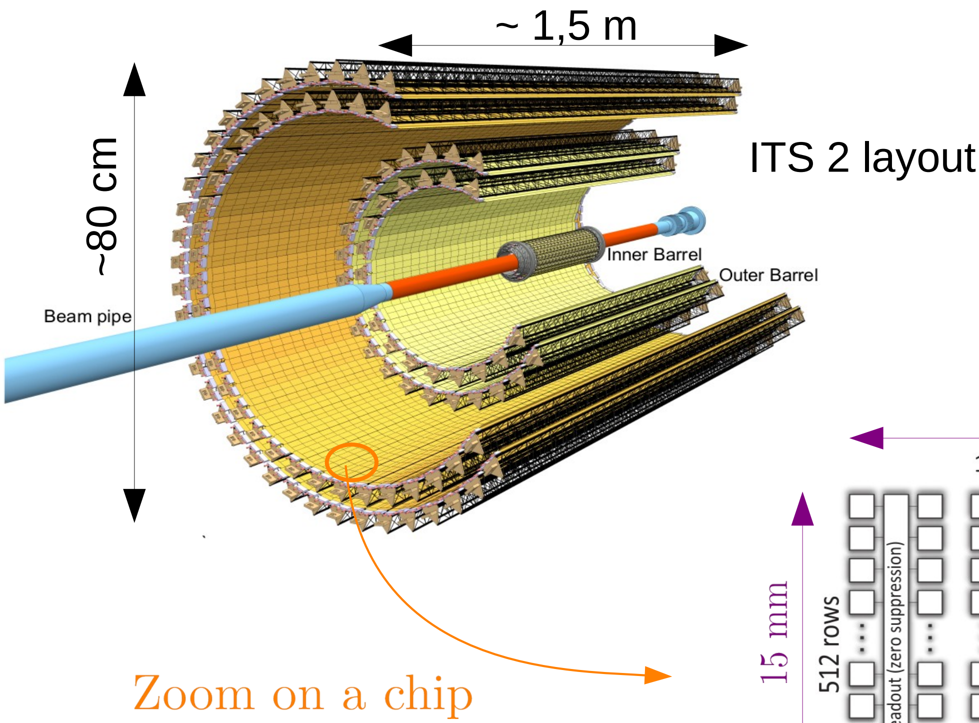

- ~ 500k pixels per chip
- ~ 24k chips on the detector
- ~ 12G pixels on the detector

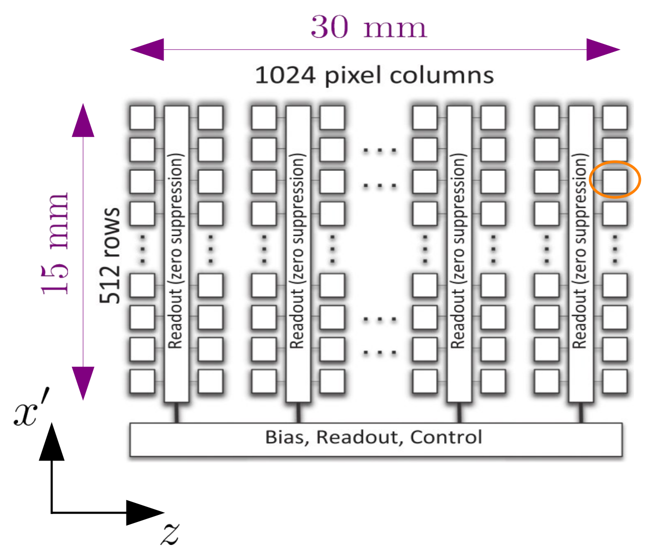

Architecture of an ALPIDE chip
in the (zx’) plane

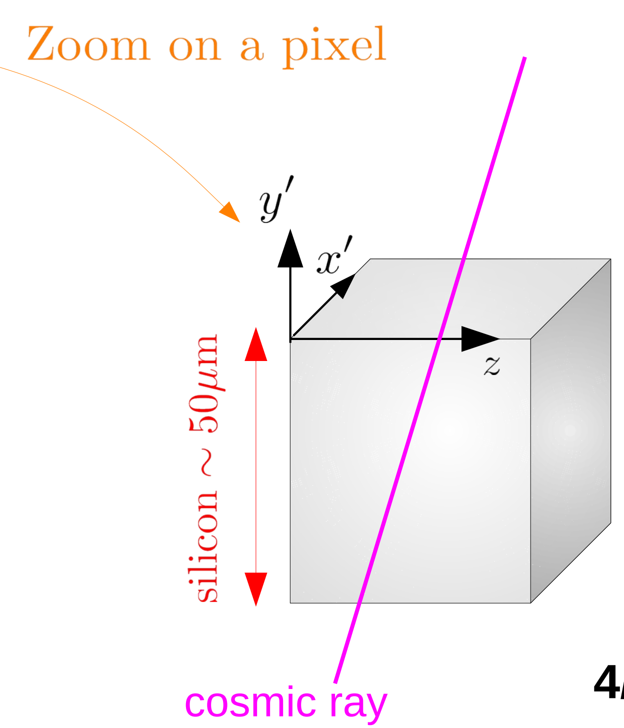

Inner Tracking System

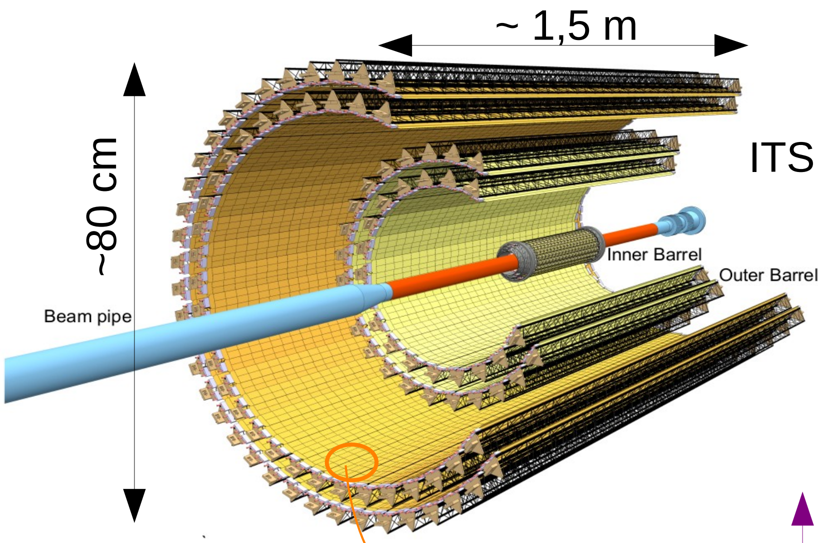

ITS 2 layout

- ~ 500k pixels per chip
- ~ 24k chips on the detector
- ~ 12G pixels on the detector

Zoom on a chip

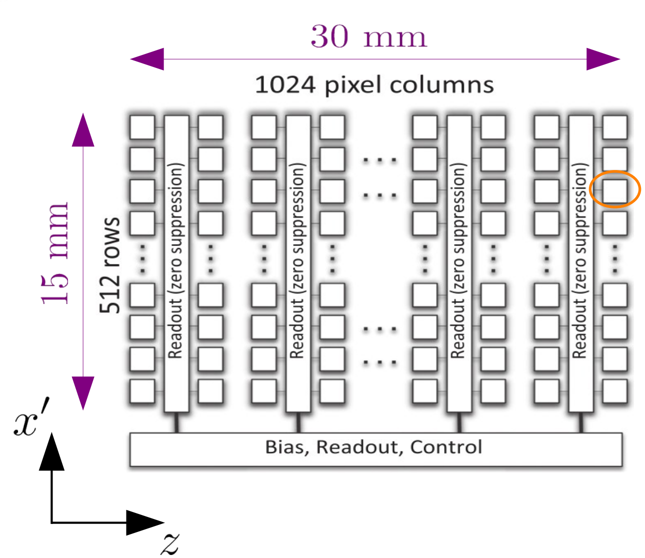

Zoom on a pixel

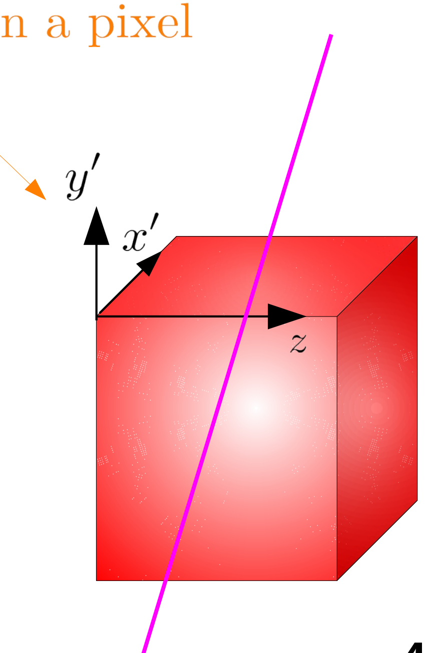

Architecture of an ALPIDE chip
in the (zx’) plane

Inner Tracking System

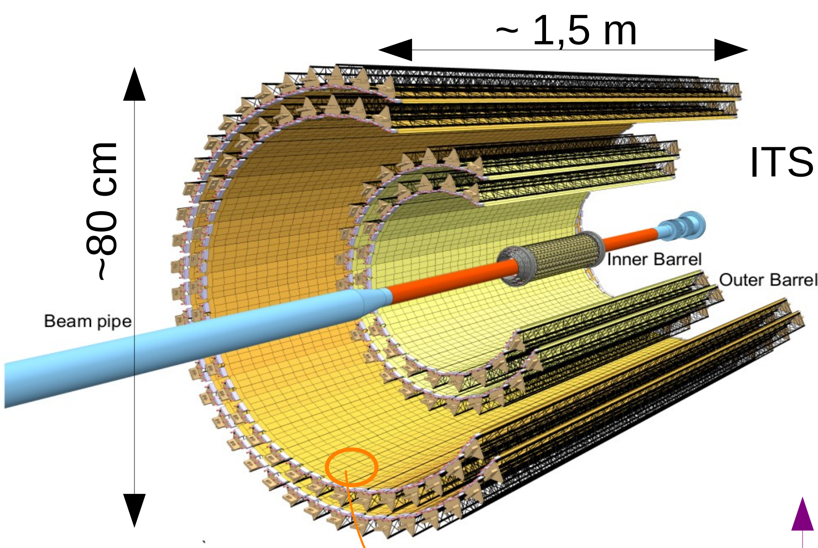

Zoom on a chip

- ~ 500k pixels per chip
- ~ 24k chips on the detector
- ~ 12G pixels on the detector

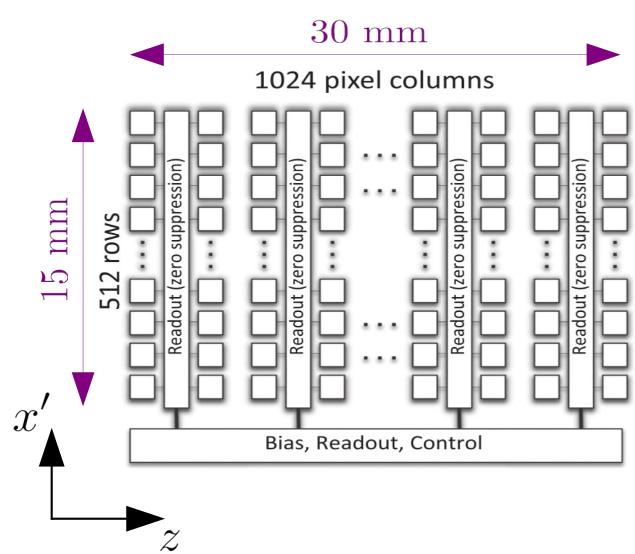

Architecture of an ALPIDE chip in the (zx’) plane

Cluster of 2 pixels

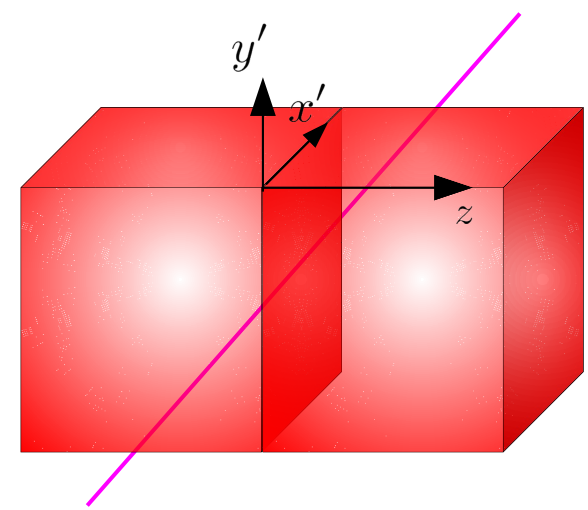

I) Track candidates selection

II) Cluster shape analysis

III) Comparison with Monte-Carlo data

Track candidates

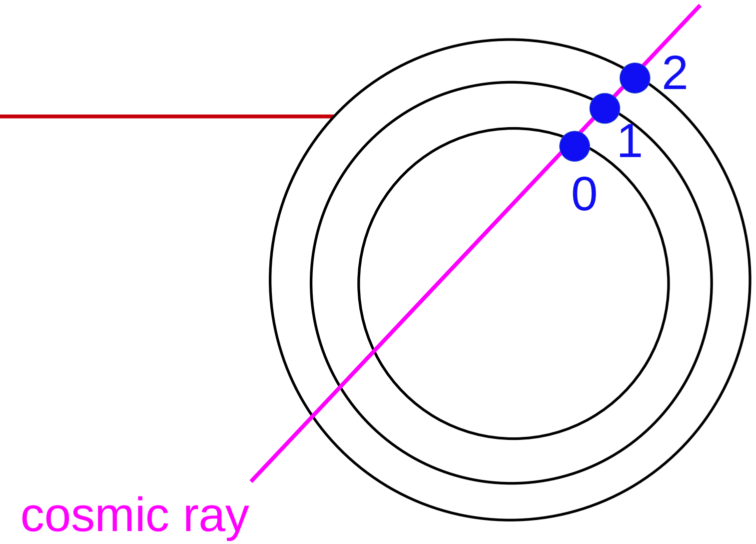

$$\boldsymbol{B} = \boldsymbol{0} \quad \Rightarrow \quad$$ track = straight line

Candidate = triplet of clusters verfifying

$$\boldsymbol{v} = \frac{\boldsymbol{v}_{01} \wedge \boldsymbol{v}_{12}}{\|\boldsymbol{v}_{01}\| \, \|\boldsymbol{v}_{12}\|} \simeq \boldsymbol{0}$$

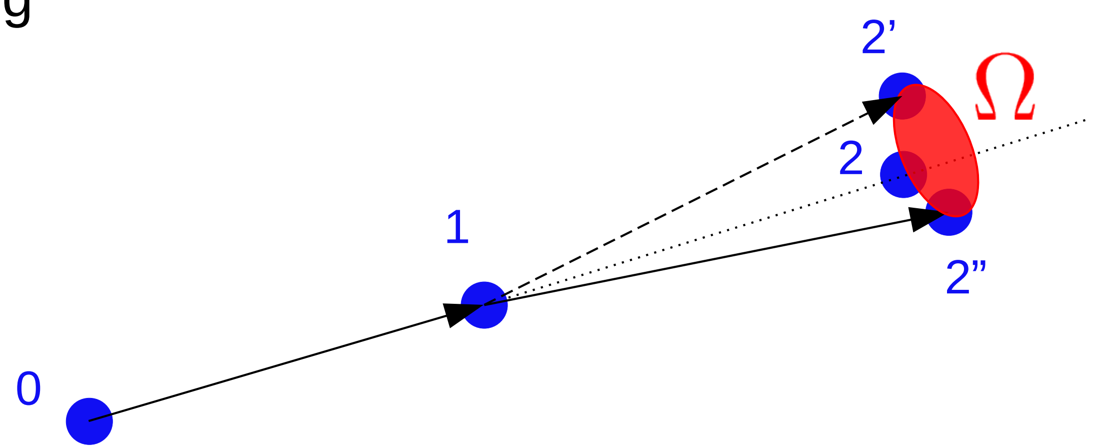

$$|v_x|, |v_y|, |v_z| \leqslant \varepsilon \;\Leftrightarrow\; 2 \in \Omega \;\Rightarrow\; (0, 1, 2) = \text{candidate}$$

"decision value" determined graphically (~0,1)

Noise map produced by studying ~12G pixels

Suppression and selection

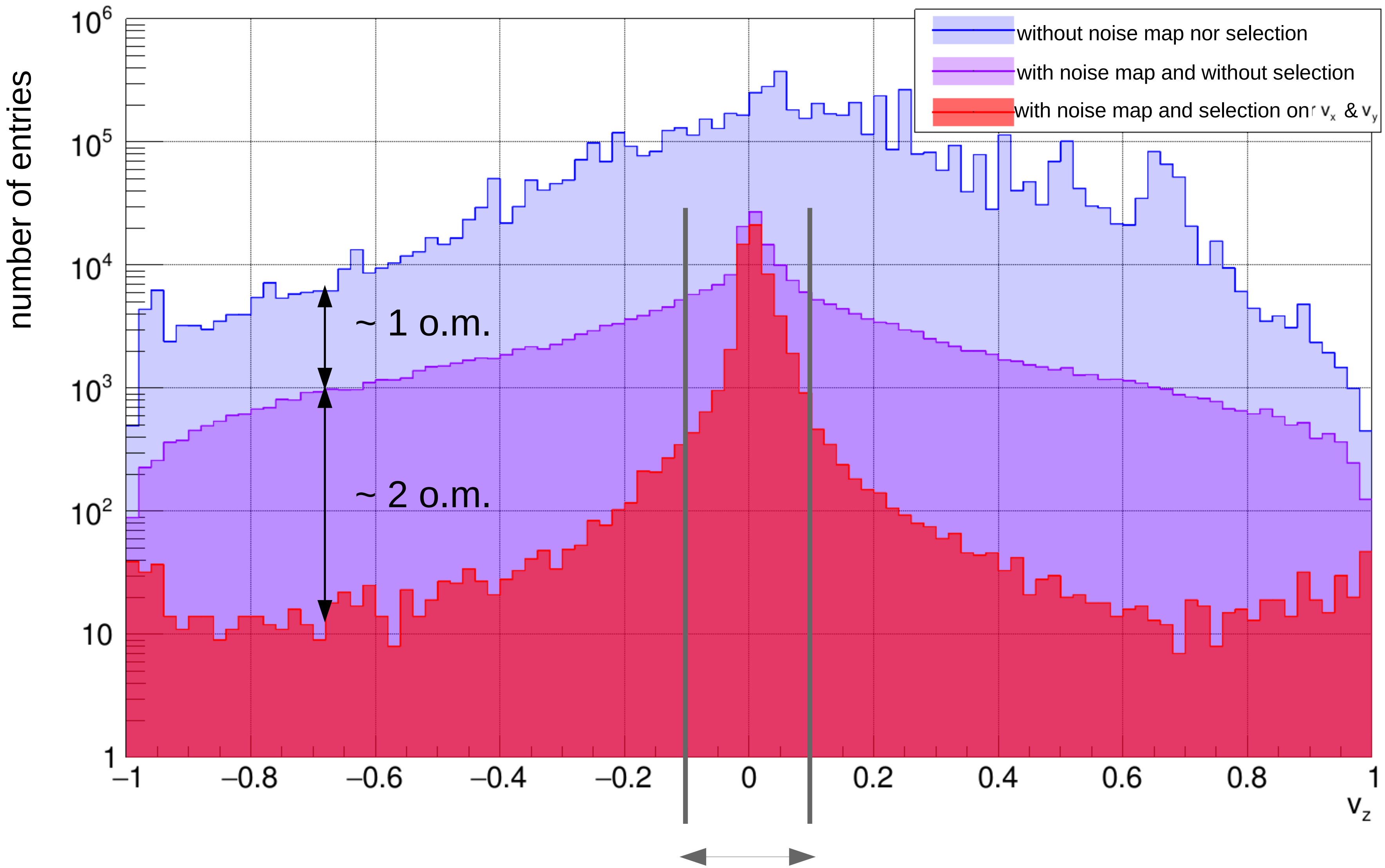

selected candidates

~6 M track candidates

Inclination angles

Plane (x,y) view

3D view

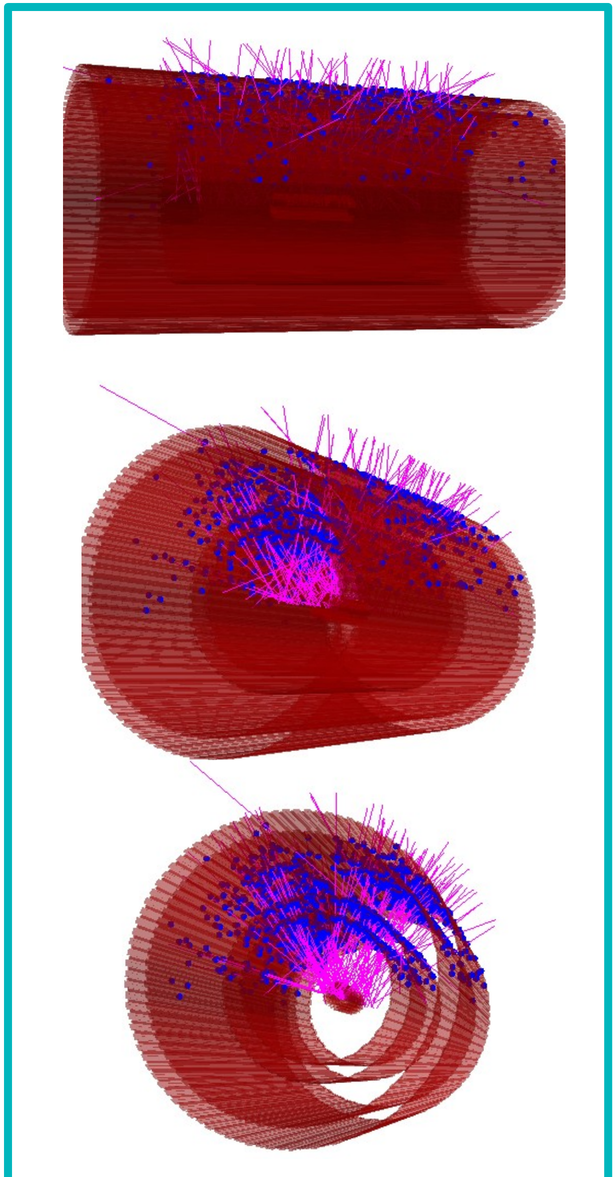

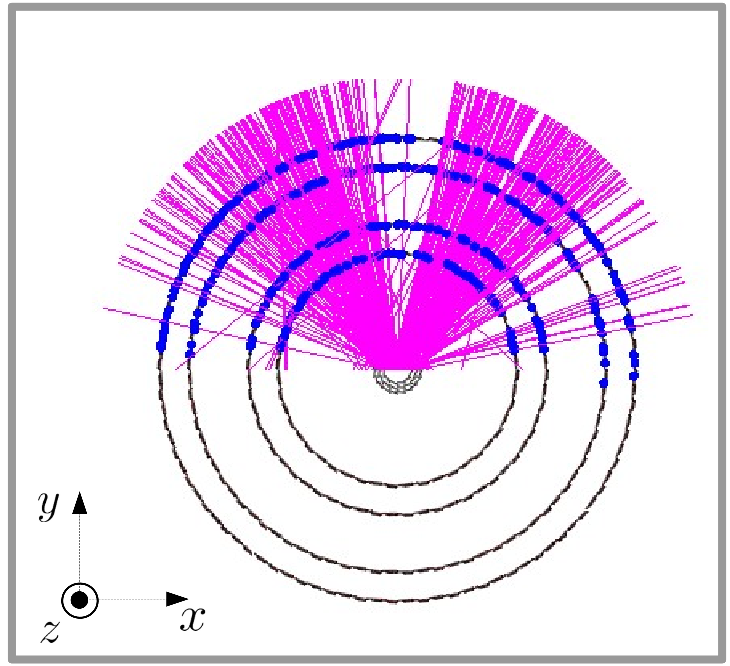

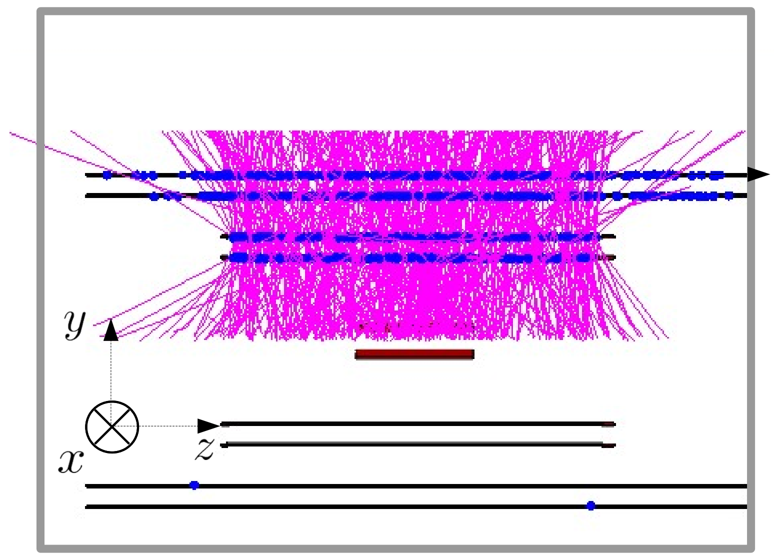

Plane (y,z) view

~6 M track candidates

Inclination angles

3D view

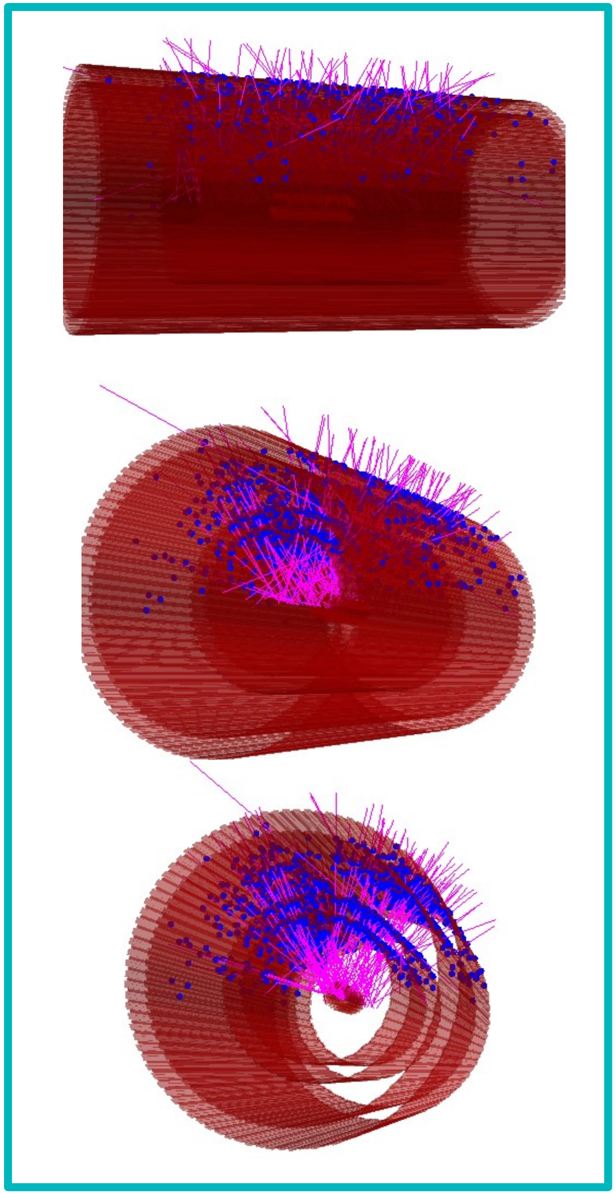

Plane (x,y) view

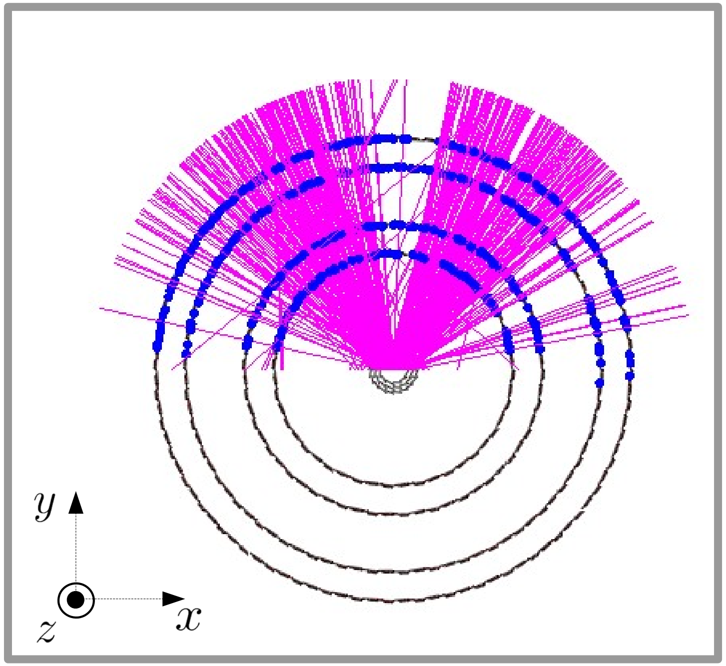

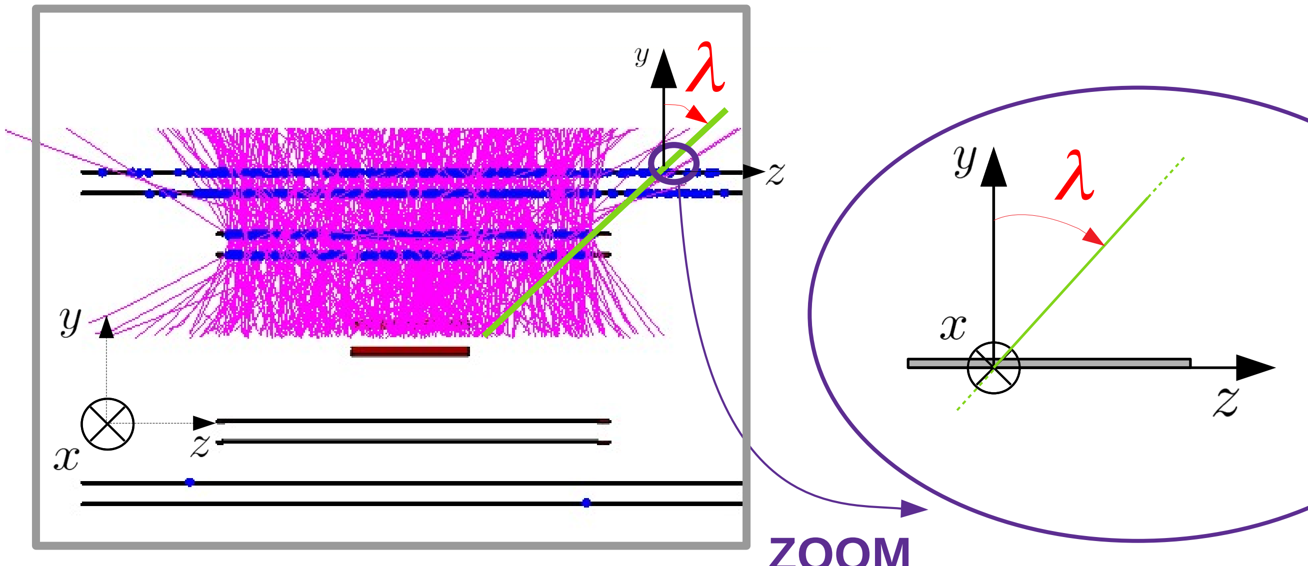

Plane (y,z) view

Inclination angles

3D view

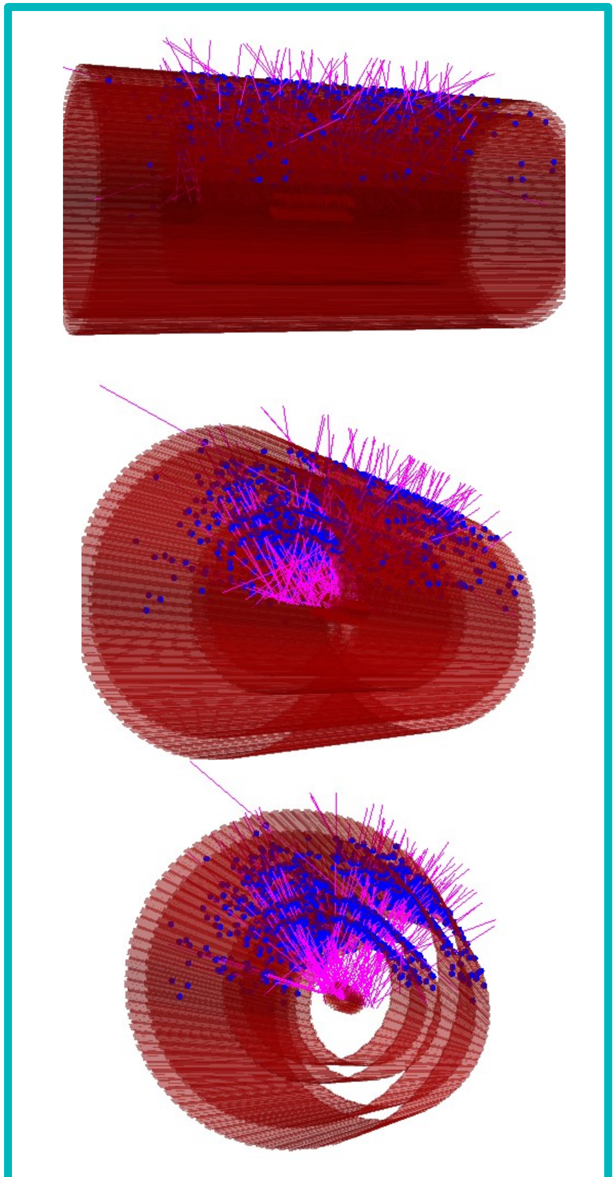

Plane (x,y) view

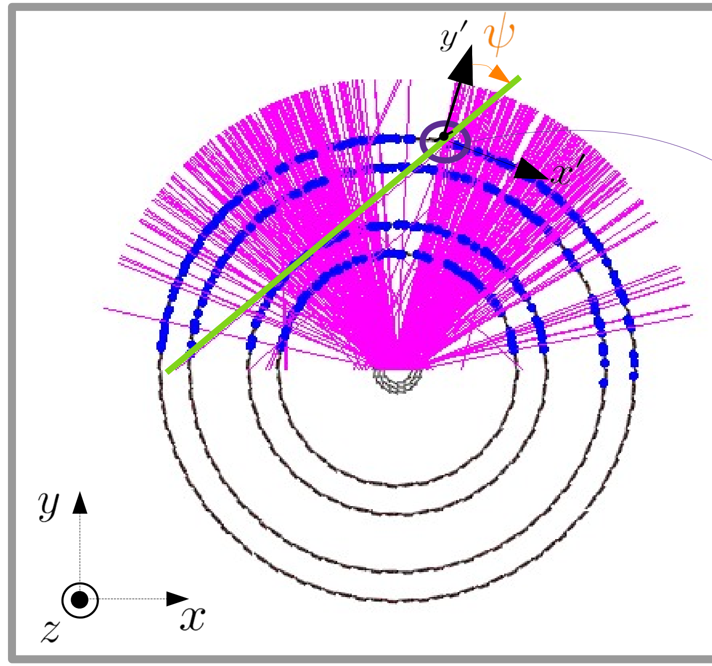

ZOOM

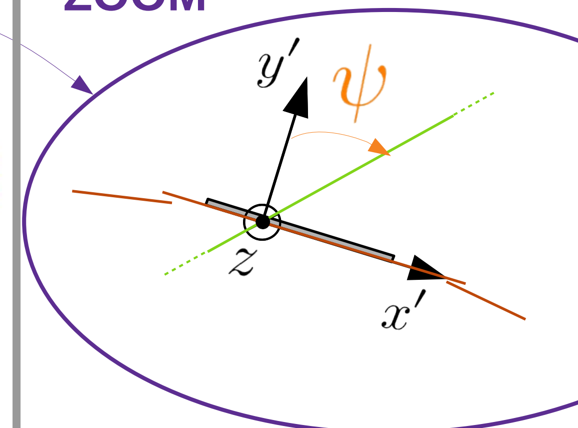

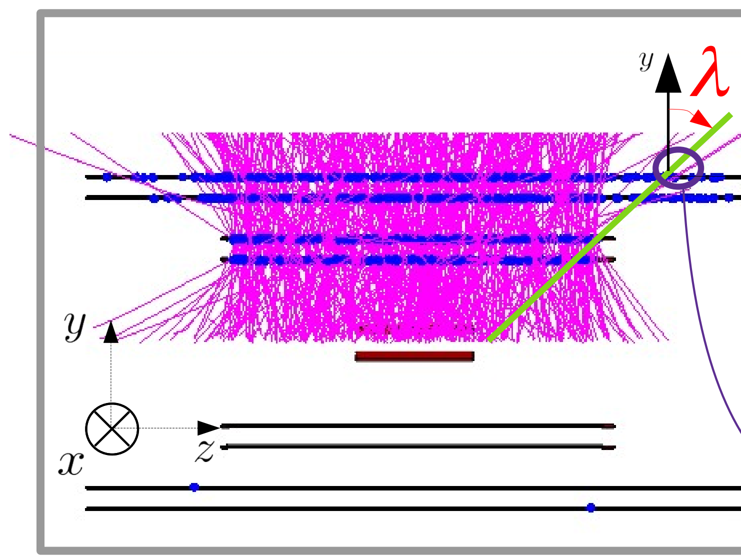

Plane (y,z) view

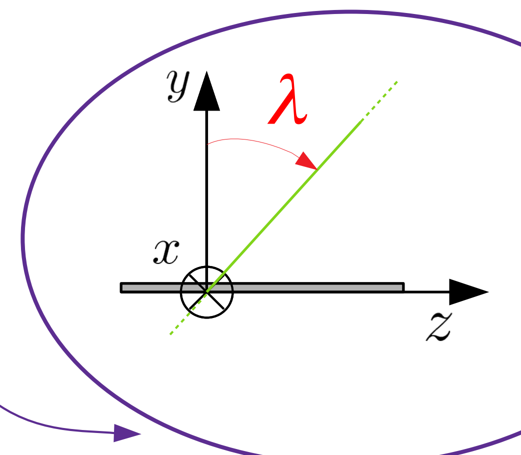

ZOOM

I) Track candidates selection

II) Cluster shape analysis

III) Comparison with Monte-Carlo data

Motivations

- Some shapes offer a better precision on position

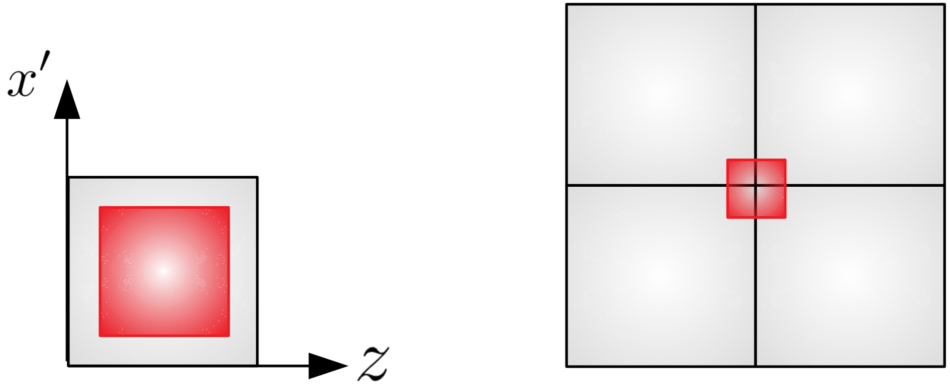

$$\sigma_z \sim \frac{d_z}{\sqrt{12}} \qquad \sigma_z \ll \frac{d_z}{\sqrt{12}}$$

$$\sigma_{x'} \sim \frac{d_{x'}}{\sqrt{12}} \qquad \sigma_{x'} \ll \frac{d_{x'}}{\sqrt{12}}$$

- It could help the tracking algorithm

Example of cluster-track assignment

- Track reconstructed on layer 5 and the algorithm looks for the next cluster on layer 4;
- Several possible clusters:

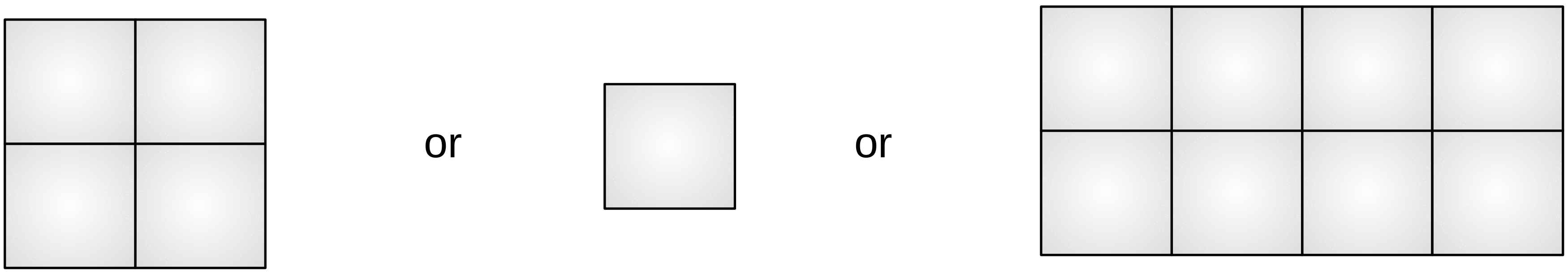

- Track orthogonal to the sensor surface → **cluster shape distribution as a function of inclination angles** offers a finer selection of the next cluster:

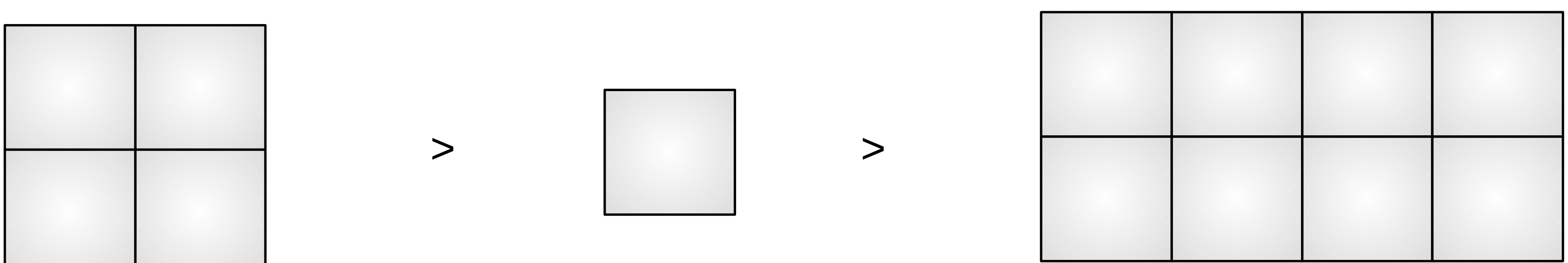

Example

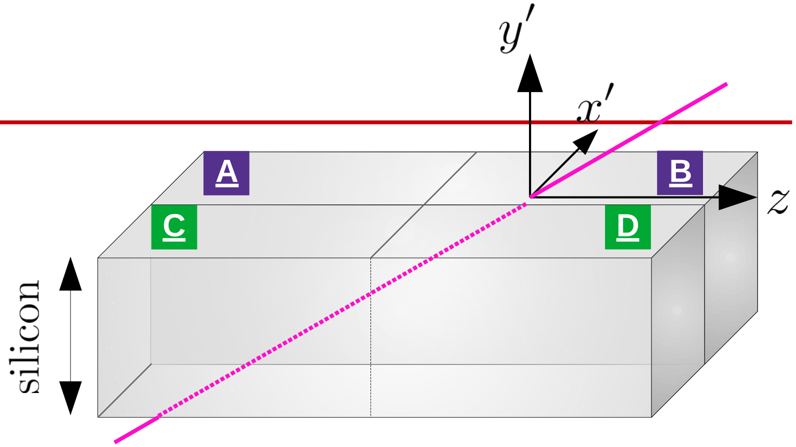

Example

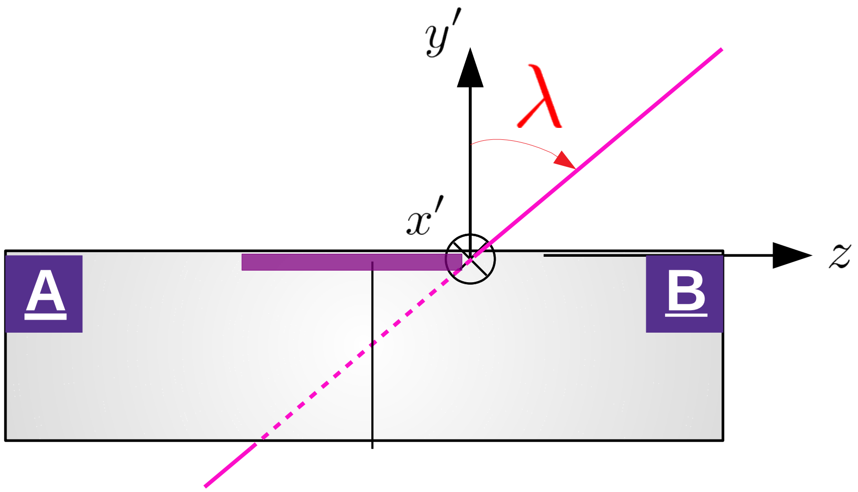

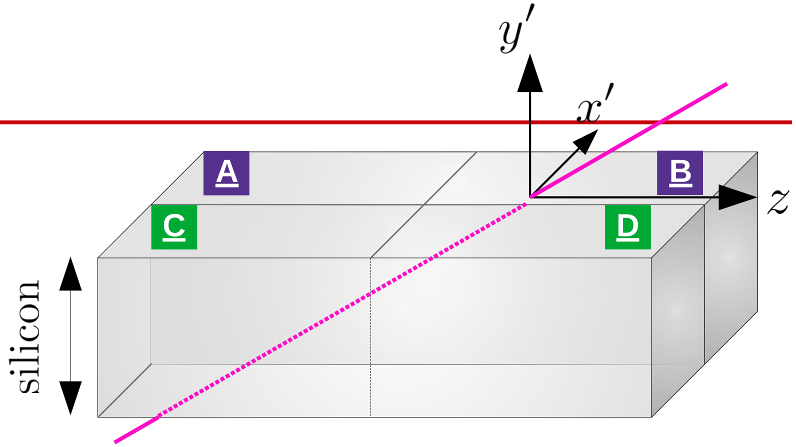

$$|\psi| = 0$$

Example

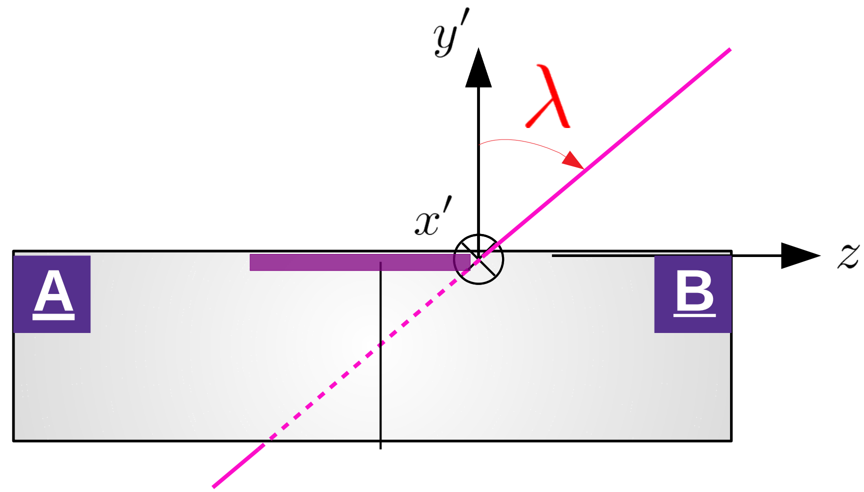

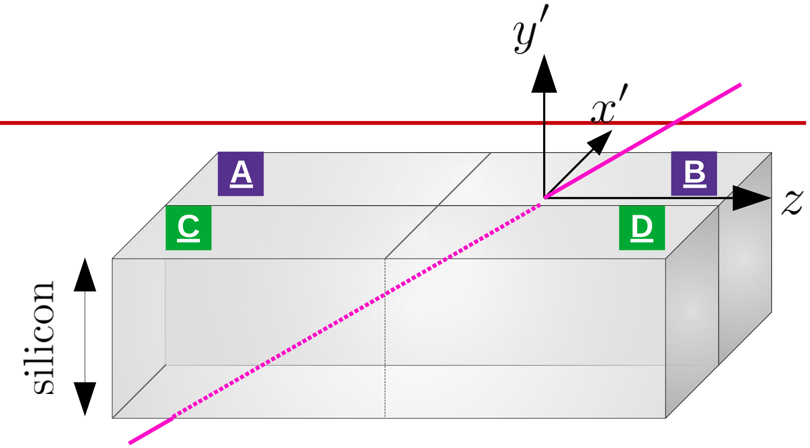

$$|\psi| = 0 \Rightarrow$$

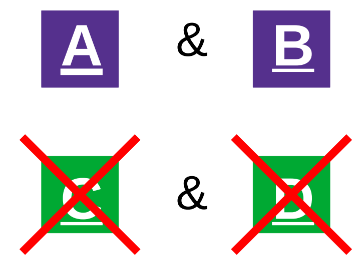

Example

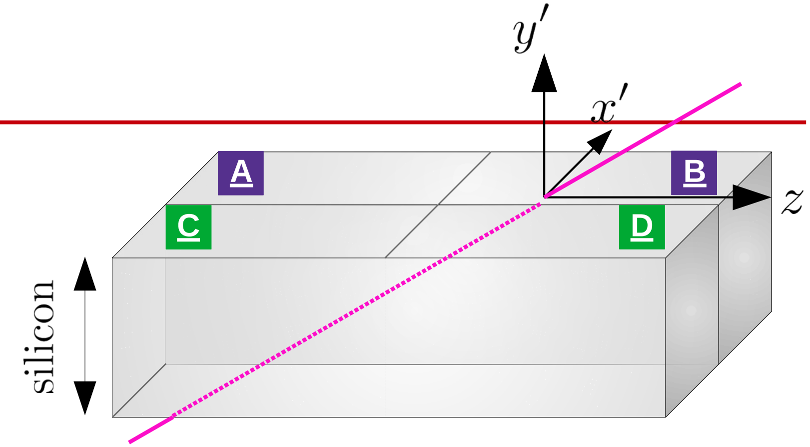

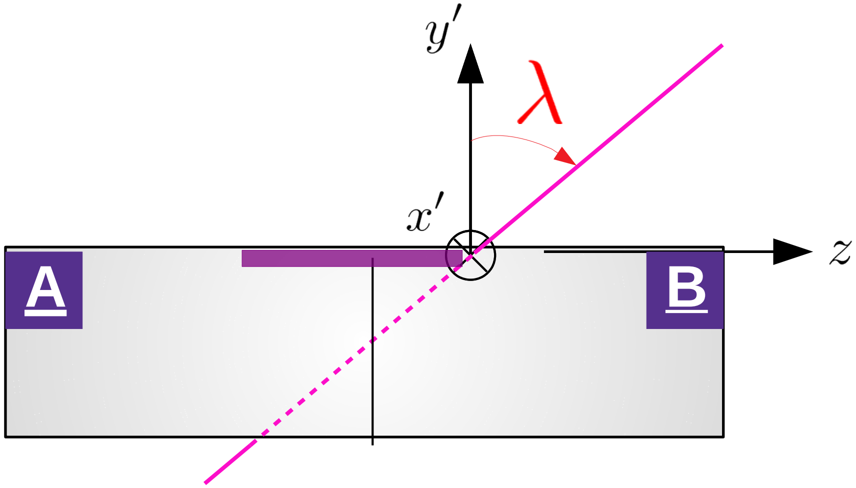

$$|\psi| = 0 \Rightarrow$$

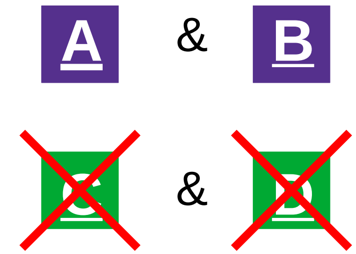

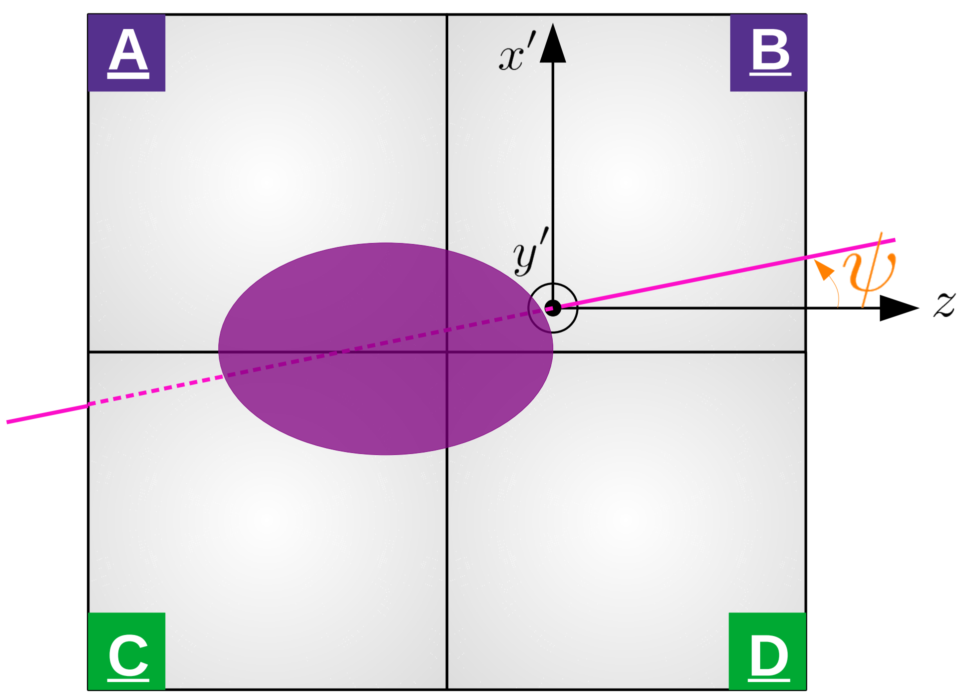

$$|\psi| > 0$$

Example

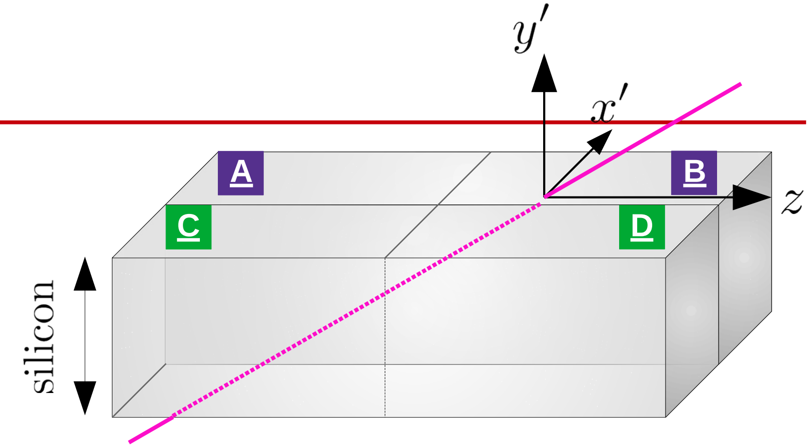

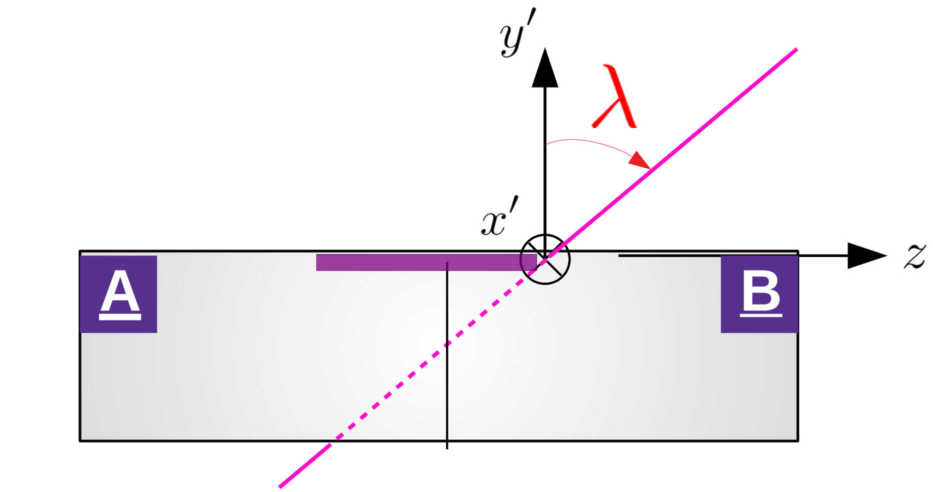

$$|\psi| = 0 \Rightarrow$$

A & B

~~C~~ & ~~D~~

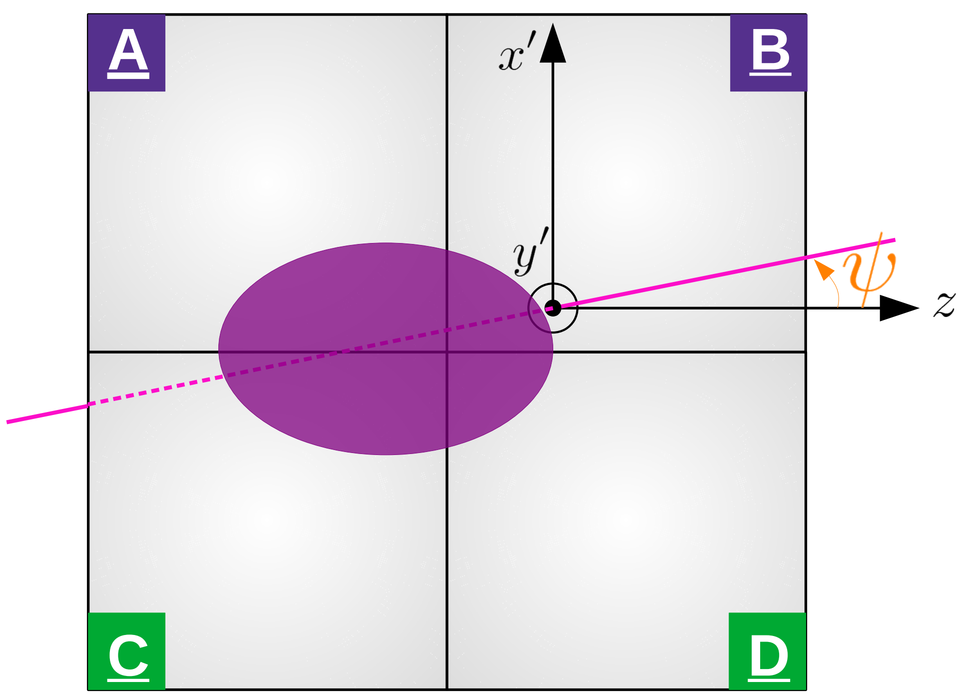

$$|\psi| > 0 \Rightarrow$$

A & B

C & D

$|\psi| < 10^\circ$

Cluster shape = $f(\lambda)$

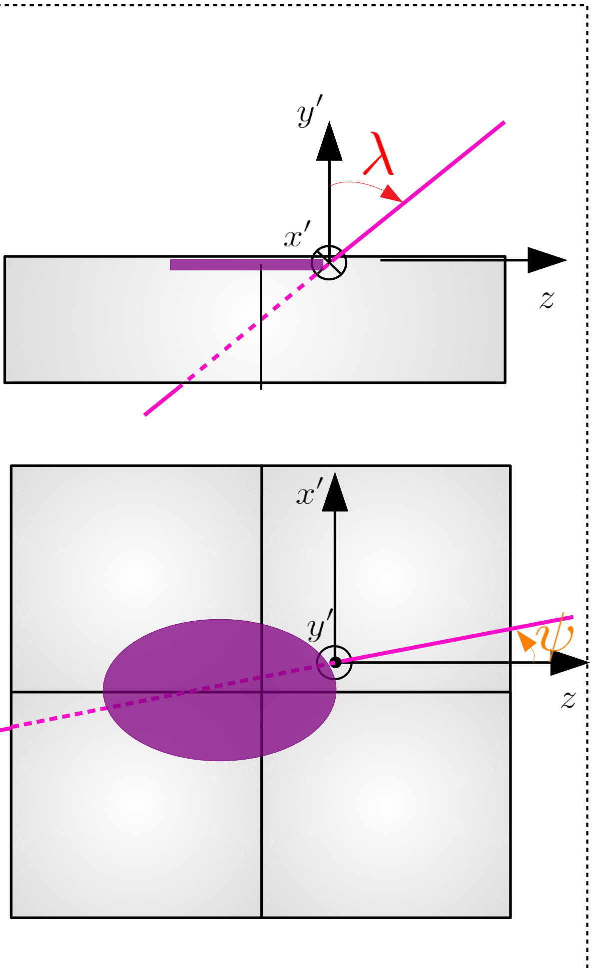

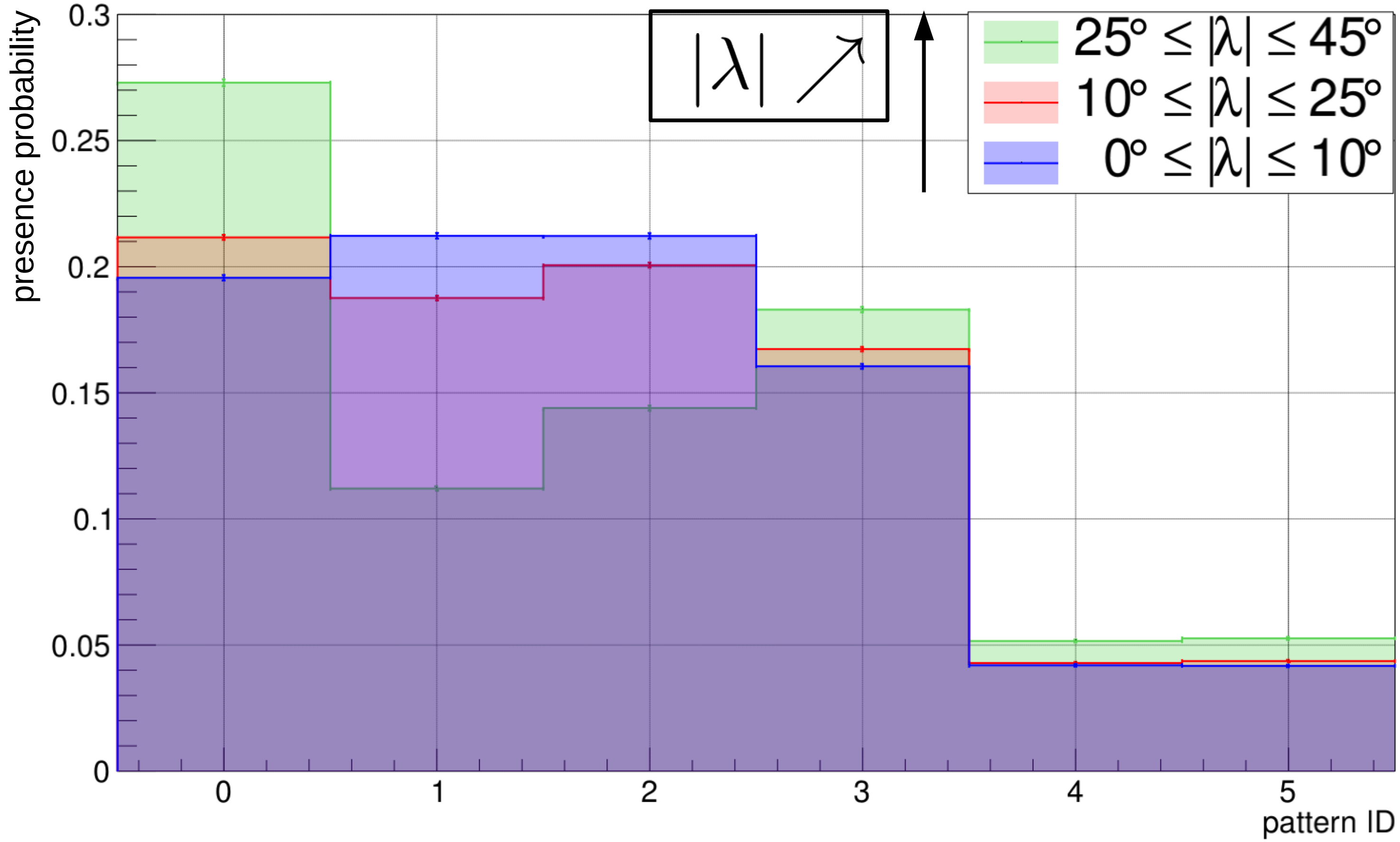

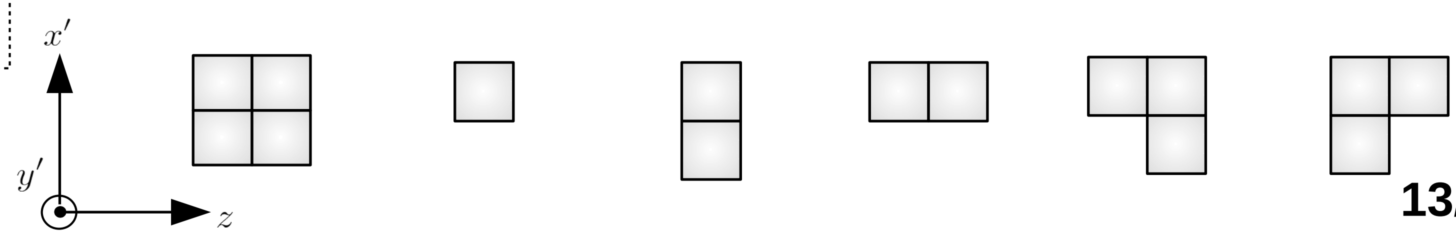

$\texttt{patternID} \in \{0; 2059\}$

$|\psi| < 10^\circ$

Cluster shape = $f(\lambda)$

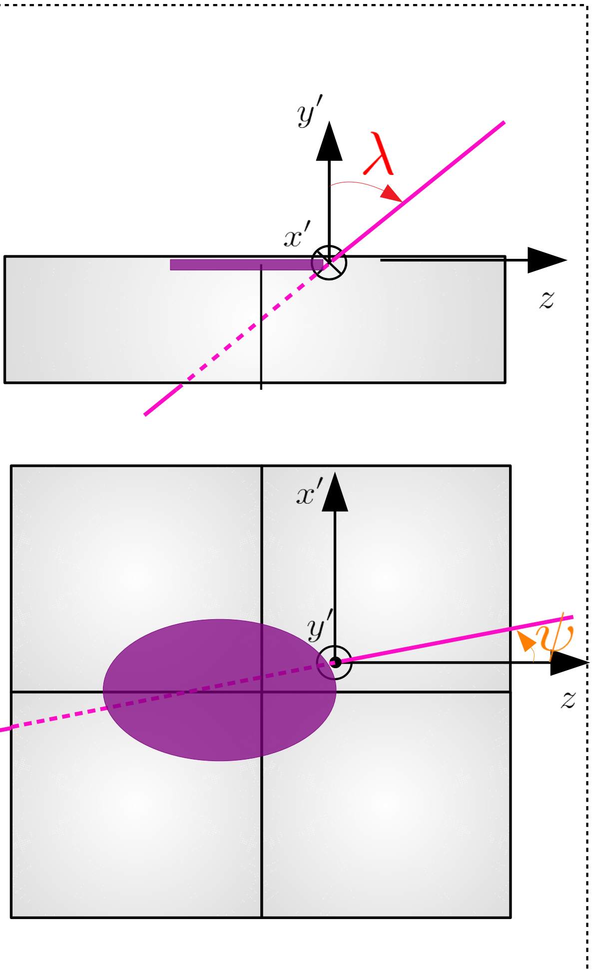

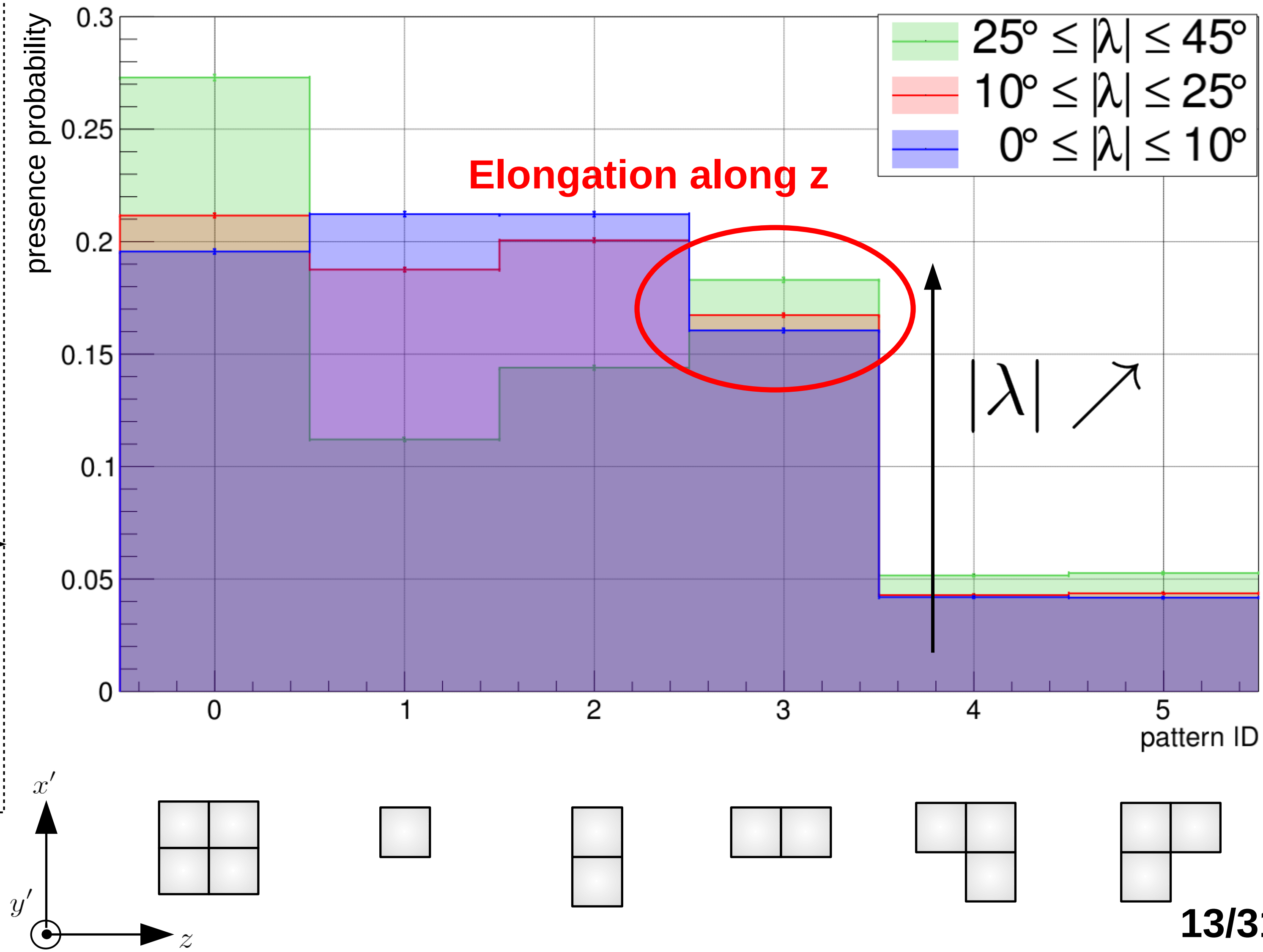

$\texttt{patternID} \in \{0; 2059\}$

$|\psi| < 10^\circ$

Cluster shape = $f(\lambda)$

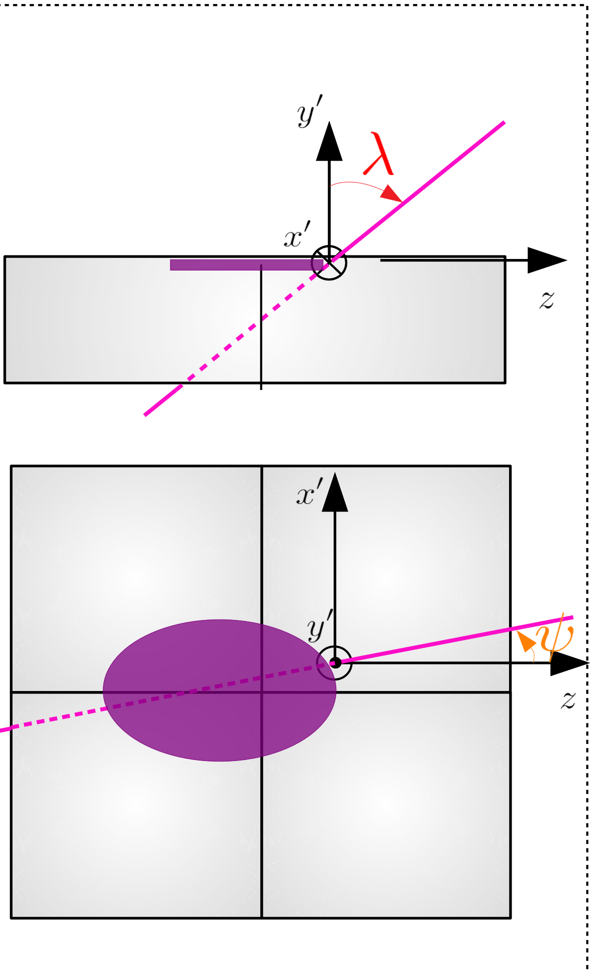

$\texttt{patternID} \in \{0; 2059\}$

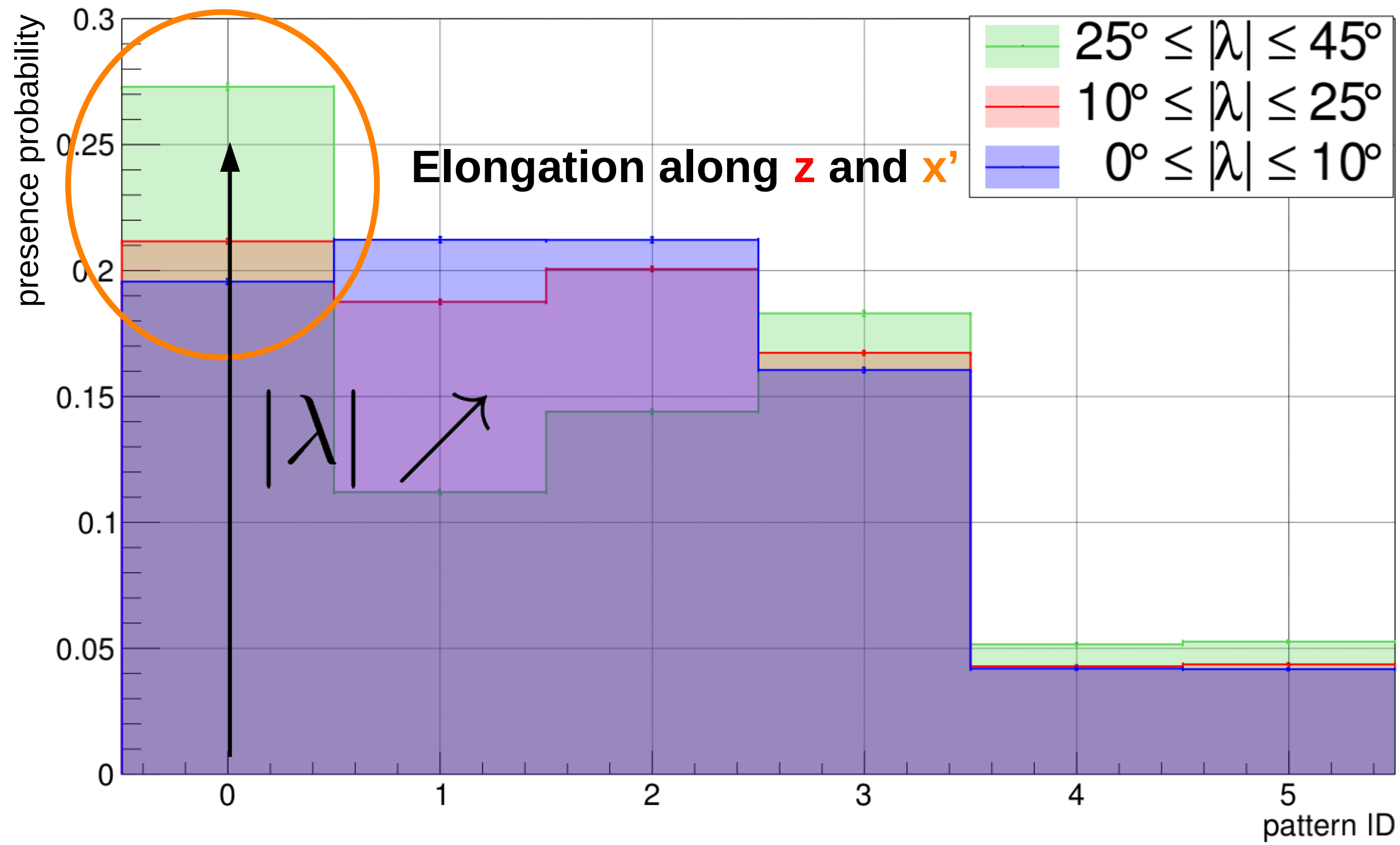

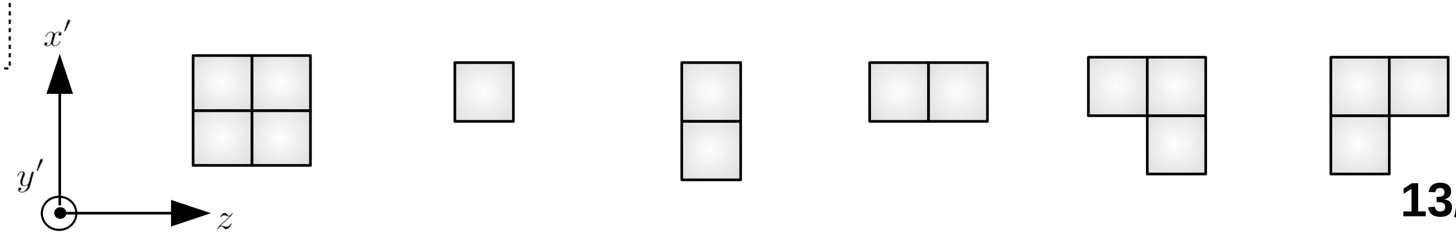

Cluster shape = $f(\lambda)$

$|\psi| < 10^\circ$

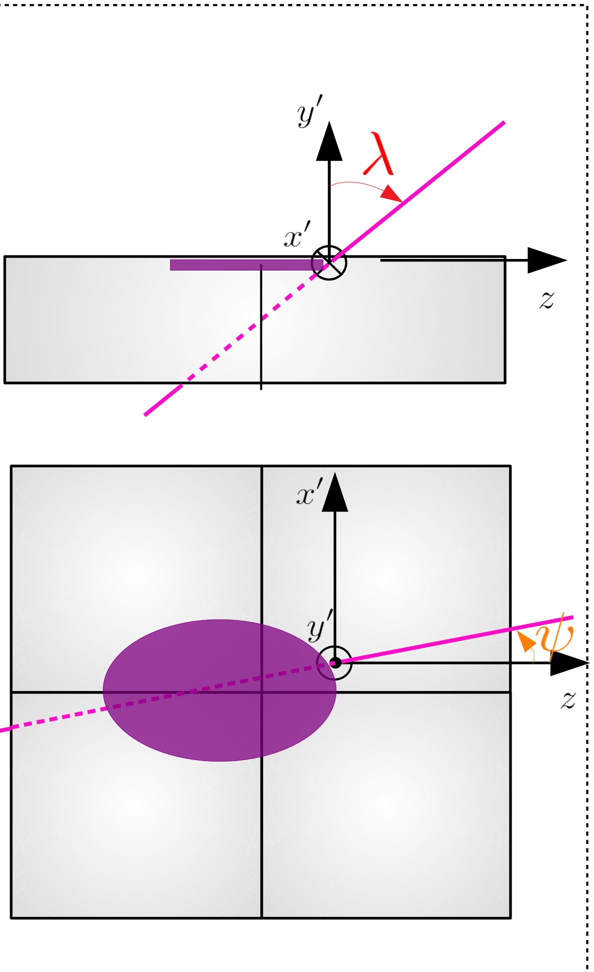

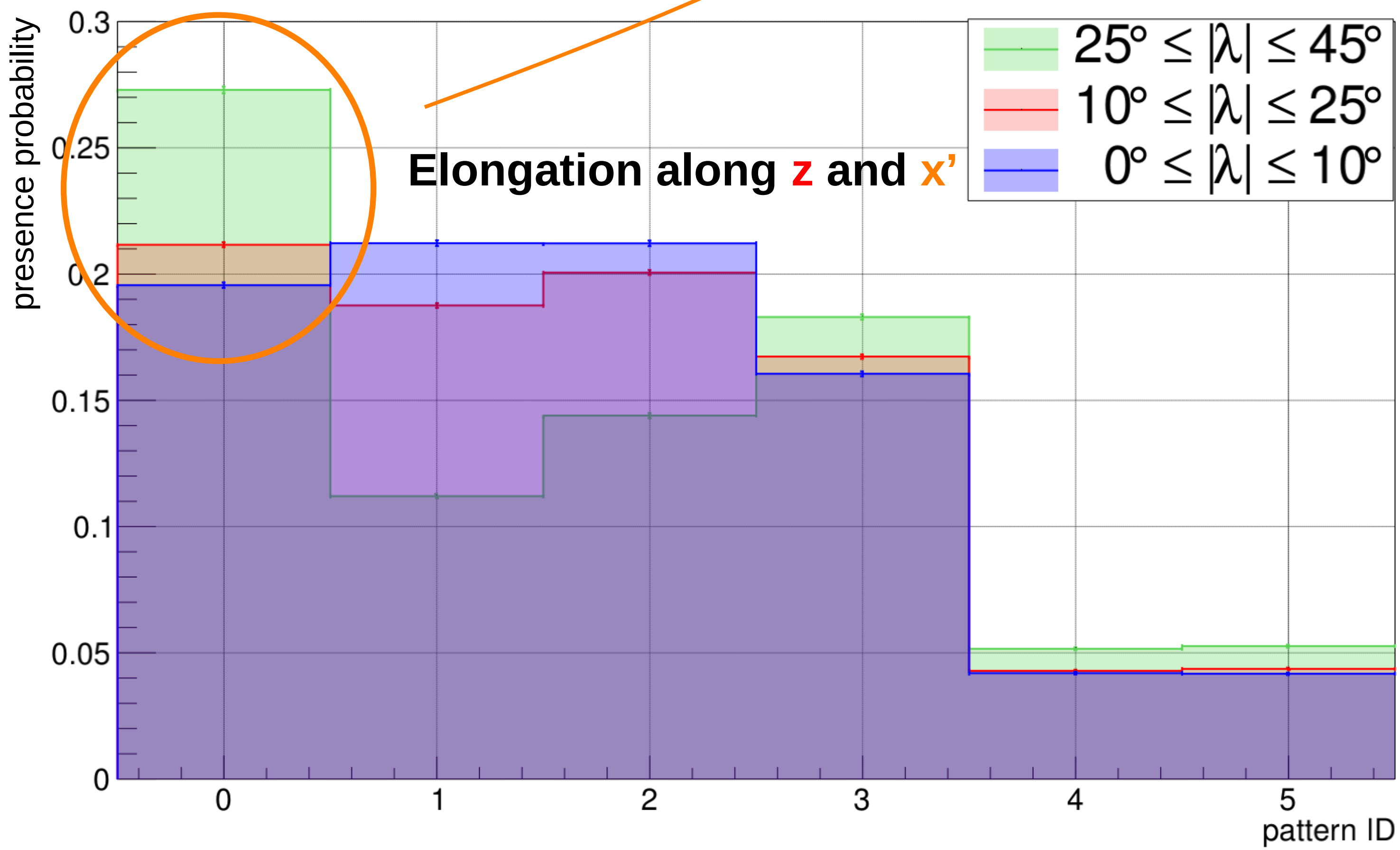

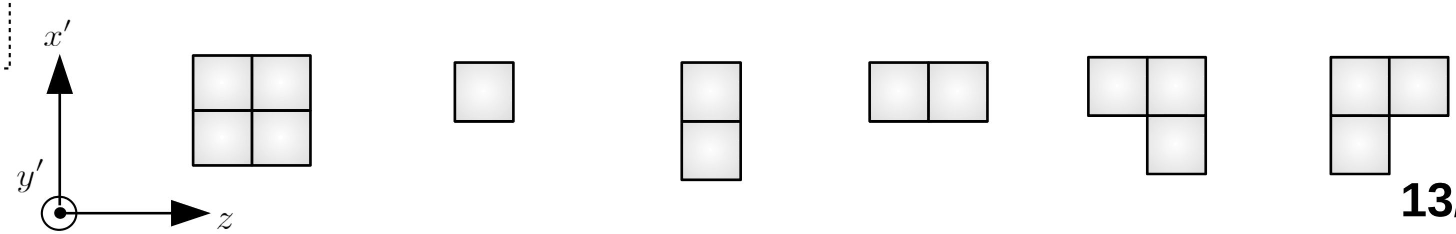

$\texttt{patternID} \in \{0; 2059\}$

Cluster shape = $f(\lambda)$

$|\psi| < 10^\circ$

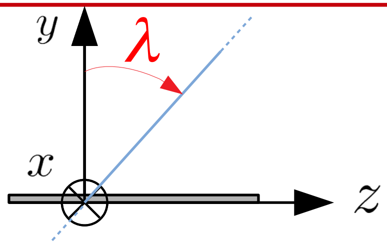

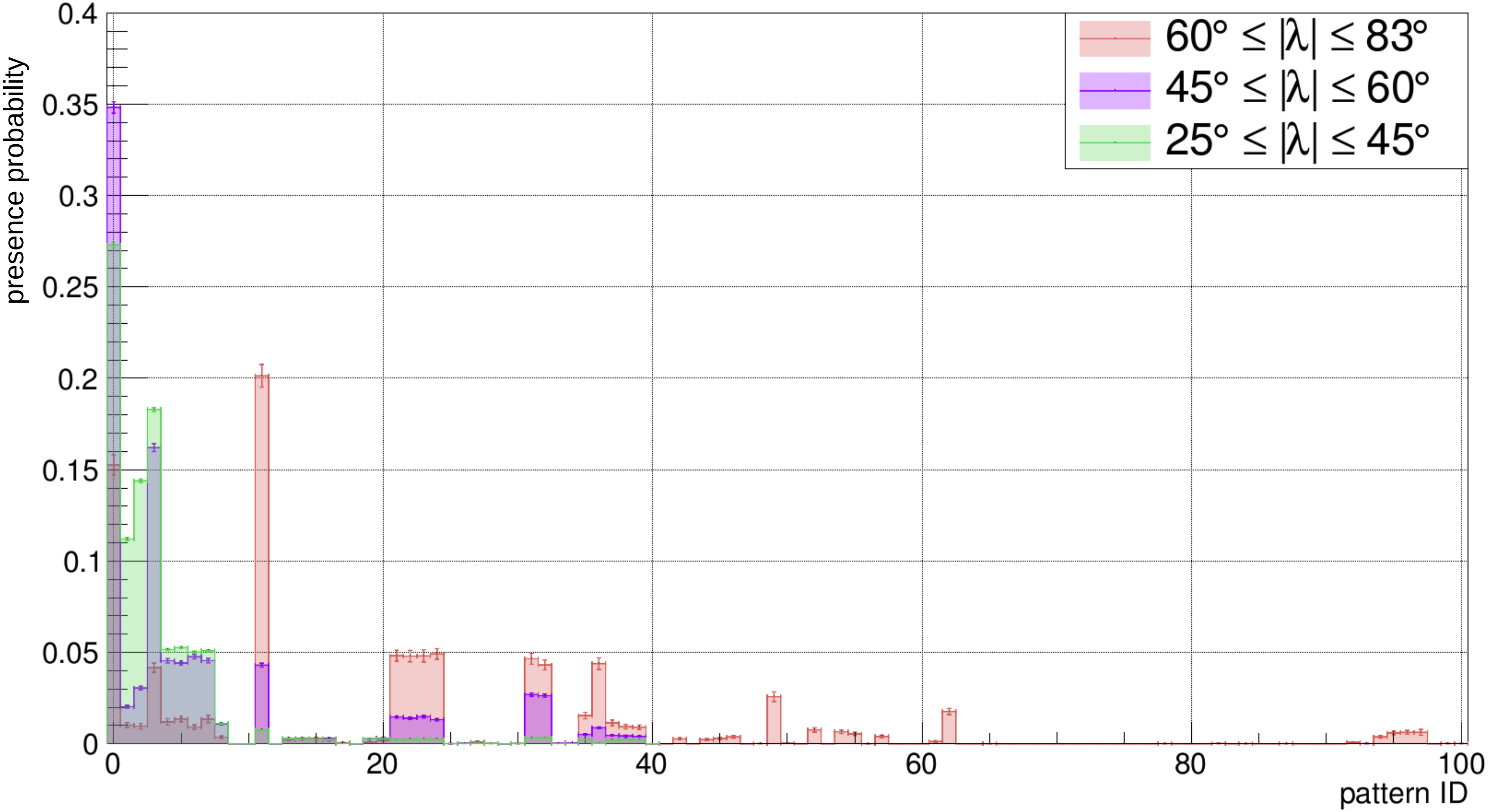

Cluster shape = $f(\lambda)$

$|\psi| < 10^\circ$

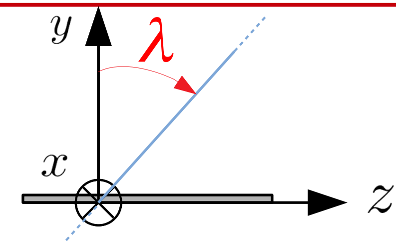

Cluster shape = $f(\lambda)$

$|\psi| < 10°$

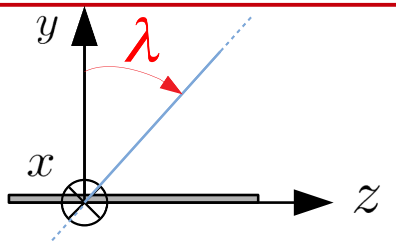

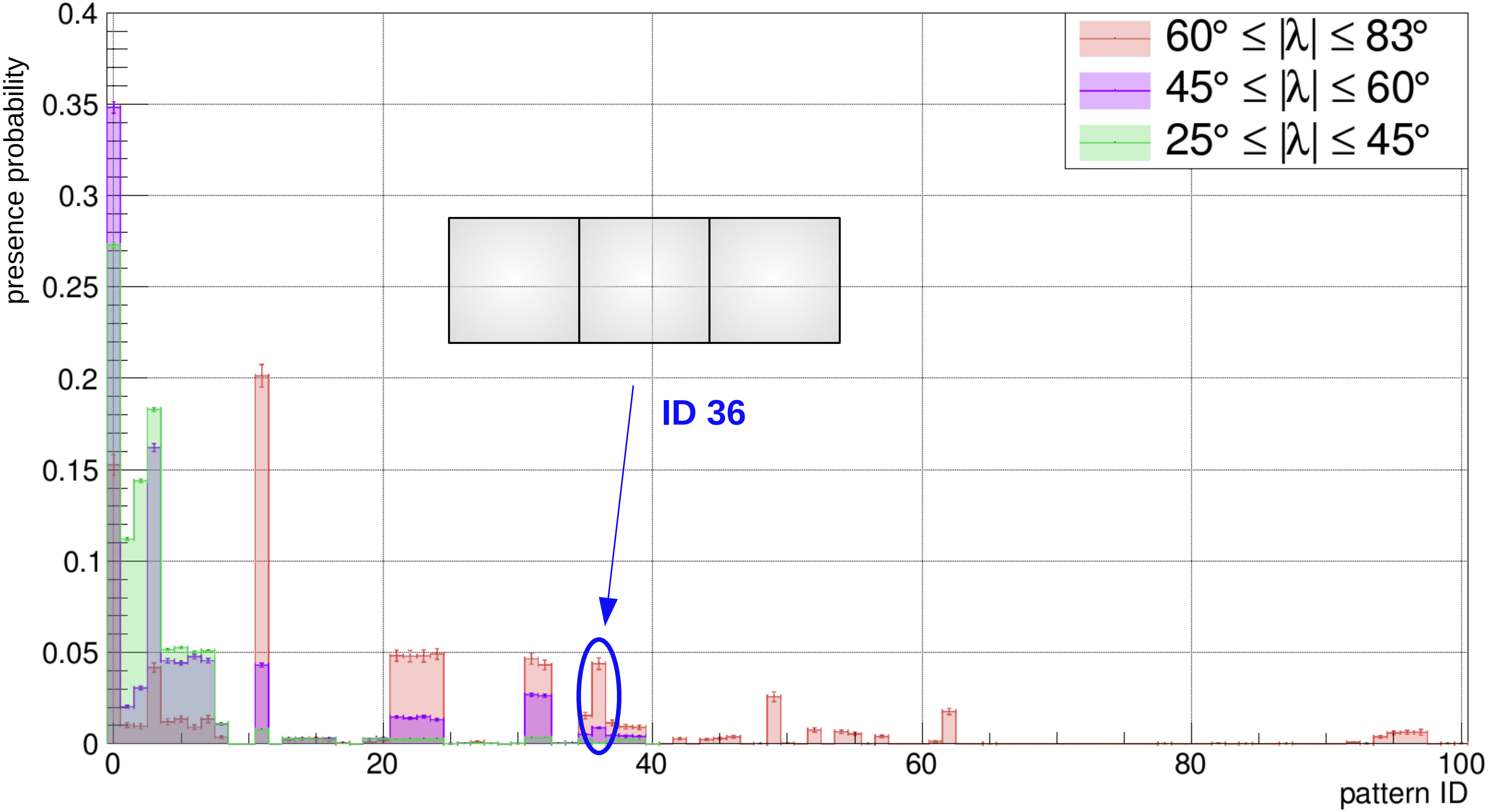

Cluster shape = $f(\lambda)$

$|\psi| < 10^{\circ}$

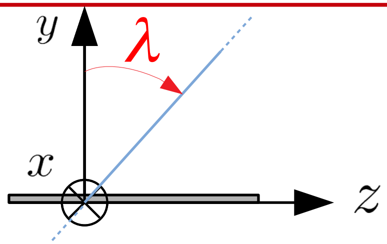

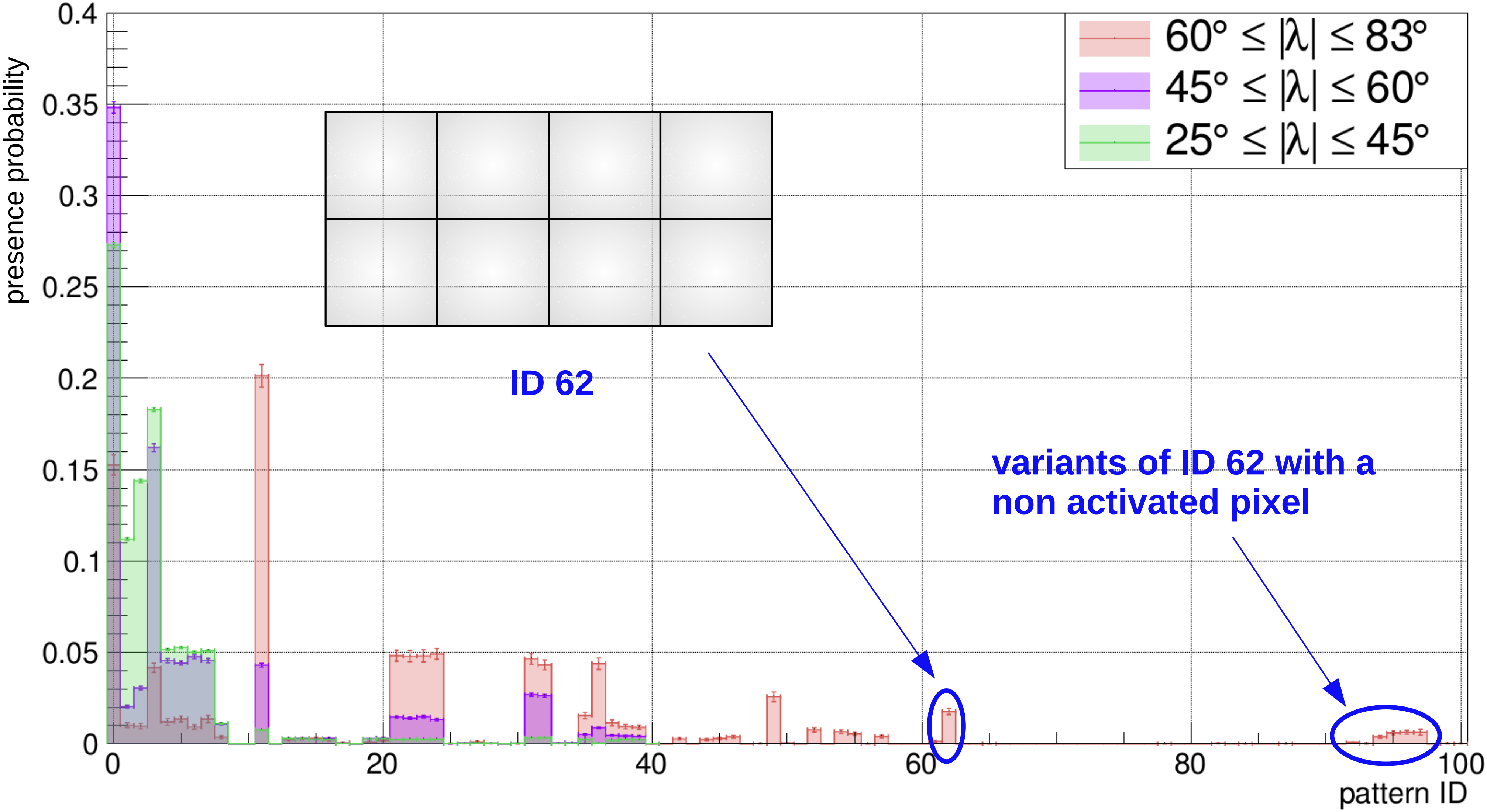

$$|\lambda| < 10^\circ$$

Cluster shape = $f(\psi)$

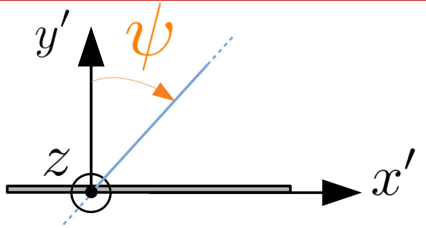

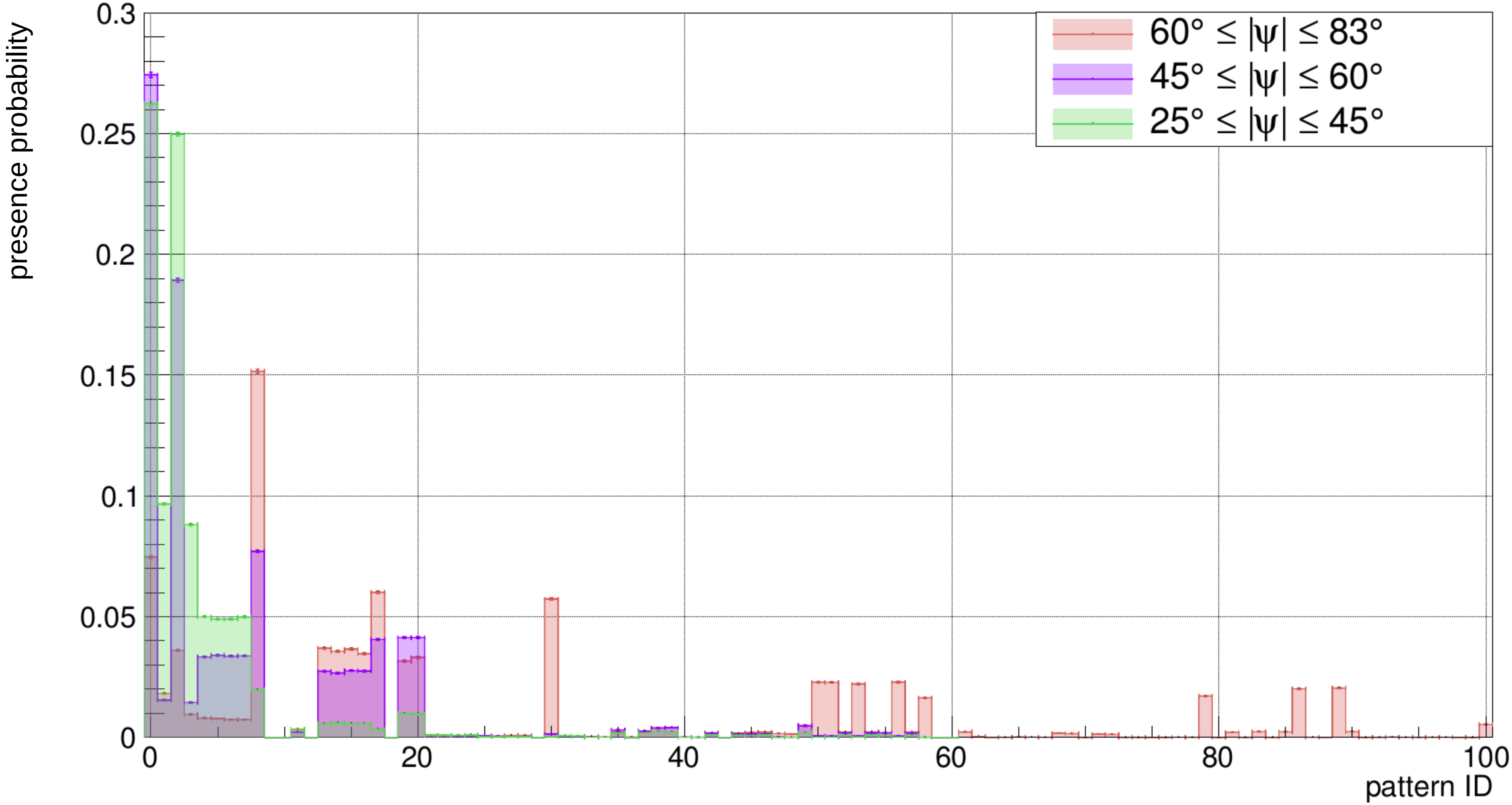

Cluster shape = $f(\psi)$

$|\lambda| < 10^\circ$

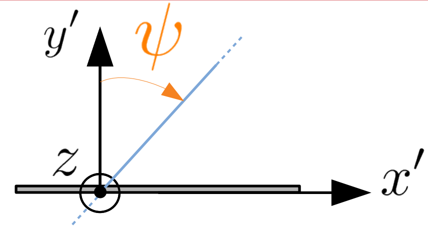

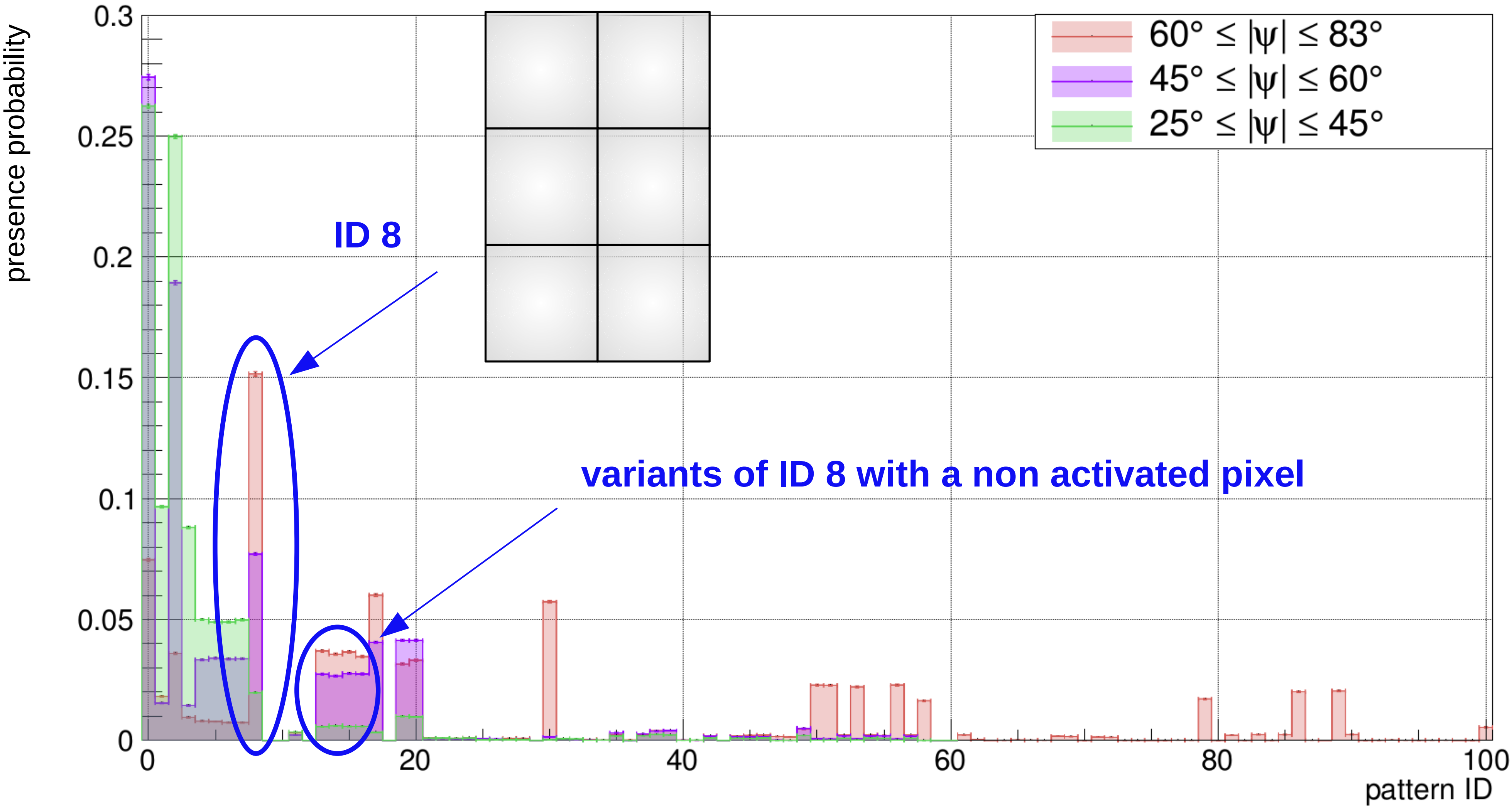

$|\lambda| < 10^\circ$

Cluster shape = $f(\psi)$

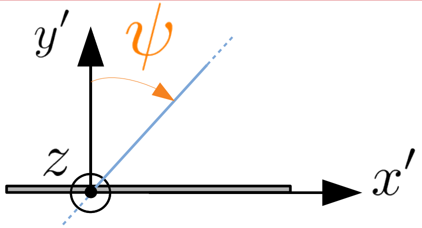

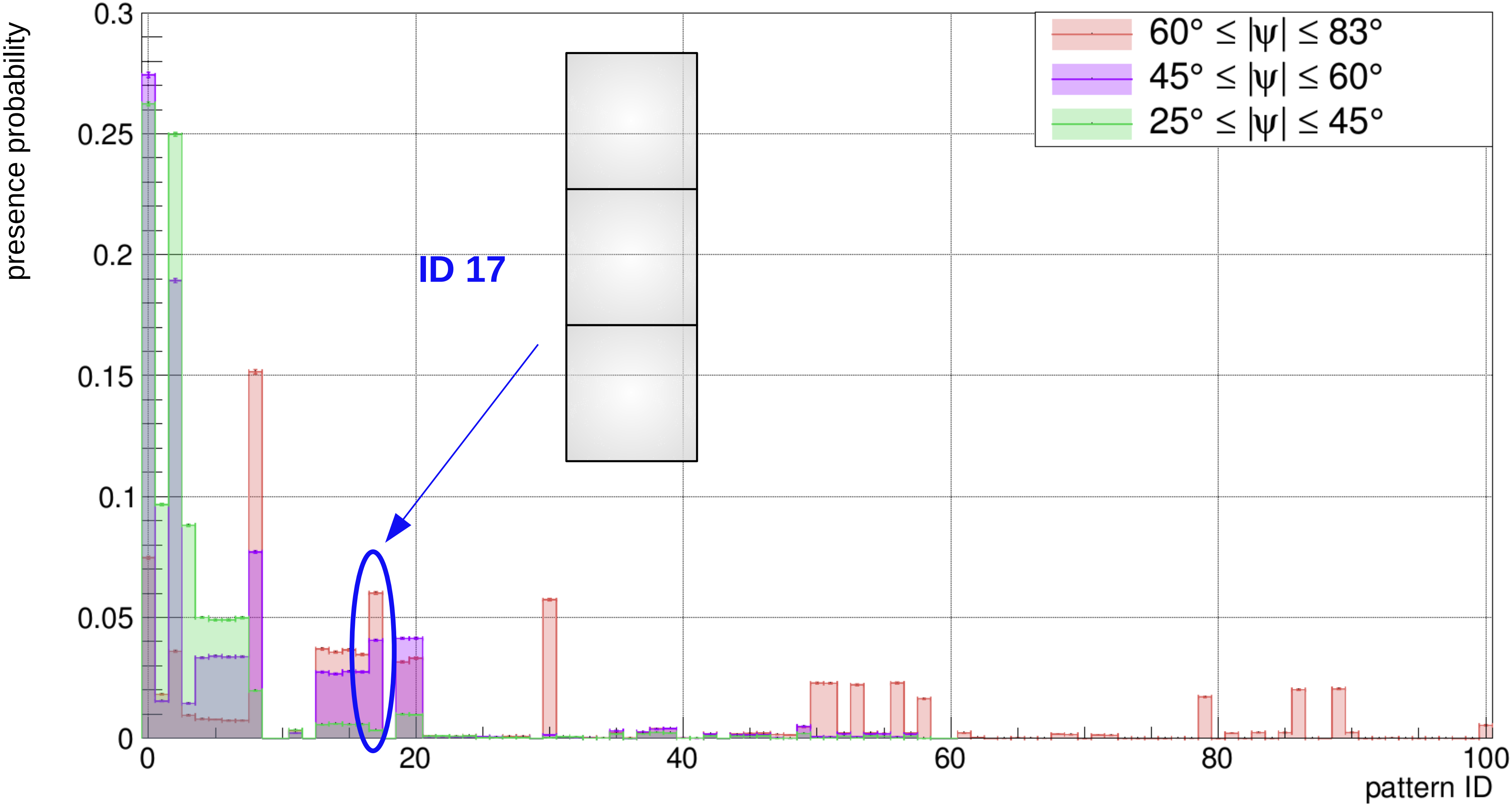

$|\lambda| < 10°$

Cluster shape = $f(\psi)$

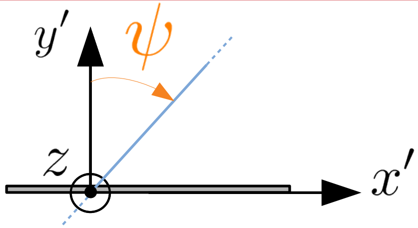

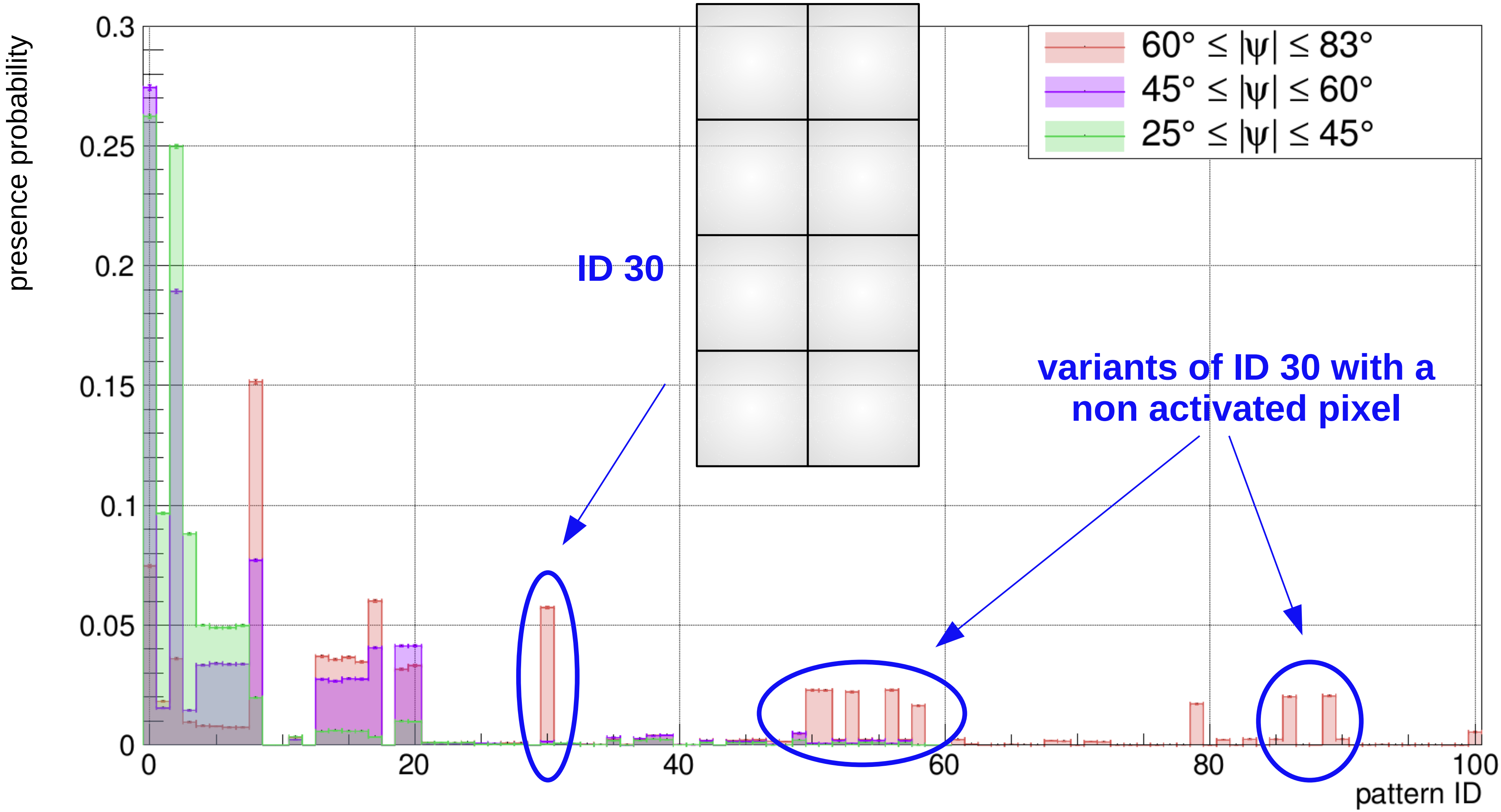

$|\lambda| < 10°$

Cluster shape = $f(\psi)$

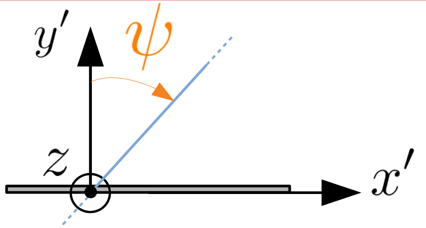

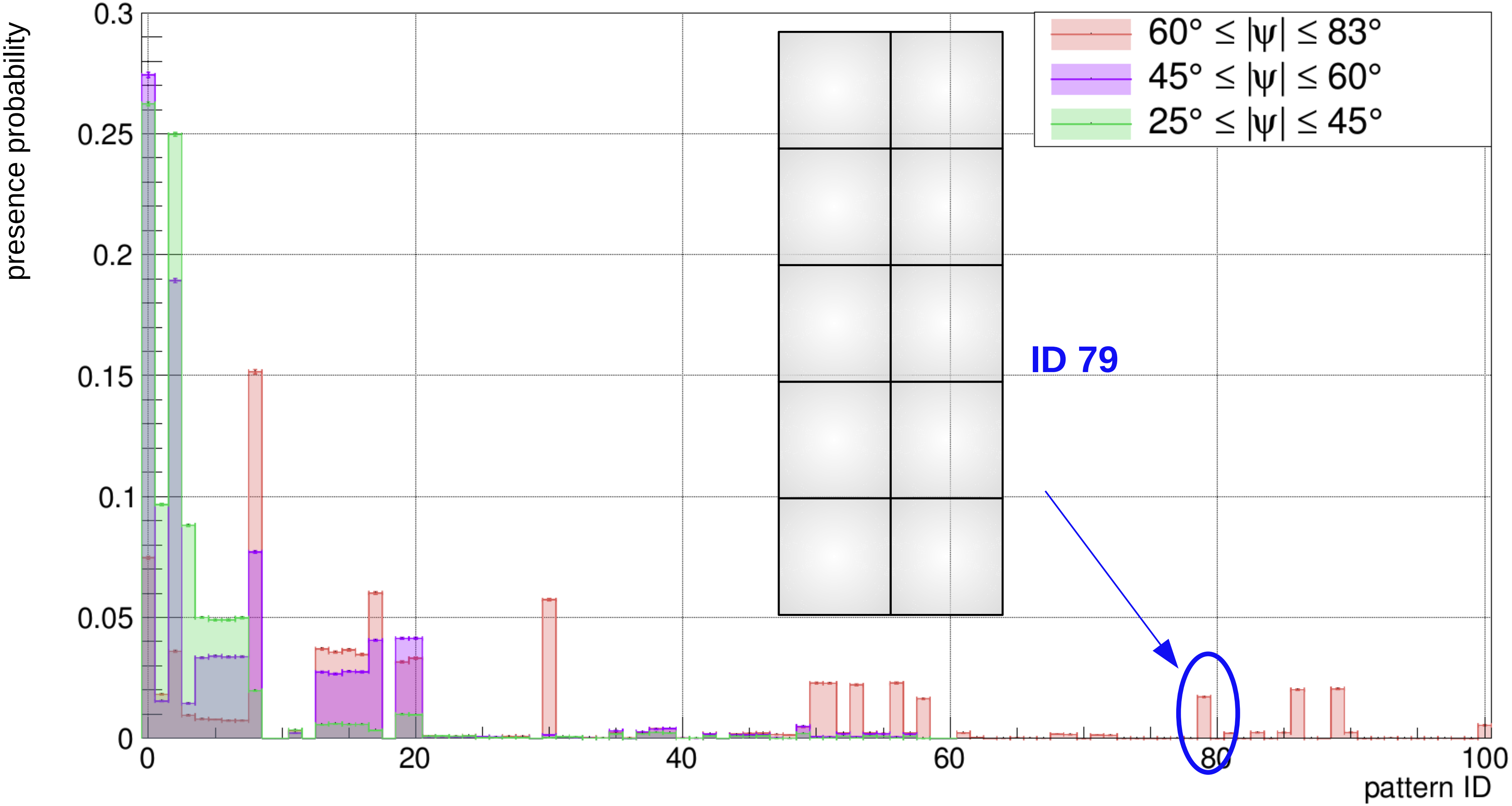

I) Track candidates selection

II) Cluster shape analysis

III) Comparison with Monte-Carlo data

ALICE

Real data vs simulated data

- Bias = potential difference applied to the width of a chip's semiconductor to compensate the effects of radiation damage
- Inner Barrel (IB): with bias and without bias
- MC : ~ 10 M tracks generated

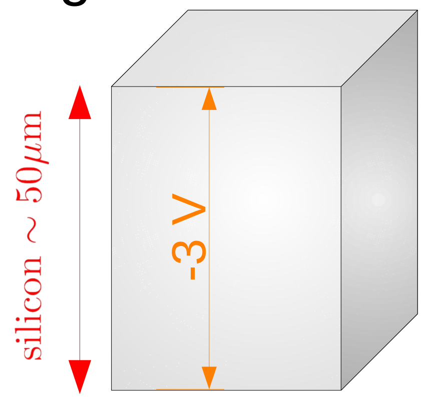

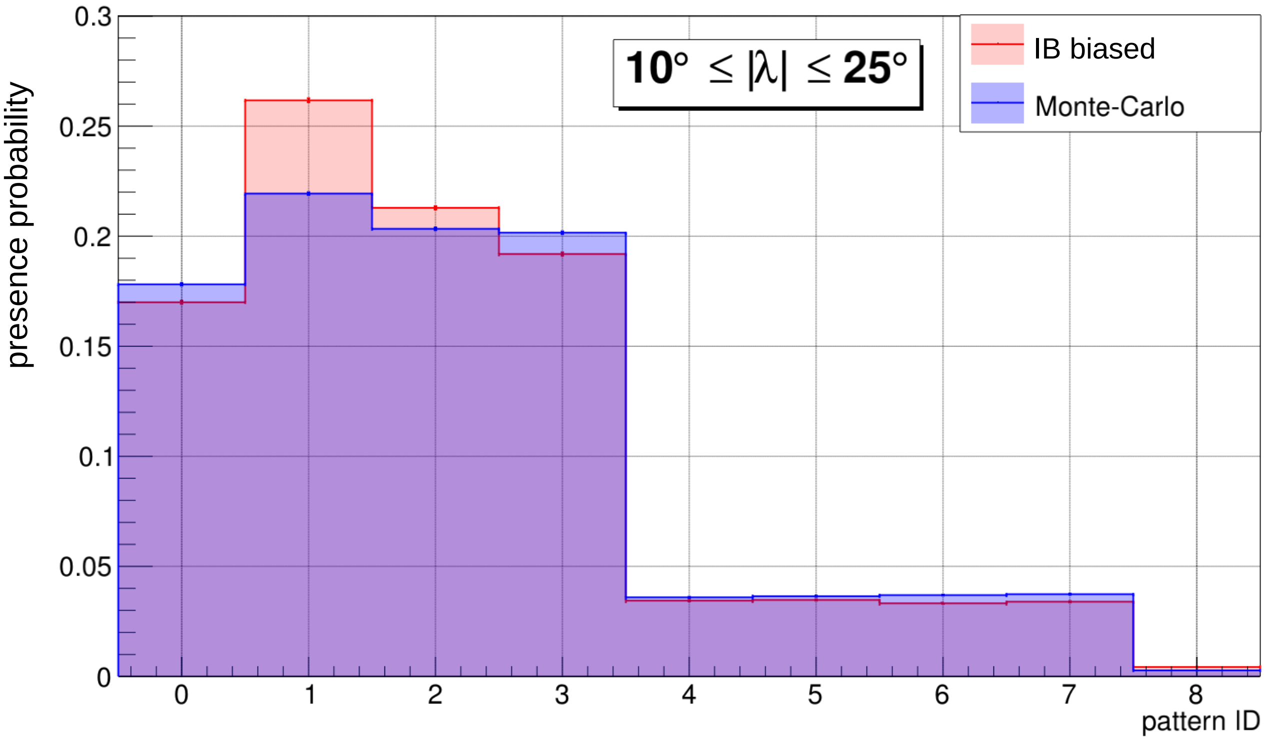

Measure of difference

$$d_\lambda = \sum_{i=1}^{n_{\mathrm{bin}}} \frac{\left[N_\lambda(i) - N_\lambda^{\mathrm{MC}}(i)\right]^2}{N_\lambda(i) + N_\lambda^{\mathrm{MC}}(i)}$$

Real data vs simulated data

$$d_\lambda + d_\psi = \sum_{i=1}^{n_{\text{bin}}} \frac{\left[N_\lambda(i) - N_\lambda^{\text{MC}}(i)\right]^2}{N_\lambda(i) + N_\lambda^{\text{MC}}(i)} + \sum_{j=1}^{n_{\text{bin}}} \frac{\left[N_\psi(j) - N_\psi^{\text{MC}}(j)\right]^2}{N_\psi(j) + N_\psi^{\text{MC}}(j)}$$

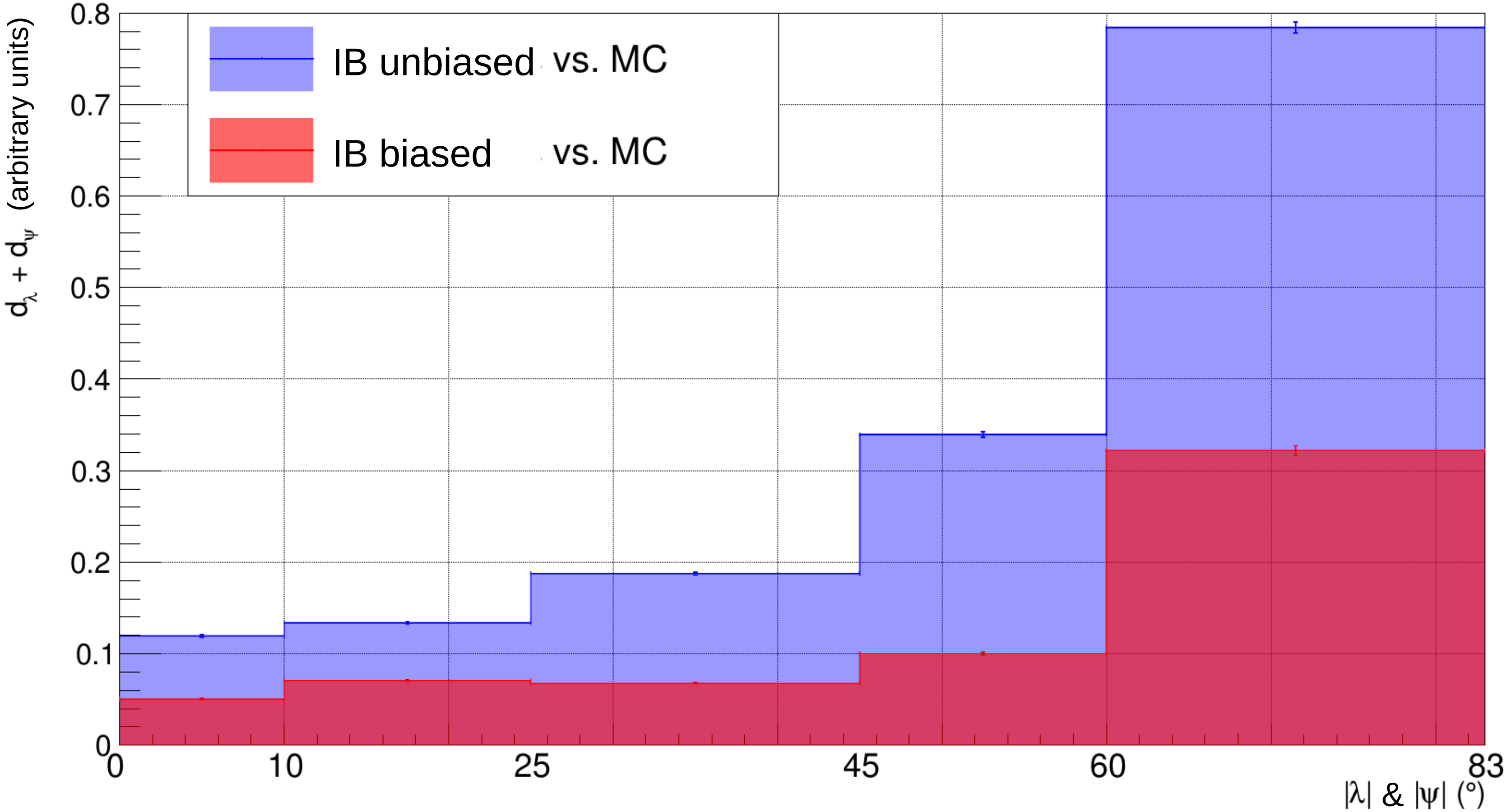

Real data vs simulated data

$$d_\lambda + d_\psi = \sum_{i=1}^{n_{\text{bin}}} \frac{\left[N_\lambda(i) - N_\lambda^{\text{MC}}(i)\right]^2}{N_\lambda(i) + N_\lambda^{\text{MC}}(i)} + \sum_{j=1}^{n_{\text{bin}}} \frac{\left[N_\psi(j) - N_\psi^{\text{MC}}(j)\right]^2}{N_\psi(j) + N_\psi^{\text{MC}}(j)}$$

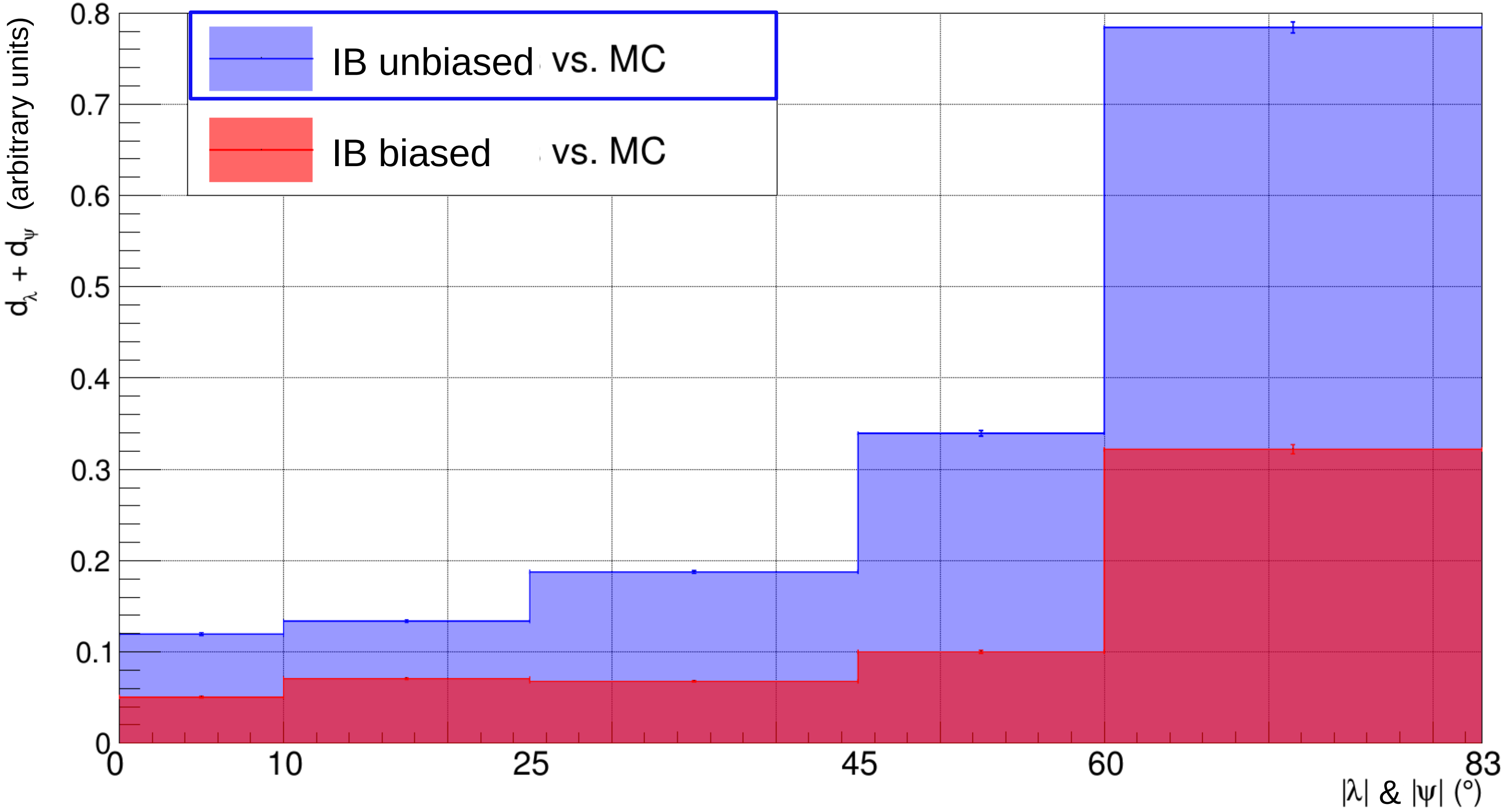

Real data vs simulated data

$$d_\lambda + d_\psi = \sum_{i=1}^{n_{\rm bin}} \frac{\left[N_\lambda(i) - N_\lambda^{\rm MC}(i)\right]^2}{N_\lambda(i) + N_\lambda^{\rm MC}(i)} + \sum_{j=1}^{n_{\rm bin}} \frac{\left[N_\psi(j) - N_\psi^{\rm MC}(j)\right]^2}{N_\psi(j) + N_\psi^{\rm MC}(j)}$$

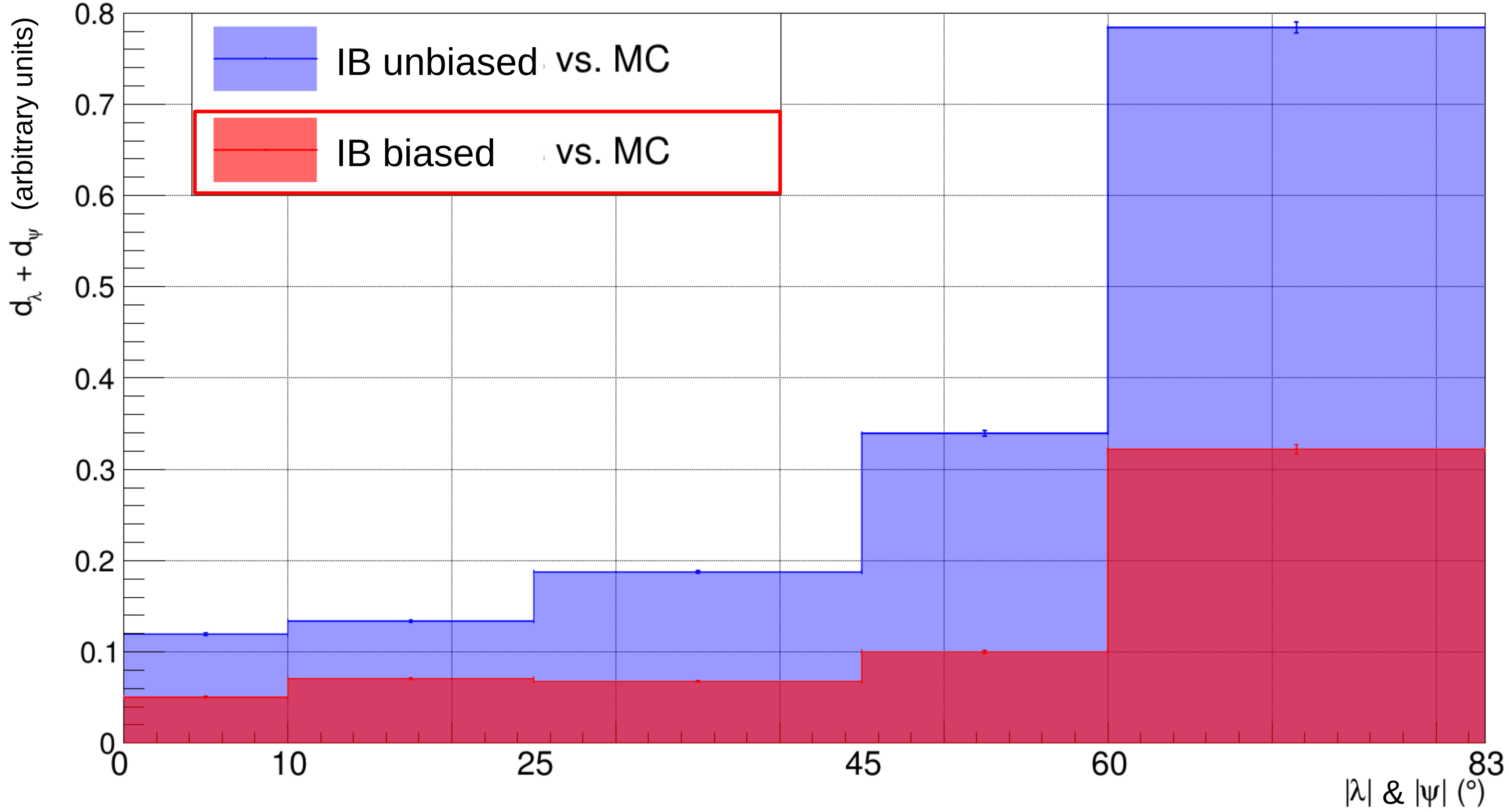

Real data vs simulated data

$$d_\lambda + d_\psi = \sum_{i=1}^{n_{\rm bin}} \frac{\left[N_\lambda(i) - N_\lambda^{\rm MC}(i)\right]^2}{N_\lambda(i) + N_\lambda^{\rm MC}(i)} + \sum_{j=1}^{n_{\rm bin}} \frac{\left[N_\psi(j) - N_\psi^{\rm MC}(j)\right]^2}{N_\psi(j) + N_\psi^{\rm MC}(j)}$$

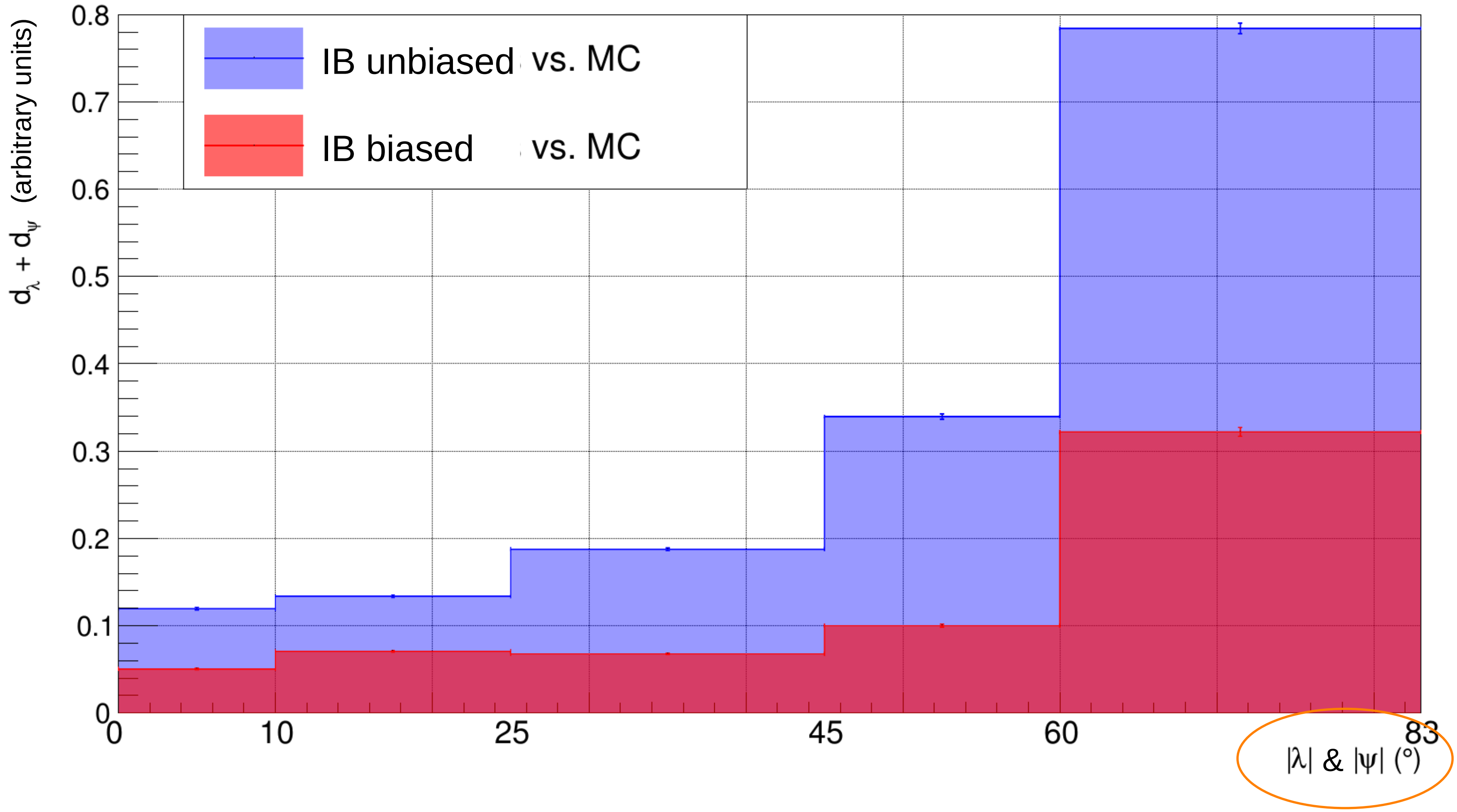

Real data vs simulated data

$$d_\lambda + d_\psi = \sum_{i=1}^{n_{\text{bin}}} \frac{\left[N_\lambda(i) - N_\lambda^{\text{MC}}(i)\right]^2}{N_\lambda(i) + N_\lambda^{\text{MC}}(i)} + \sum_{j=1}^{n_{\text{bin}}} \frac{\left[N_\psi(j) - N_\psi^{\text{MC}}(j)\right]^2}{N_\psi(j) + N_\psi^{\text{MC}}(j)}$$

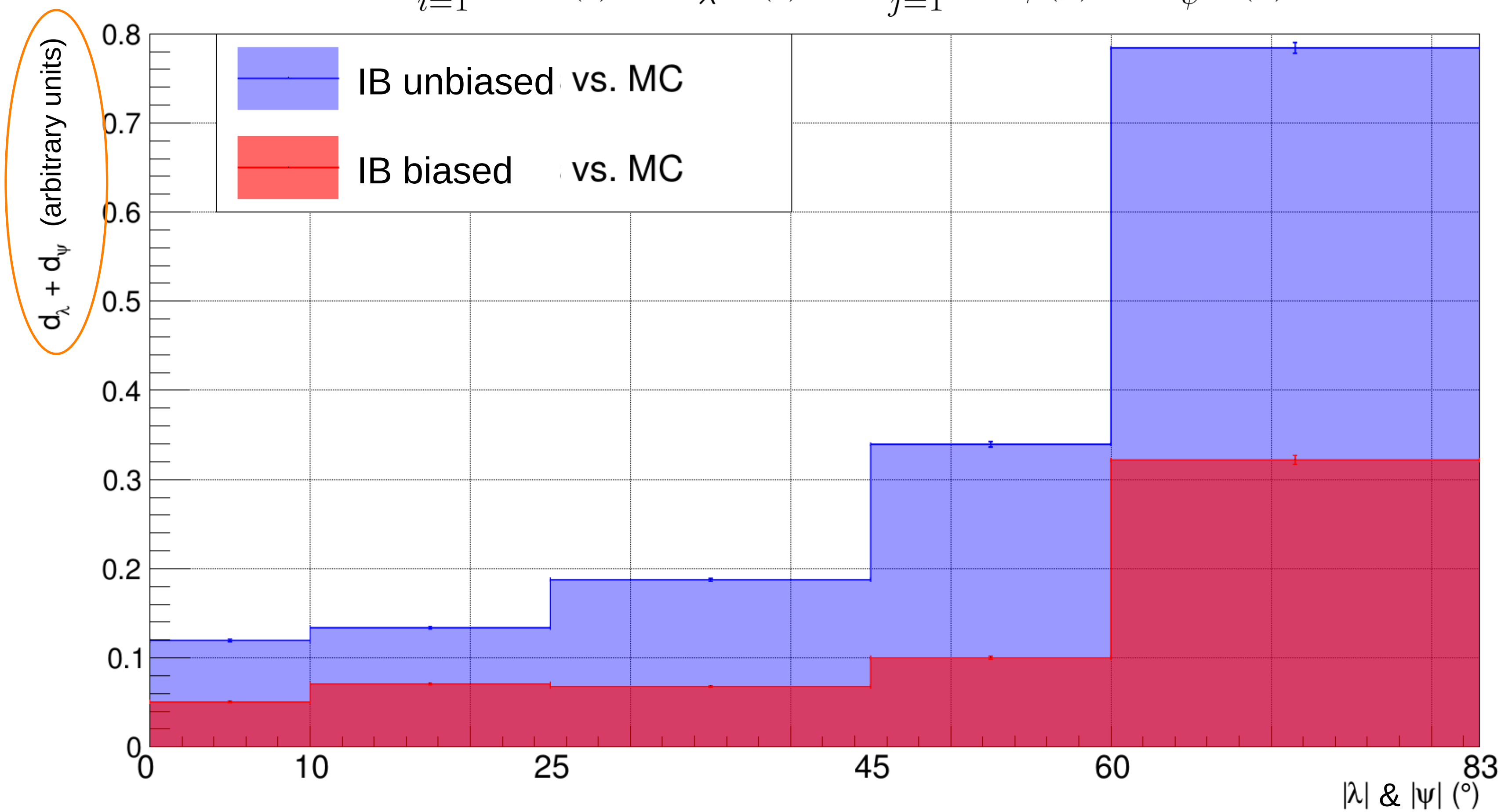

Real data vs simulated data

$$d_\lambda + d_\psi = \sum_{i=1}^{n_{\text{bin}}} \frac{\left[N_\lambda(i) - N_\lambda^{\text{MC}}(i)\right]^2}{N_\lambda(i) + N_\lambda^{\text{MC}}(i)} + \sum_{j=1}^{n_{\text{bin}}} \frac{\left[N_\psi(j) - N_\psi^{\text{MC}}(j)\right]^2}{N_\psi(j) + N_\psi^{\text{MC}}(j)}$$

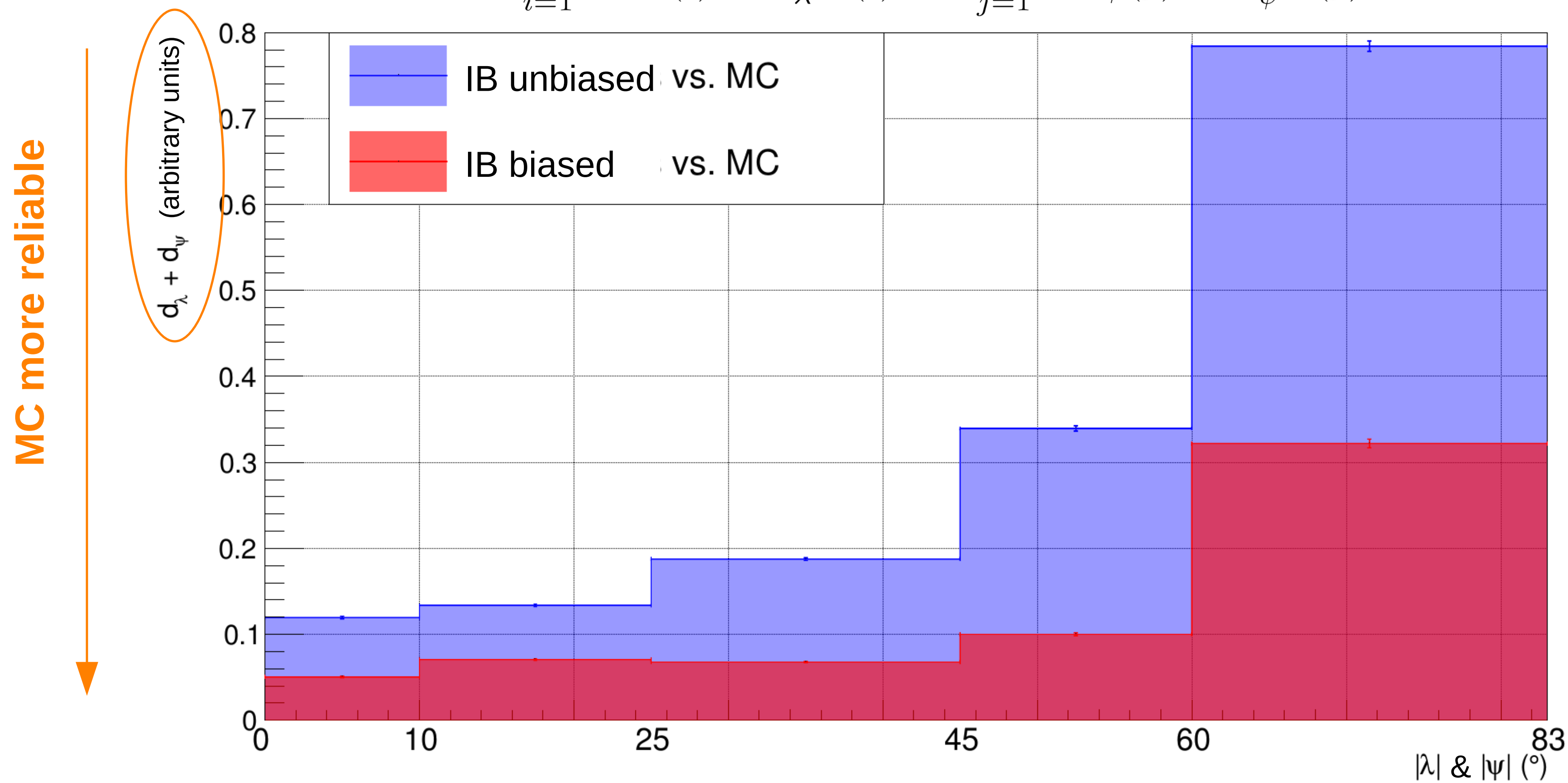

Real data vs simulated data

$$d_\lambda + d_\psi = \sum_{i=1}^{n_{\rm bin}} \frac{\left[N_\lambda(i) - N_\lambda^{\rm MC}(i)\right]^2}{N_\lambda(i) + N_\lambda^{\rm MC}(i)} + \sum_{j=1}^{n_{\rm bin}} \frac{\left[N_\psi(j) - N_\psi^{\rm MC}(j)\right]^2}{N_\psi(j) + N_\psi^{\rm MC}(j)}$$

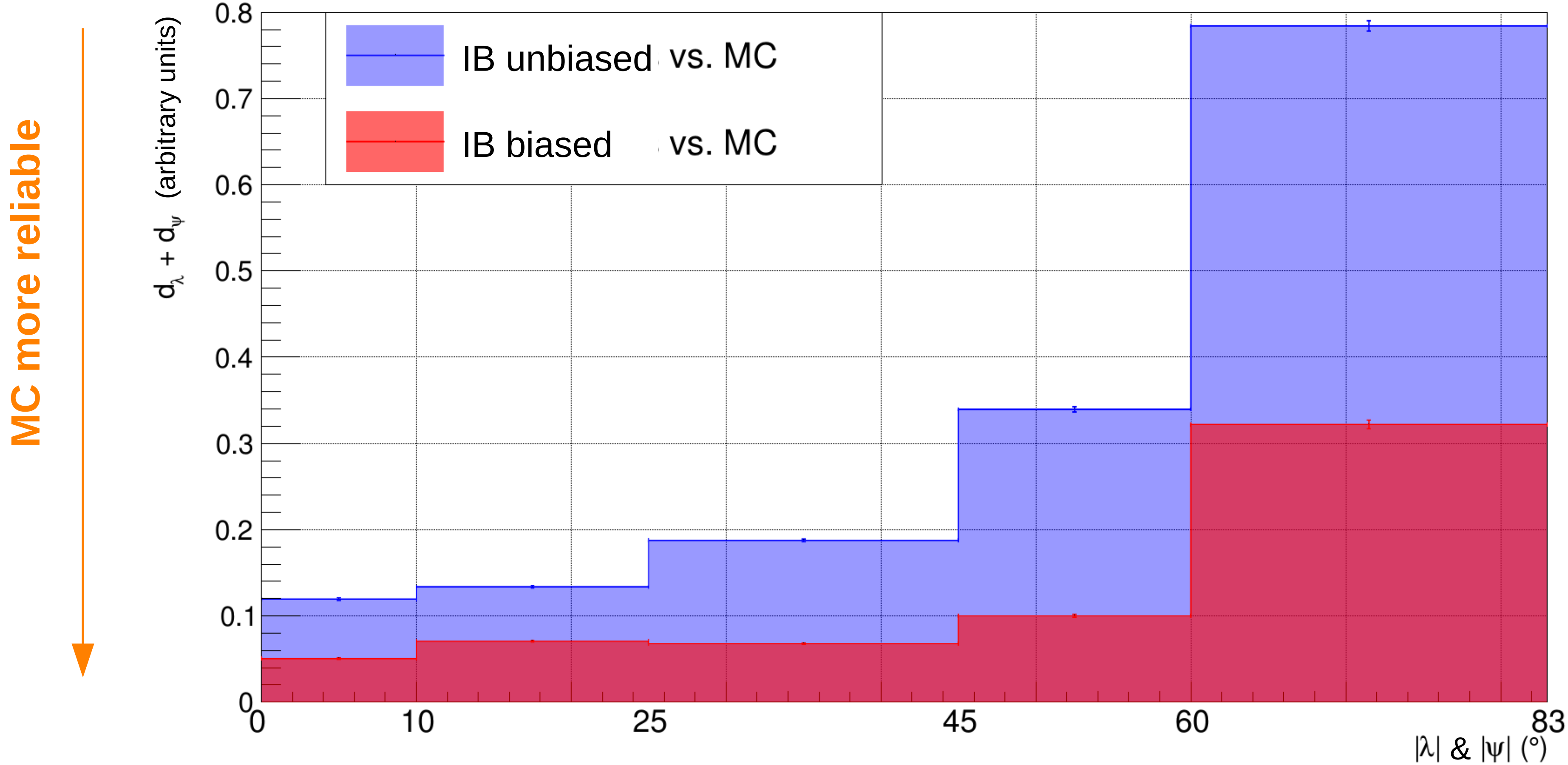

- MC better reproduces real biaised data than real unbiaised data

Real data vs simulated data

$$d_\lambda + d_\psi = \sum_{i=1}^{n_{\rm bin}} \frac{\left[N_\lambda(i) - N_\lambda^{\rm MC}(i)\right]^2}{N_\lambda(i) + N_\lambda^{\rm MC}(i)} + \sum_{j=1}^{n_{\rm bin}} \frac{\left[N_\psi(j) - N_\psi^{\rm MC}(j)\right]^2}{N_\psi(j) + N_\psi^{\rm MC}(j)}$$

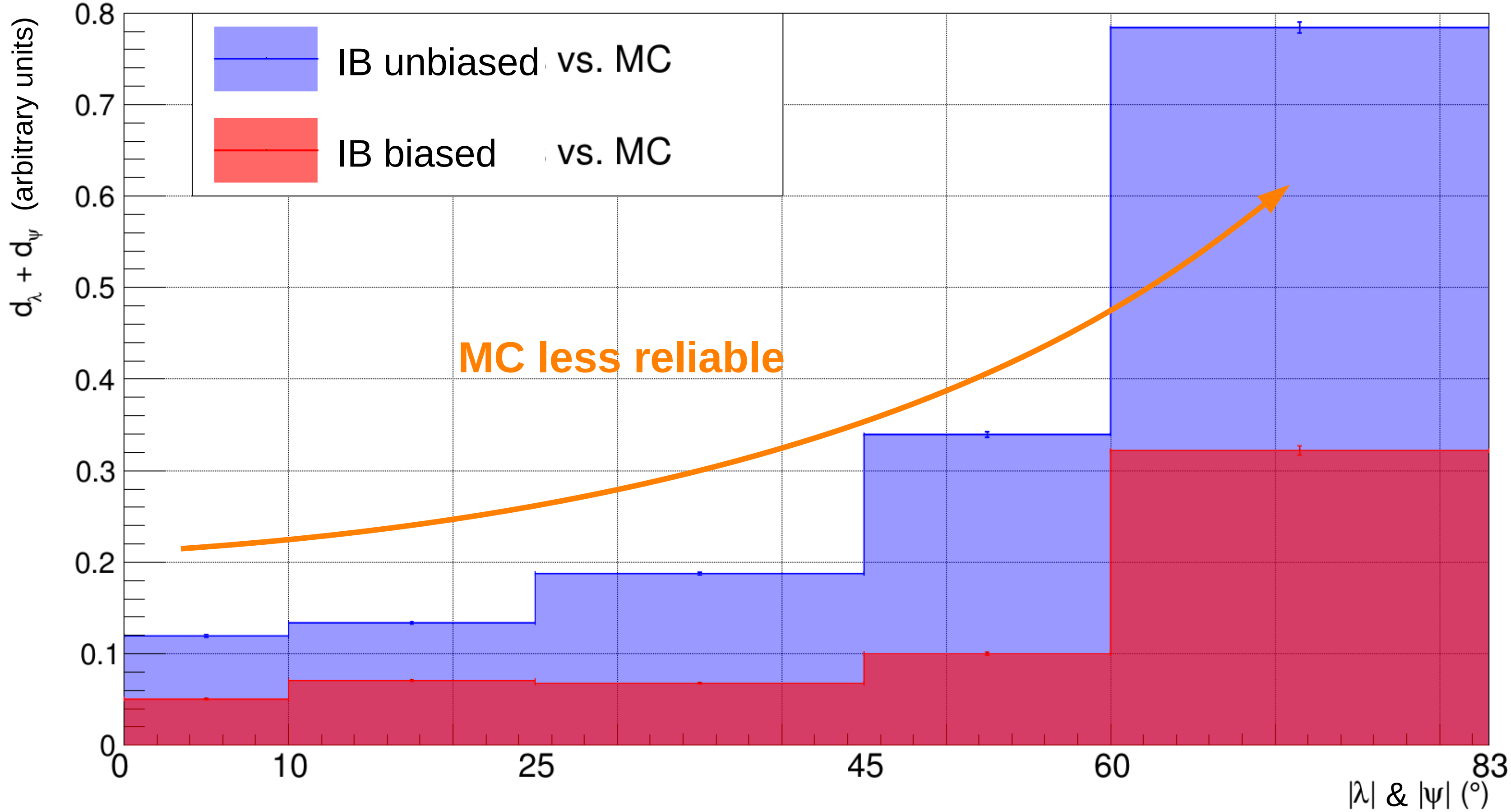

- Differences between MC and real data rise when inclination increases

Real data vs simulated data

$$d_\lambda + d_\psi = \sum_{i=1}^{n_{\mathrm{bin}}} \frac{\left[N_\lambda(i) - N_\lambda^{\mathrm{MC}}(i)\right]^2}{N_\lambda(i) + N_\lambda^{\mathrm{MC}}(i)} + \sum_{j=1}^{n_{\mathrm{bin}}} \frac{\left[N_\psi(j) - N_\psi^{\mathrm{MC}}(j)\right]^2}{N_\psi(j) + N_\psi^{\mathrm{MC}}(j)}$$

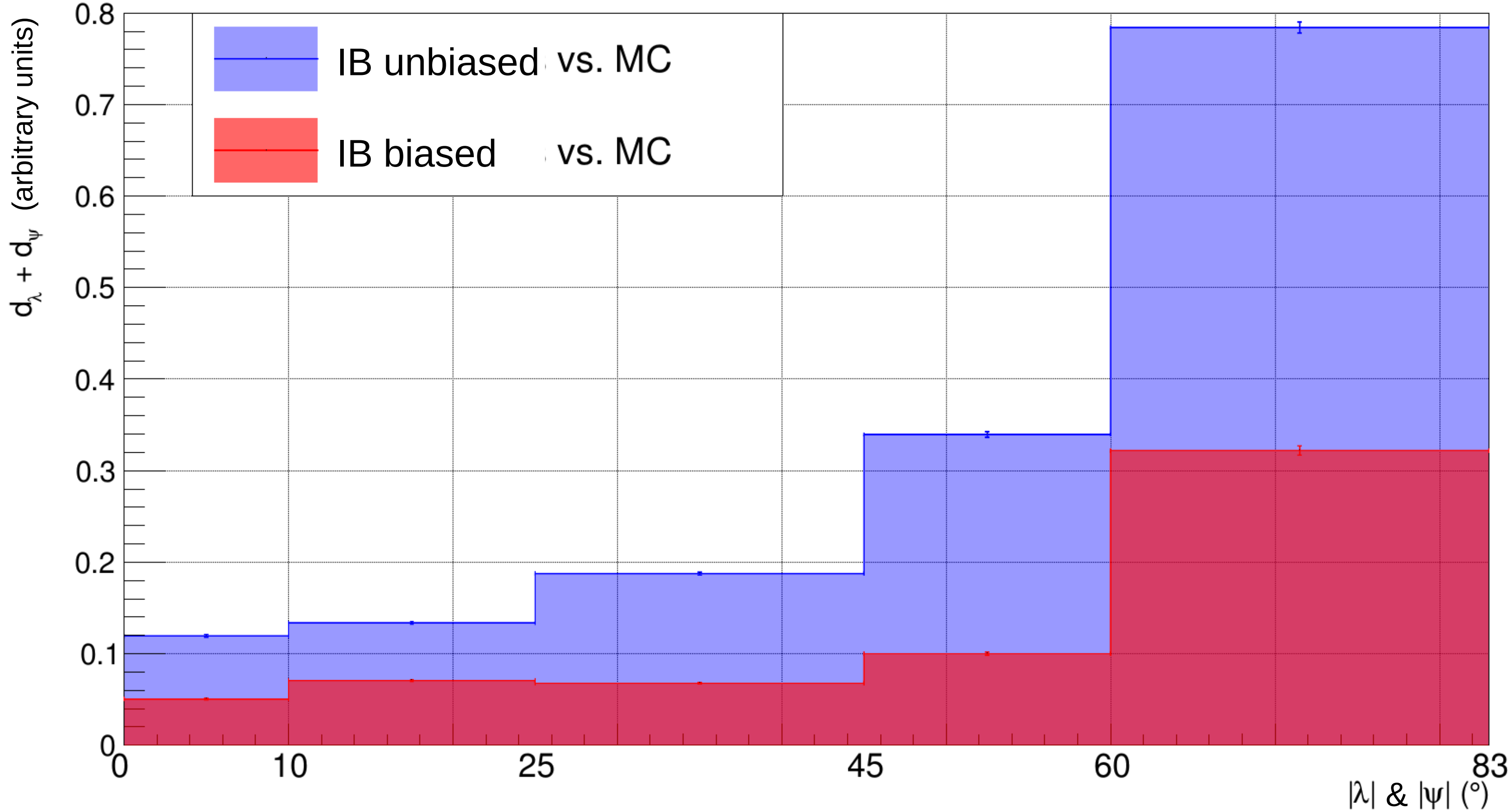

→ **improve the Monte-Carlo code**

Conclusions

- Suppression of background noise (noise map)

  + selection of track candidates

- Cluster shape analysis as a function of track inclination
  - will **help the tracking algorithm**
- Monte-Carlo simulation and comparison with real data
  - calls for **improvements of the Monte-Carlo code**

Conclusions

- Suppression of background noise (noise map)

  + track candidates selection

- Cluster shape analysis as a function of track inclination
  - will **help the tracking algorithm**
- Monte-Carlo simulation and comparison with real data
  - calls for **improvements of the Monte-Carlo code**

next step

Bias has to evolve through time
→ work in progress in the MC code

Motivations

Study Ξ_b^- (d s b)

→ production cross section in pp and Pb-Pb collisions to constrain theoretical models

Decay channel studied:

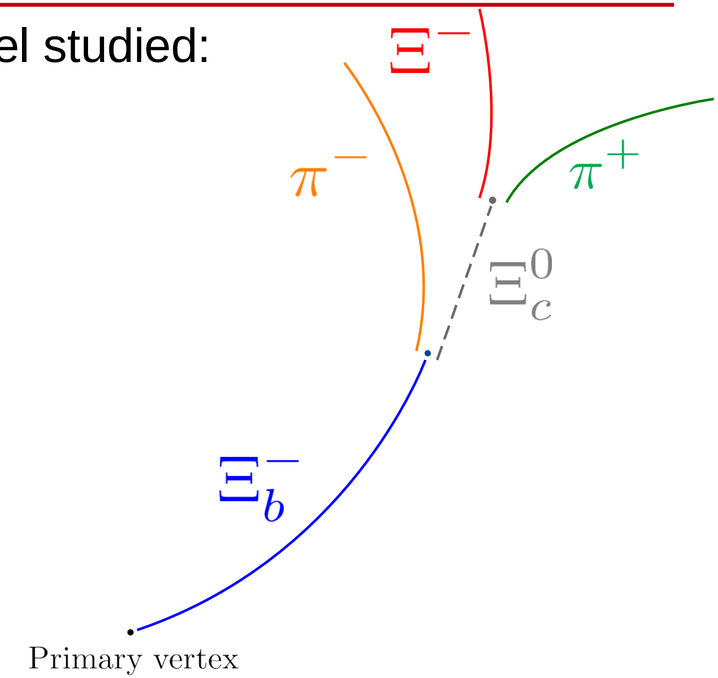

ALICE 1 unable to efficiently reconstruct this channel

upgrades needed

Ξ_c^0 ← ALICE Run 3 (2022) **Cluster shape analysis**

(Master 2 project)

Ξ_b^- → ALICE 3 (~ 2030) **Strangeness tracking**

(CERN Summer School project)

Motivations

Study Ξ_b^- (d s b)

→ production cross section in pp and Pb-Pb collisions to constrain theoretical models

Decay channel studied:

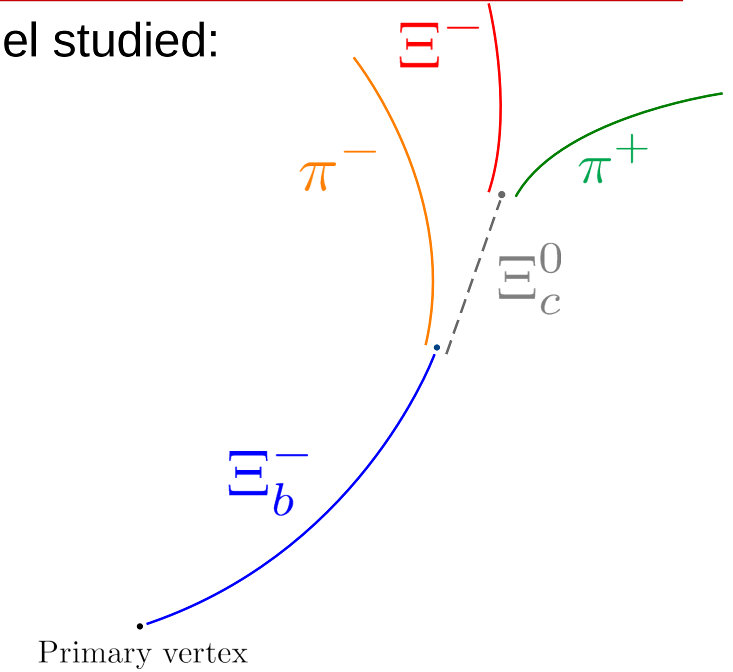

ALICE 1 unable to efficiently reconstruct this channel

upgrades needed

ALICE Run 3 (2022)
Cluster shape analysis
(Master 2 project)

ALICE 3 (~ 2030)
Strangeness tracking
(CERN Summer School project)

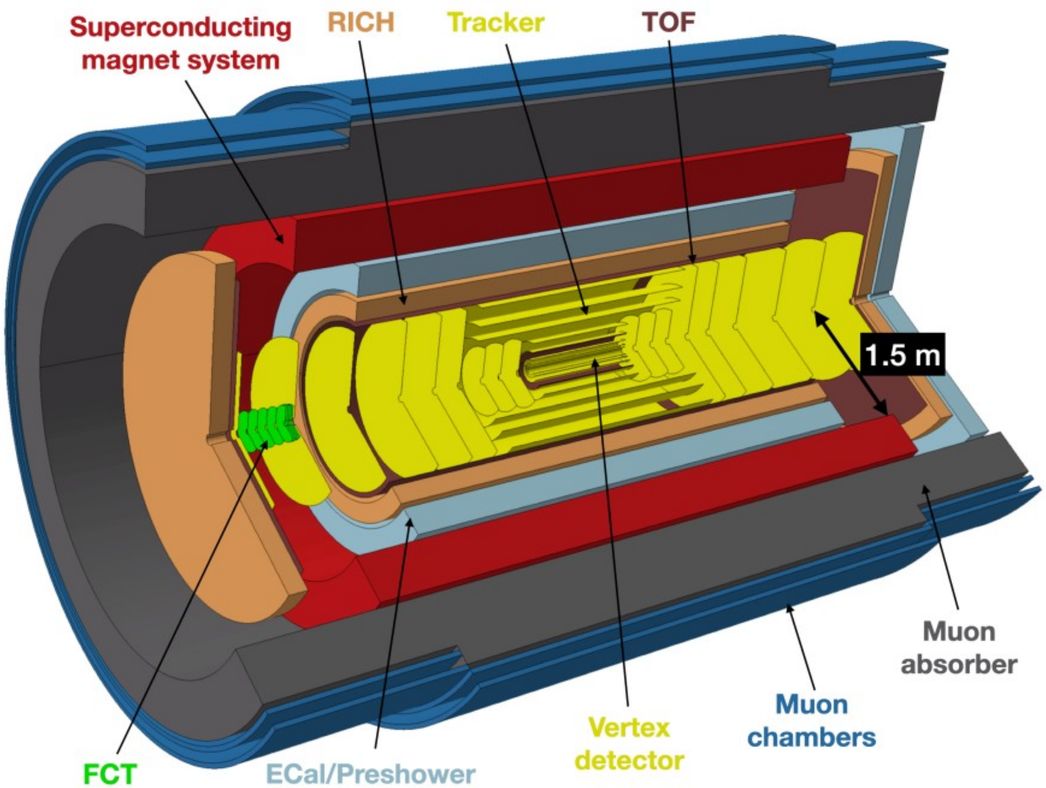

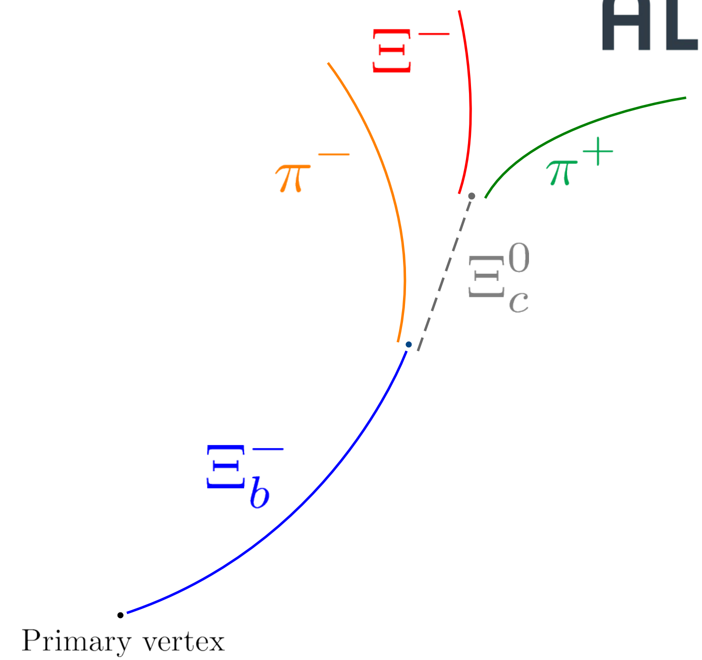

Strangeness tracking in ALICE 3:

Study of $\Xi_b^- \rightarrow (\Xi_c^0 \rightarrow \Xi^- \pi^+)\pi^-$

under the supervision of D.CHINELLATO & M.CONCAS

Strangeness tracking: example of Ξ^-

ALICE

detected before its decay

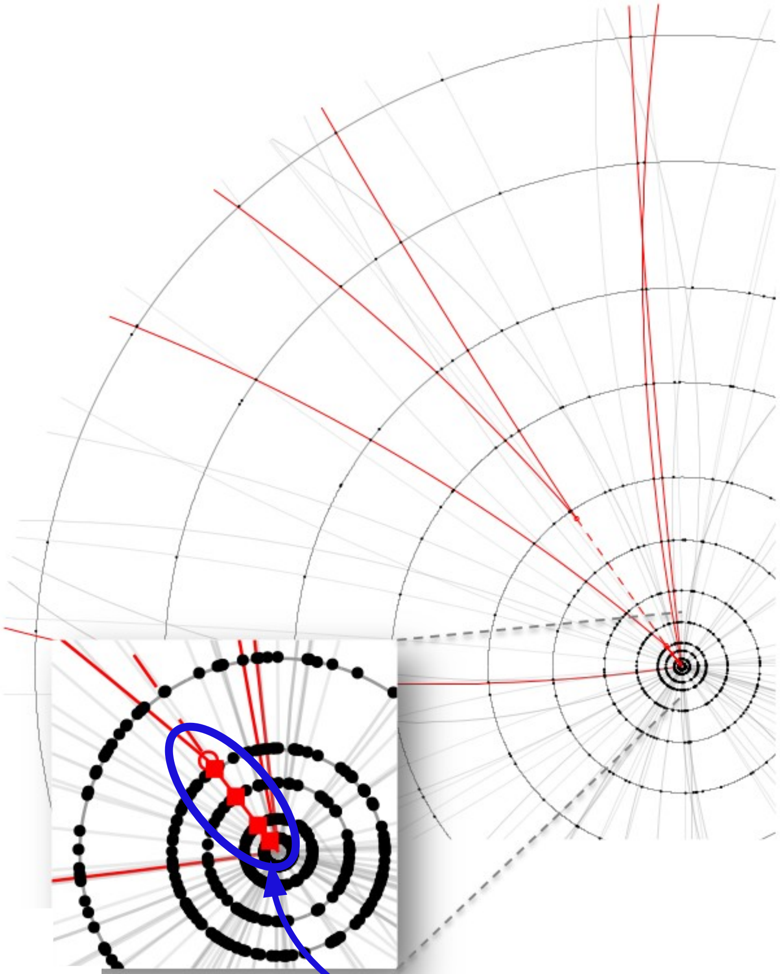

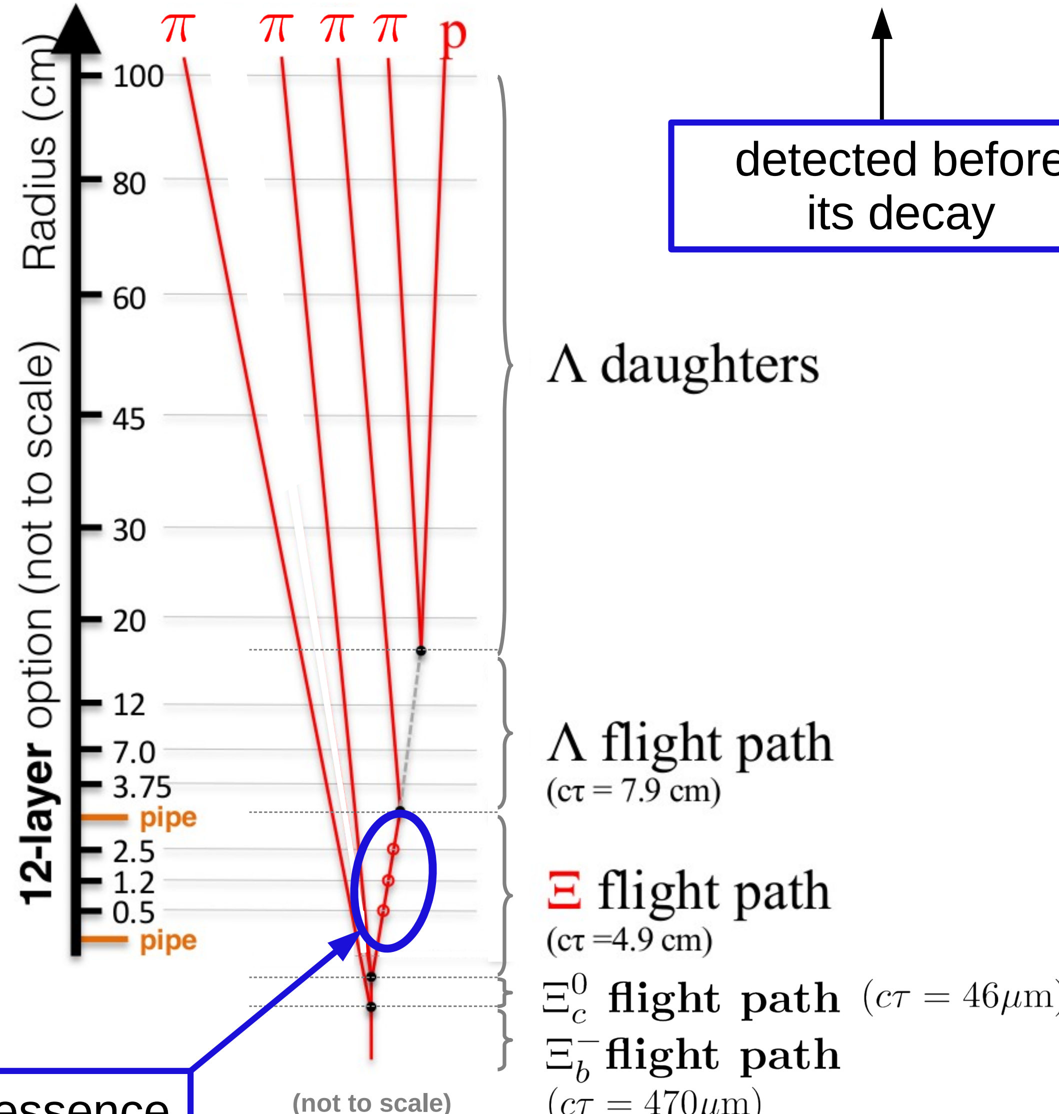

These hits are the essence of strangeness tracking !

Adapted from D. Chinellato

Motivations

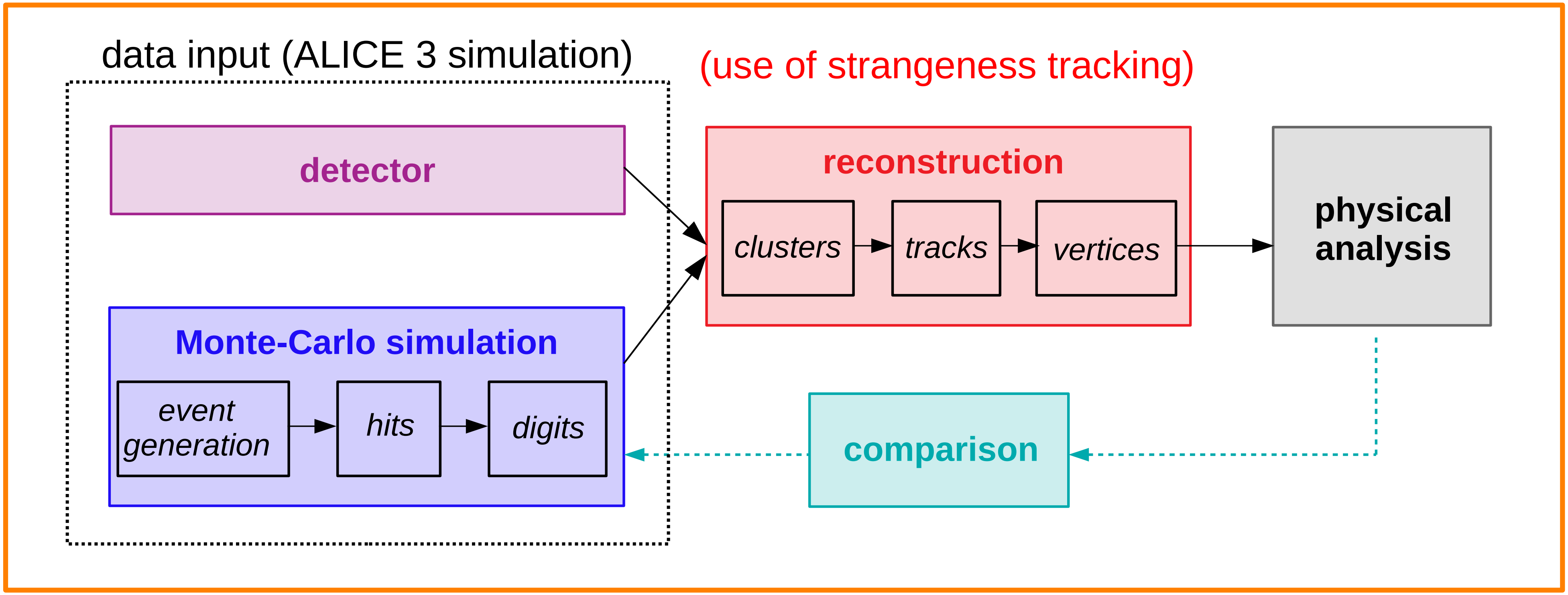

Goal: analysis prototype using a state-of-the-art detector (ALICE 3)

The ultimate goal: study the evolution of the ***b*** quark through QGP

Simulating collisions

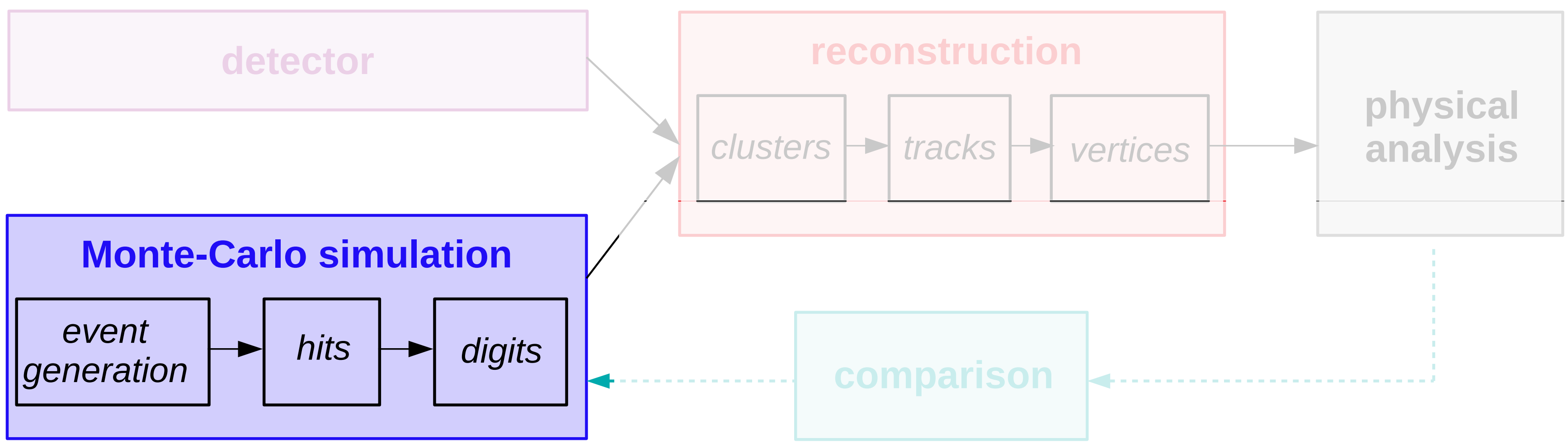

- New ALICE software: Online/Offline (O2)
- 1 minimum bias Pythia event (up to 1 particle of interest), pp collision @ 13 TeV
- GEANT3 propagator
- Simulating hits: TRK geometry (beam pipe+ALICE3)

Simulating collisions

Name	mass (GeV/c^2)
Ξ_b^- (dsb)	5.797

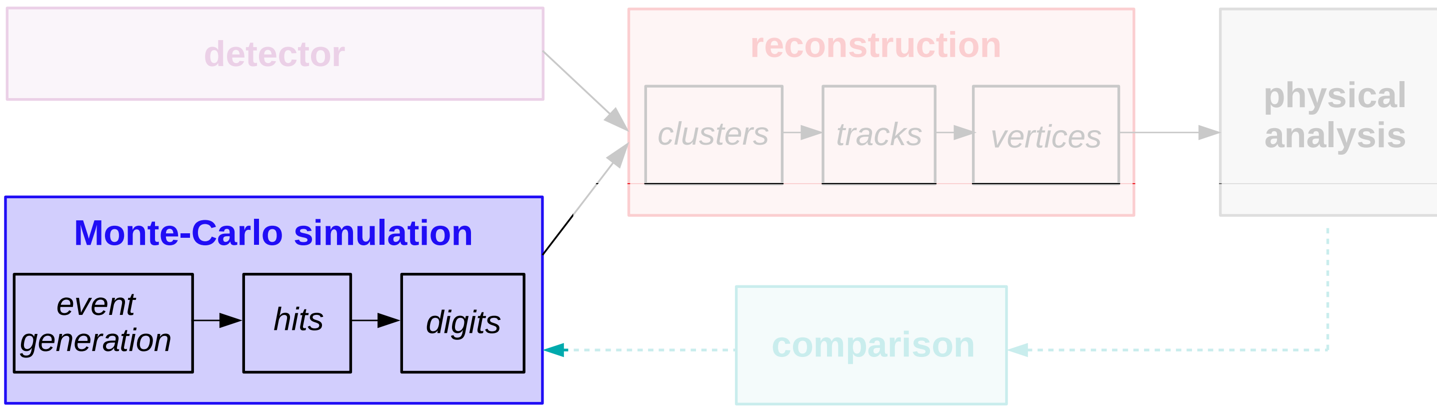

Ξ_b^-

Generation of the particle of interest

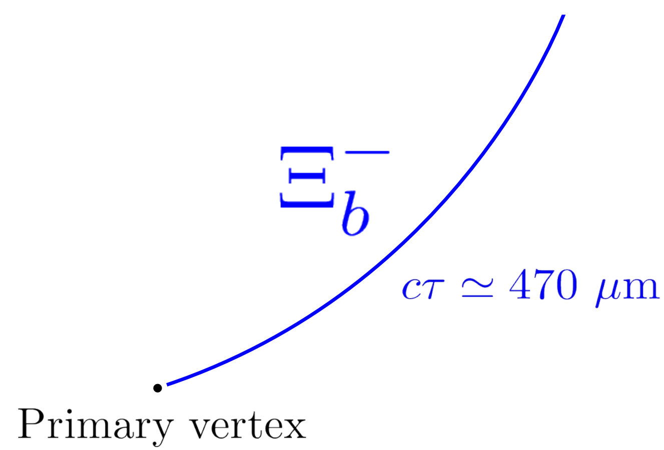

Simulating collisions

Name	mass (GeV/c^2)
Ξ_b^- (dsb)	5.797
Ξ_c^0 (dsc)	2.470
Ξ^- (dss)	1.3217
π^- ($\bar{u}$d)	0.139
π^+ (u$\bar{d}$)	0.139

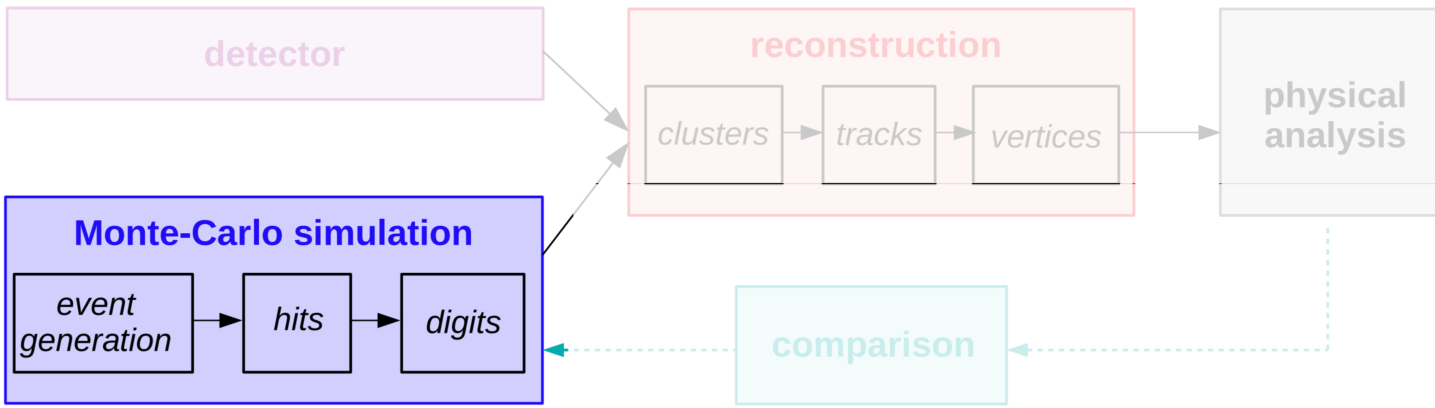

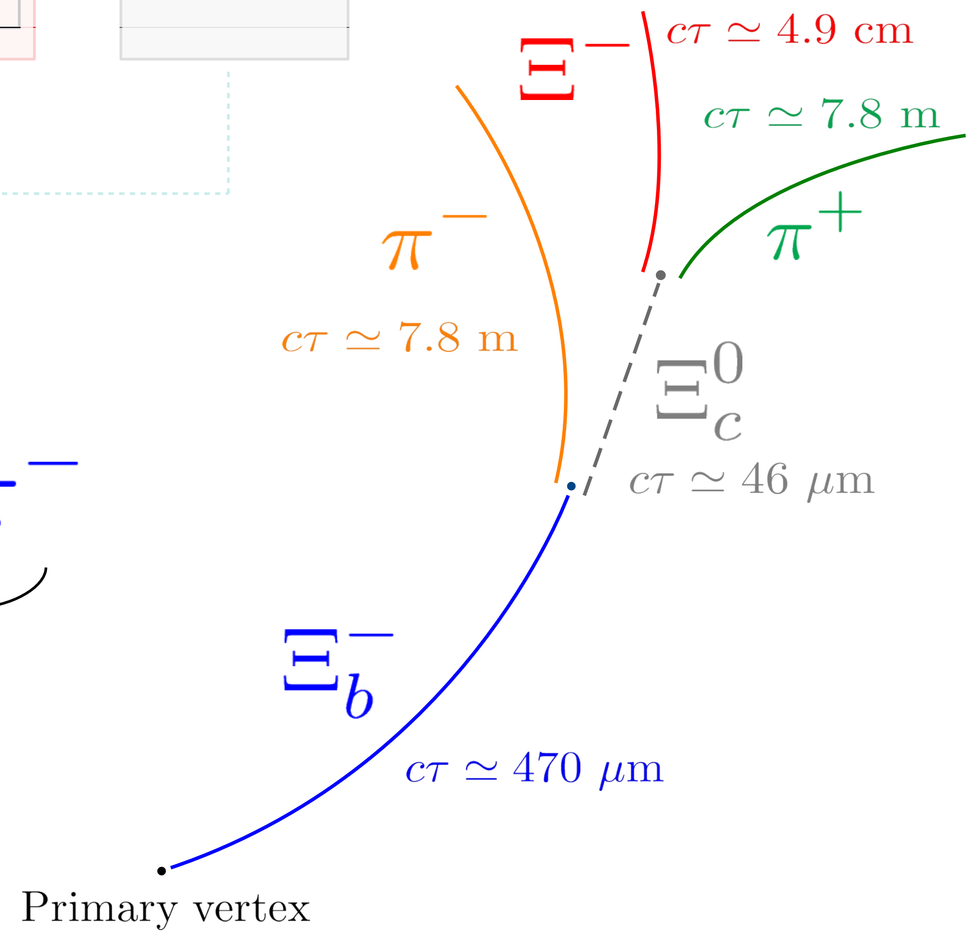

$$\Xi_b^- \rightarrow (\Xi_c^0 \rightarrow \Xi^- \pi^+)\pi^-$$

Generation of the particle of interest (Ξ_b^-)

Imposed decay channel ($\rightarrow (\Xi_c^0 \rightarrow \Xi^- \pi^+)\pi^-$)

Simulating collisions

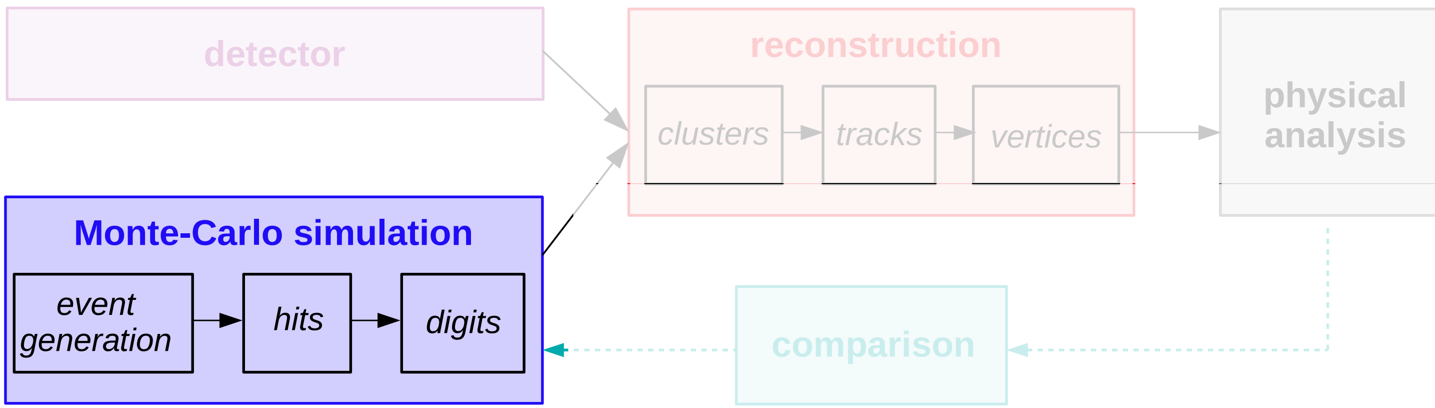

$$\Xi_b^- \to (\Xi_c^0 \to \Xi^- \pi^+)\pi^-$$

Generation of the particle of interest

Imposed decay channel

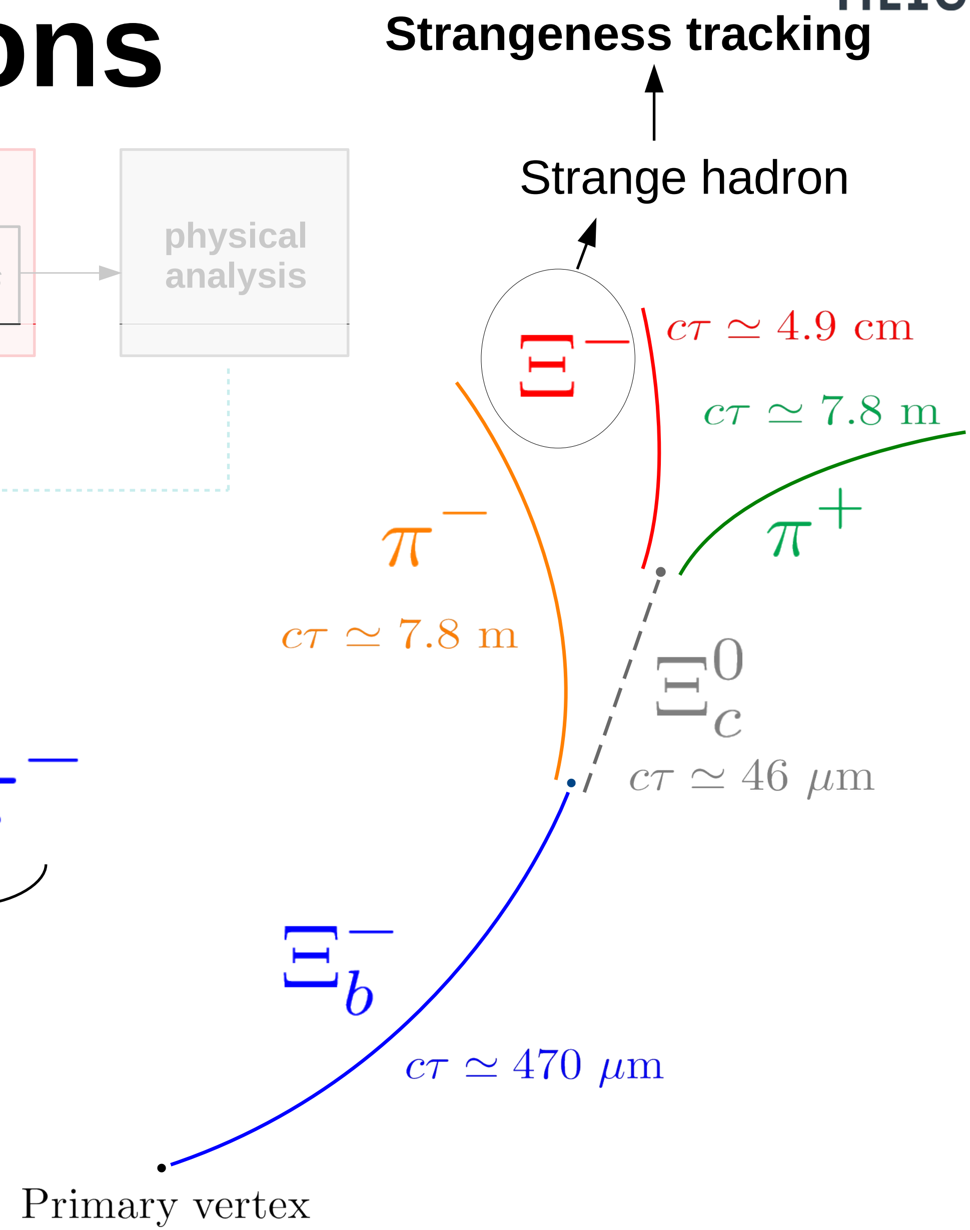

Reconstruction

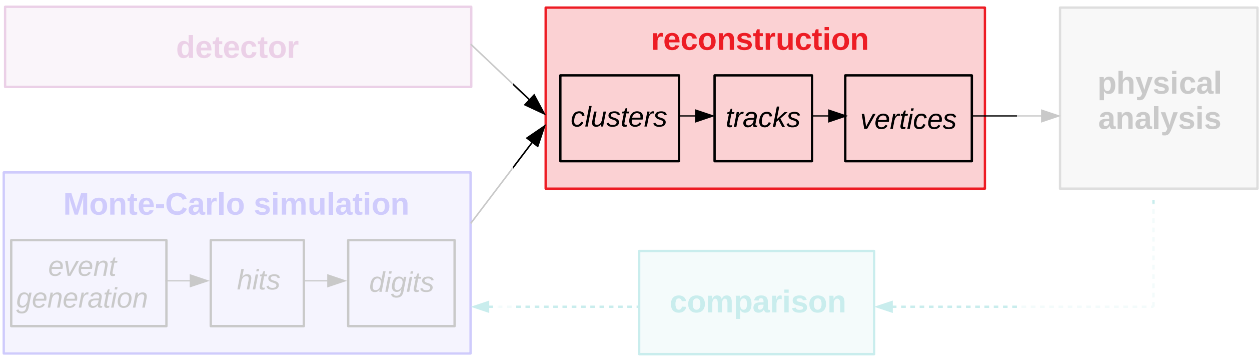

$$\Xi_b^- \to (\Xi_c^0 \to \Xi^- \pi^+)\pi^-$$

Name	mass (GeV/c^2)
Ξ_b^- (dsb)	5.797
Ξ_c^0 (dsc)	2.470
Ξ^- (dss)	1.3217
π^- ($\bar{u}$d)	0.139
π^+ (u$\bar{d}$)	0.139

Reconstruction

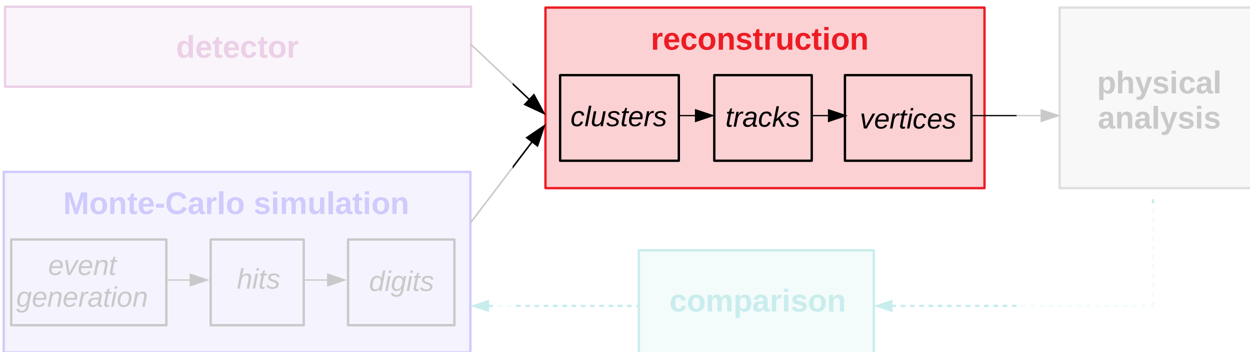

carries the benefits of strangeness tracking

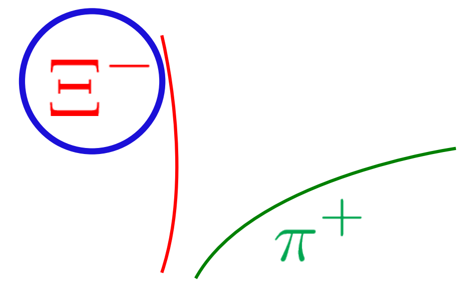

$$\Xi_b^- \rightarrow (\Xi_c^0 \rightarrow \Xi^- \pi^+)\pi^-$$

Name	mass (GeV/c^2)
Ξ_b^- (dsb)	5.797
Ξ_c^0 (dsc)	2.470
Ξ^- (dss)	1.3217
π^- ($\bar{\text{u}}$d)	0.139
π^+ (u$\bar{\text{d}}$)	0.139

Primary vertex

Reconstruction

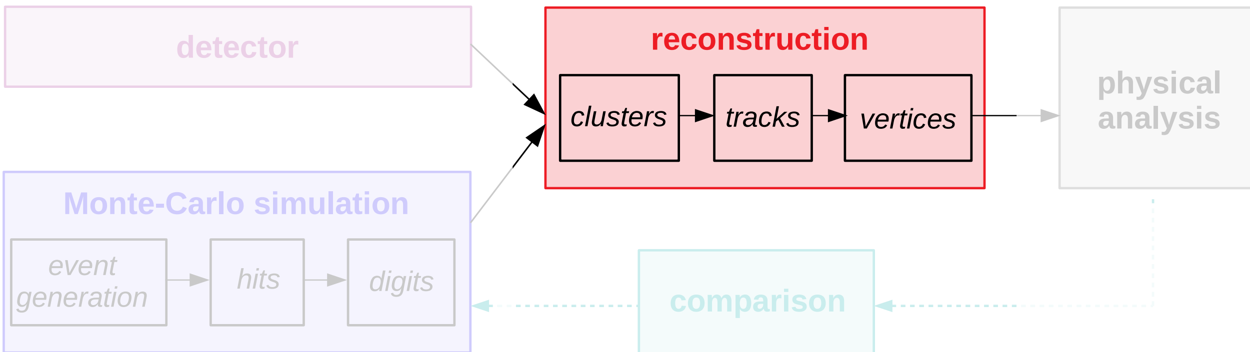

$$\Xi_b^- \rightarrow (\Xi_c^0 \rightarrow \Xi^- \pi^+)\pi^-$$

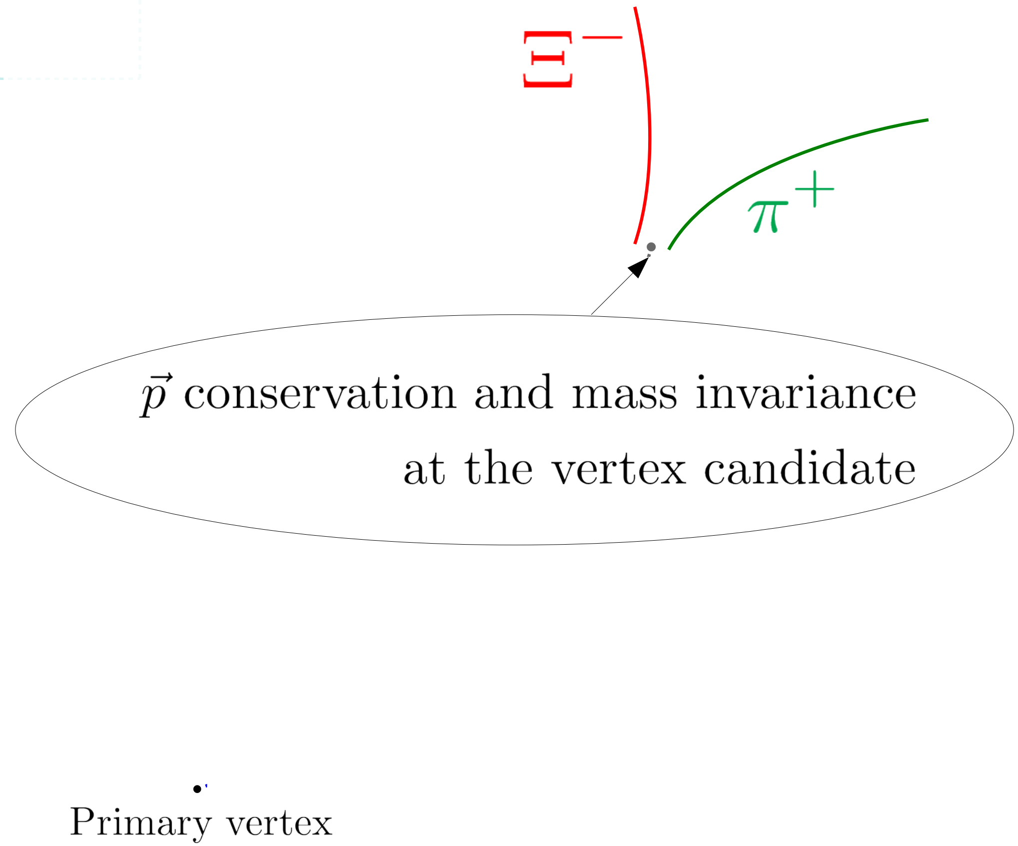

Name	mass (GeV/c^2)
Ξ_b^- (dsb)	5.797
Ξ_c^0 (dsc)	2.470
Ξ^- (dss)	1.3217
π^- ($\bar{u}$d)	0.139
π^+ (u$\bar{d}$)	0.139

Reconstruction

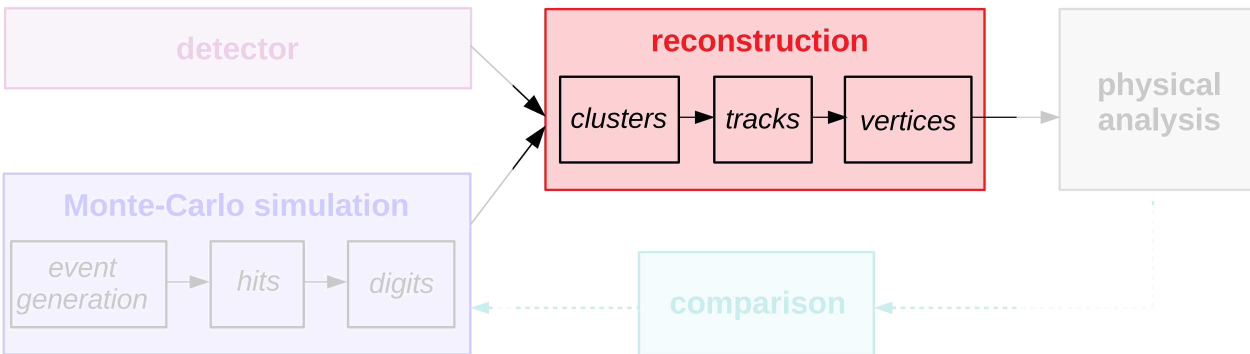

$$\Xi_b^- \to (\Xi_c^0 \to \Xi^- \pi^+)\pi^-$$

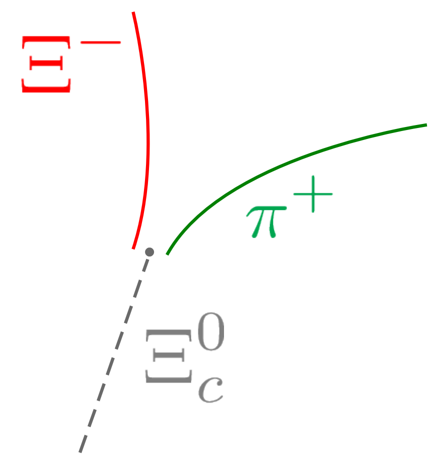

Name	mass (GeV/c^2)
Ξ_b^- (dsb)	5.797
Ξ_c^0 (dsc)	2.470
Ξ^- (dss)	1.3217
π^- ($\bar{u}$d)	0.139
π^+ (u$\bar{d}$)	0.139

Primary vertex

Reconstruction

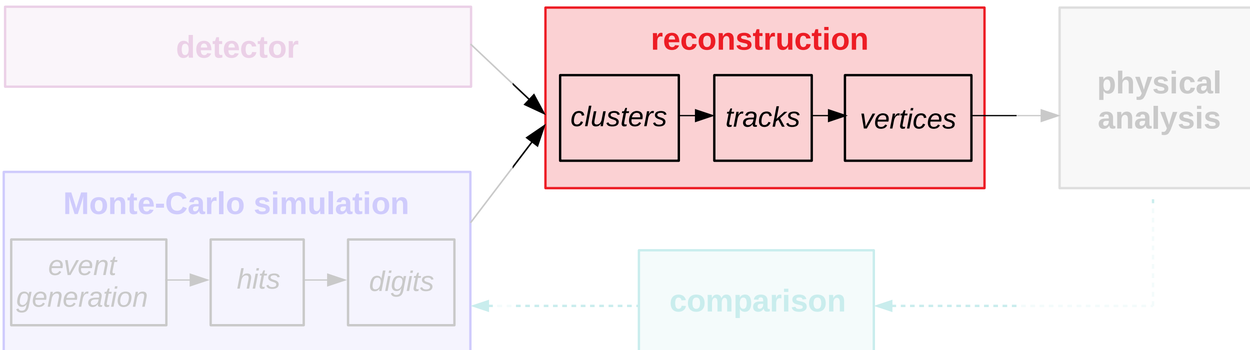

$$\Xi_b^- \rightarrow (\Xi_c^0 \rightarrow \Xi^- \pi^+)\pi^-$$

Name	mass (GeV/c^2)
Ξ_b^- (dsb)	5.797
Ξ_c^0 (dsc)	2.470
Ξ^- (dss)	1.3217
π^- ($\bar{u}$d)	0.139
π^+ (u$\bar{d}$)	0.139

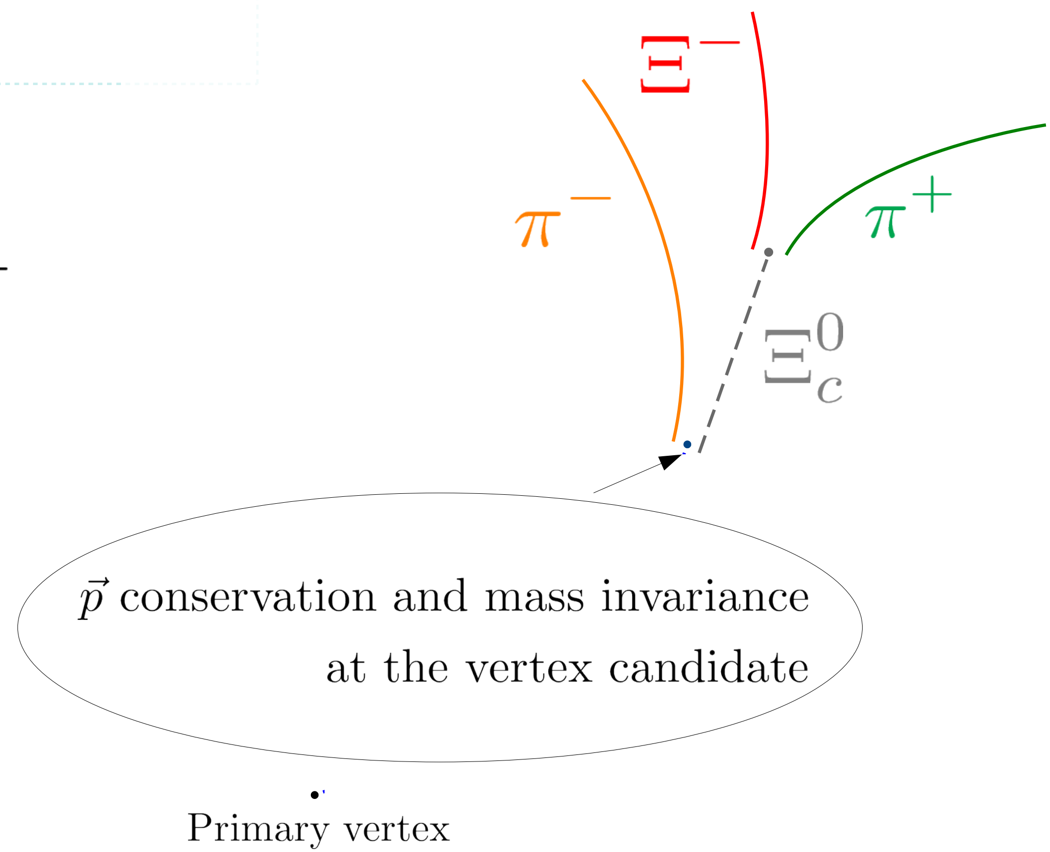

Reconstruction

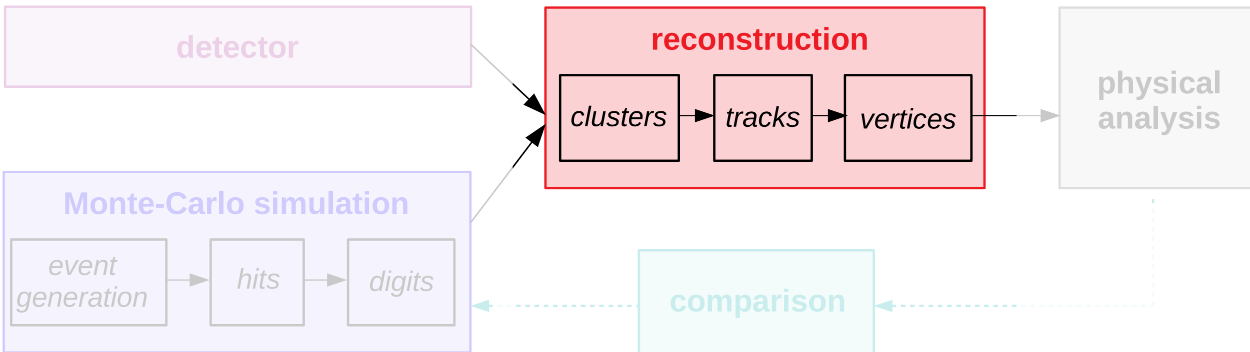

$$\Xi_b^- \rightarrow (\Xi_c^0 \rightarrow \Xi^- \pi^+)\pi^-$$

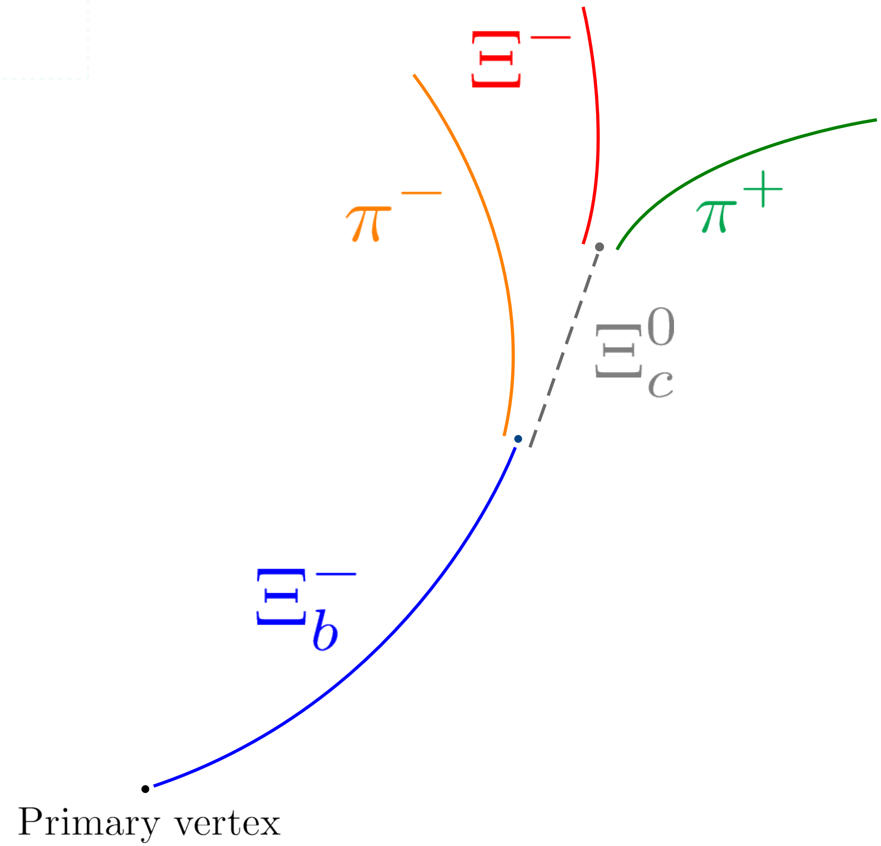

Name	mass (GeV/c^2)
Ξ_b^- (dsb)	5.797
Ξ_c^0 (dsc)	2.470
Ξ^- (dss)	1.3217
π^- ($\bar{u}$d)	0.139
π^+ (u$\bar{d}$)	0.139

repeat it for more than 2M events

Topological observables

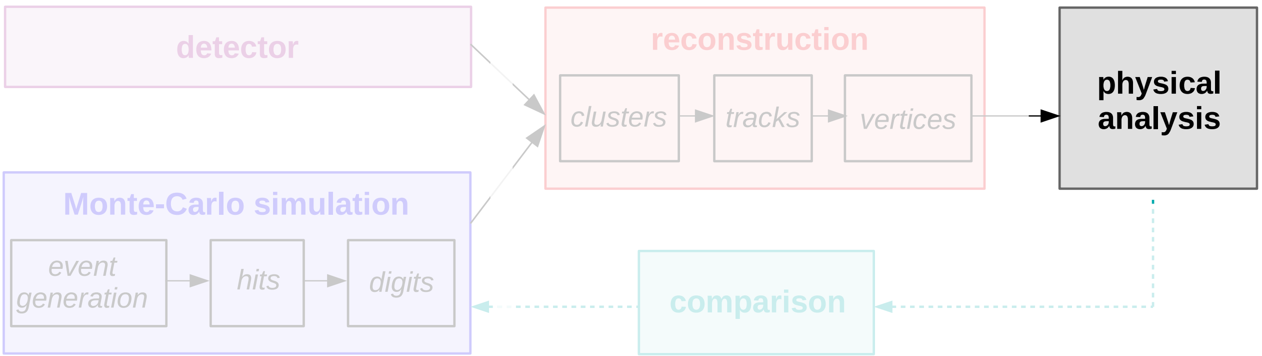

$$\Xi_b^- \rightarrow (\Xi_c^0 \rightarrow \Xi^- \pi^+)\pi^-$$

Here we study 2 observables:

- **Decay radius**

  ~ Distance between primary vertex and decay

  (in the transverse plane)

- **DCA** to primary vertex

  DCA: Distance of Closest Approach

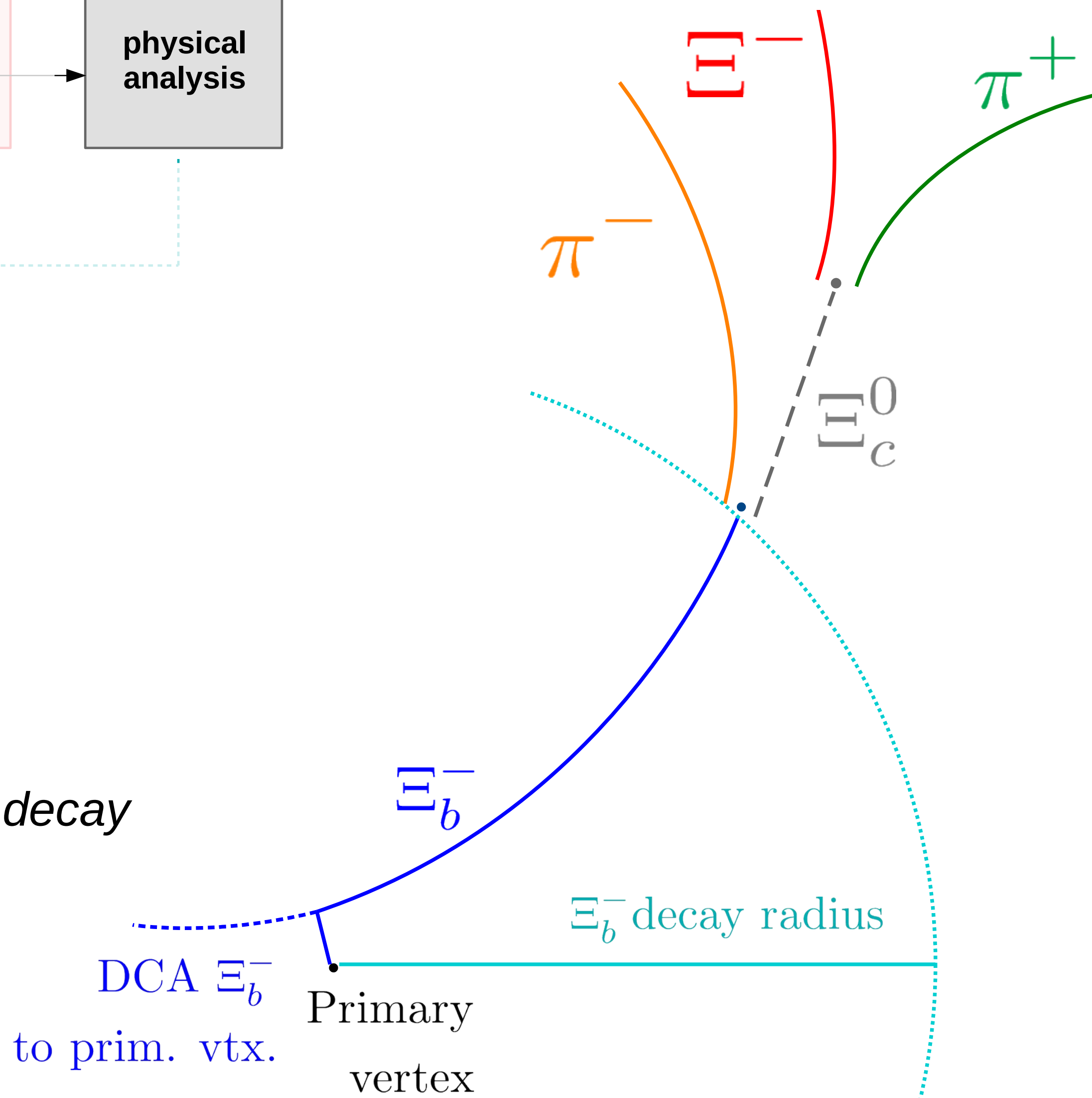

Strangeness tracking usability

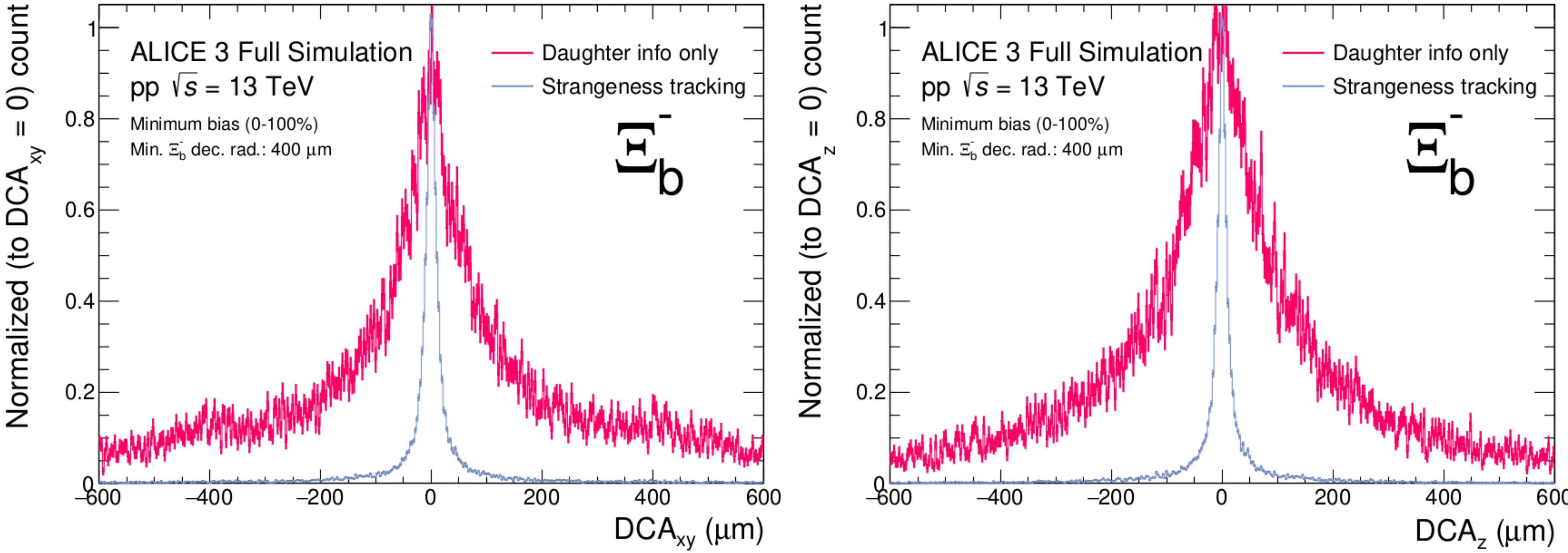

Improvement in DCA resolution by strangeness tracking

Strangeness tracking on Ξ^- → reduces combinatorial background

Background: generation of primary Ξ_c^0 instead of Ξ_b^- and no decay channel imposed

ALICE

Topological cuts

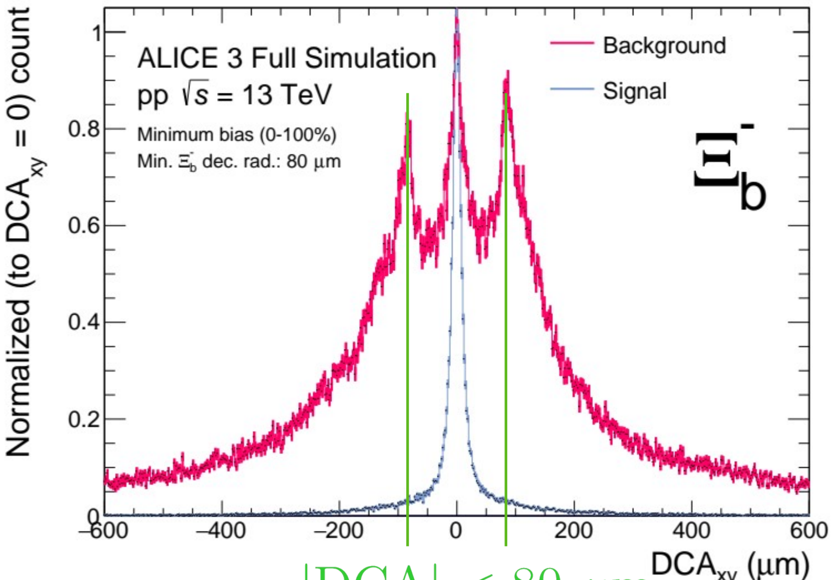

$|\mathrm{DCA}| < 80\ \mu m$

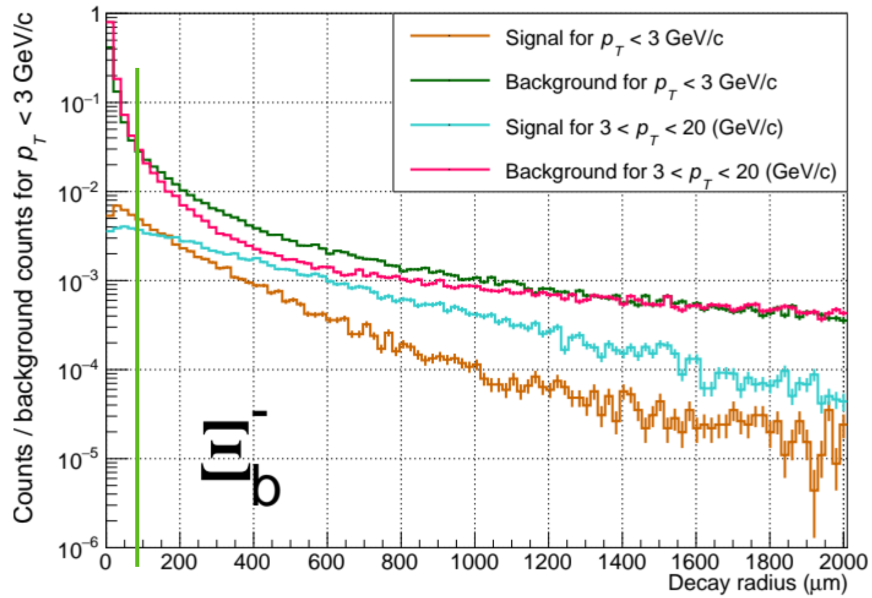

decay rad. $> 80\ \mu m$

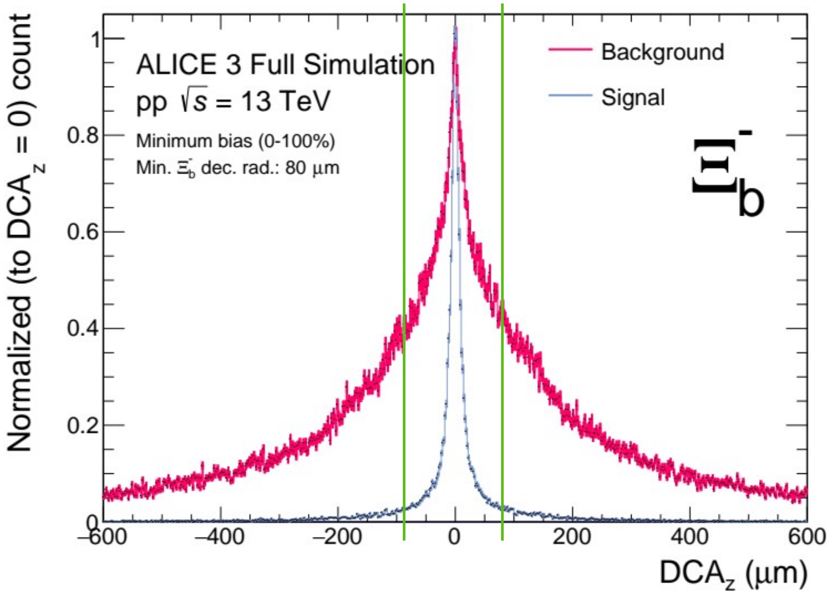

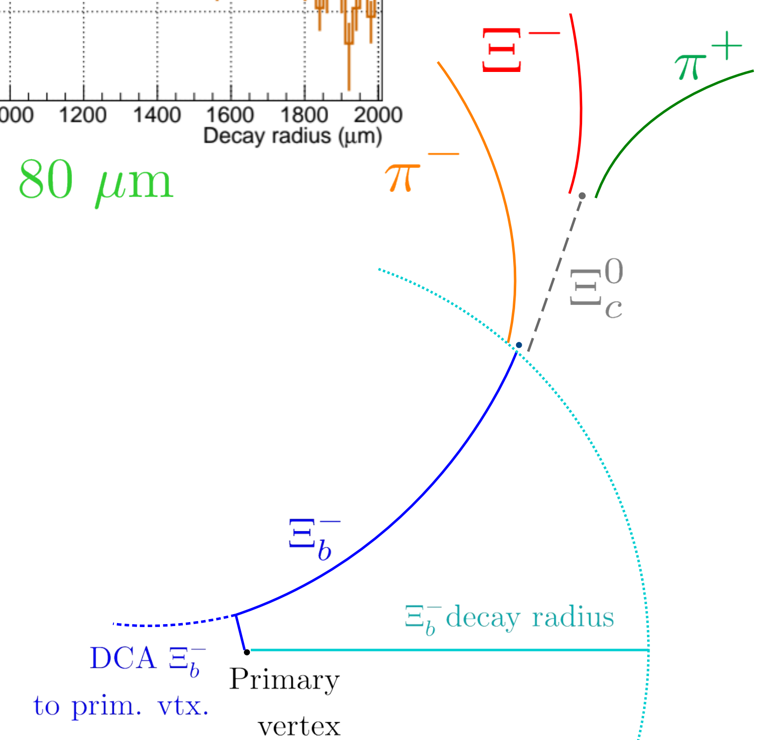

Main result

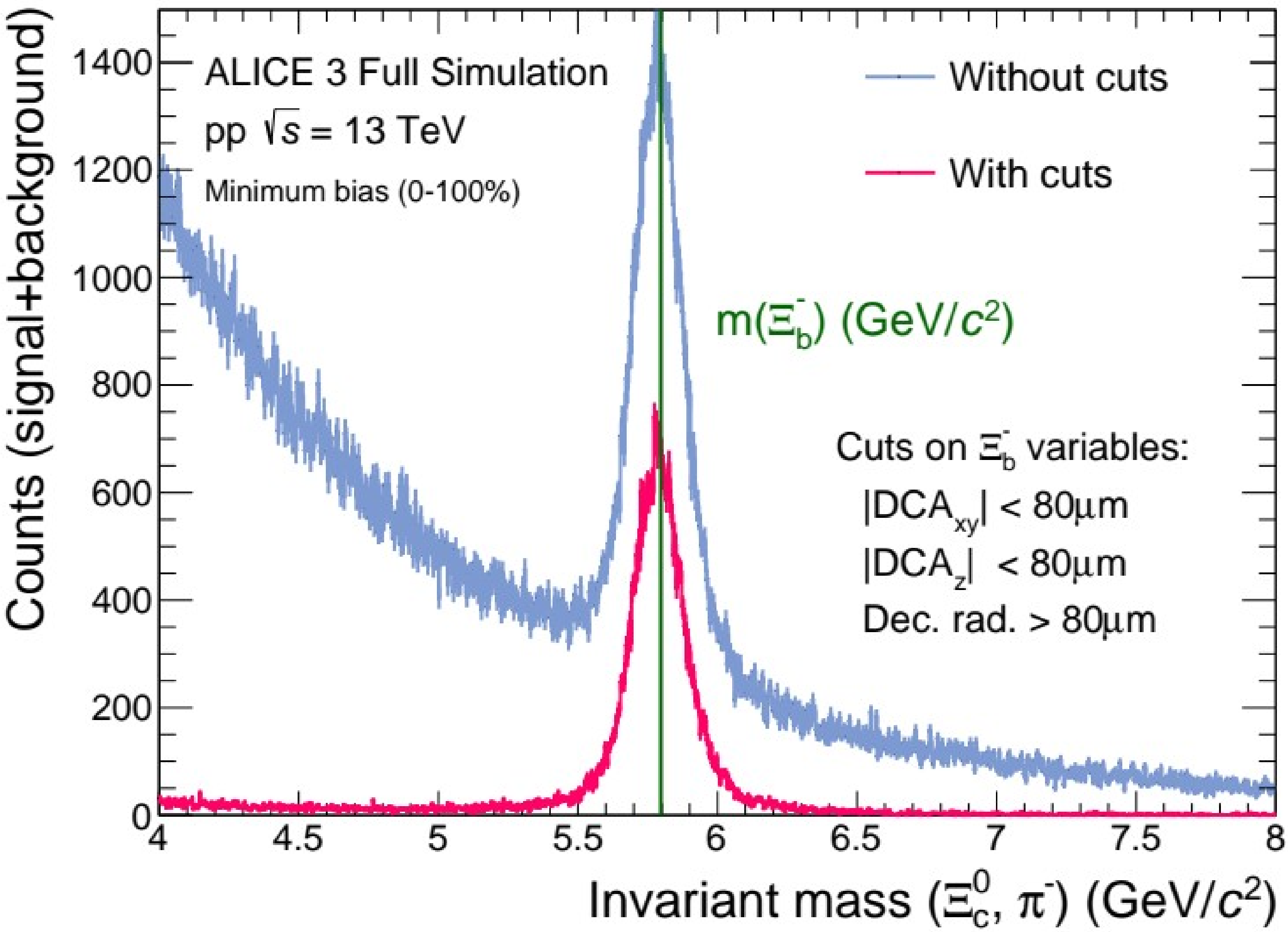

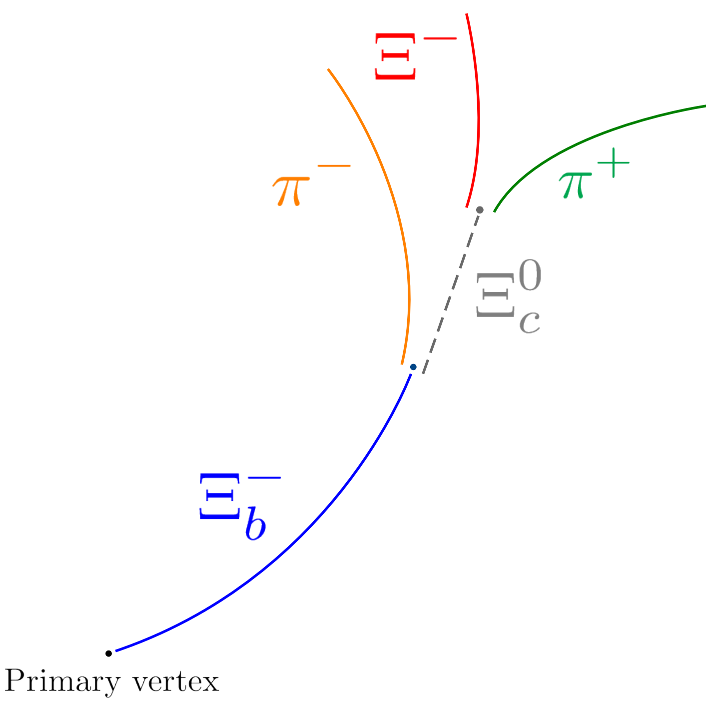

Majority of background is reduced → **functional analysis prototype**

Global conclusions

- 2 different studies:
  - Cluster shape analysis → **improvement of MC**
  - Strangeness tracking → **viable analysis prototype** offering efficiency and precision in the reconstruction procedure → **towards production cross section**

ALICE 3 Letter of Intent
https://cds.cern.ch/record/2803563

- Preparing the field to study interaction of *b* quark with QGP

→ future ALICE data (run 3 of LHC starting in June)

PhD subject

Study of open beauty production in the ALICE detector at LHC

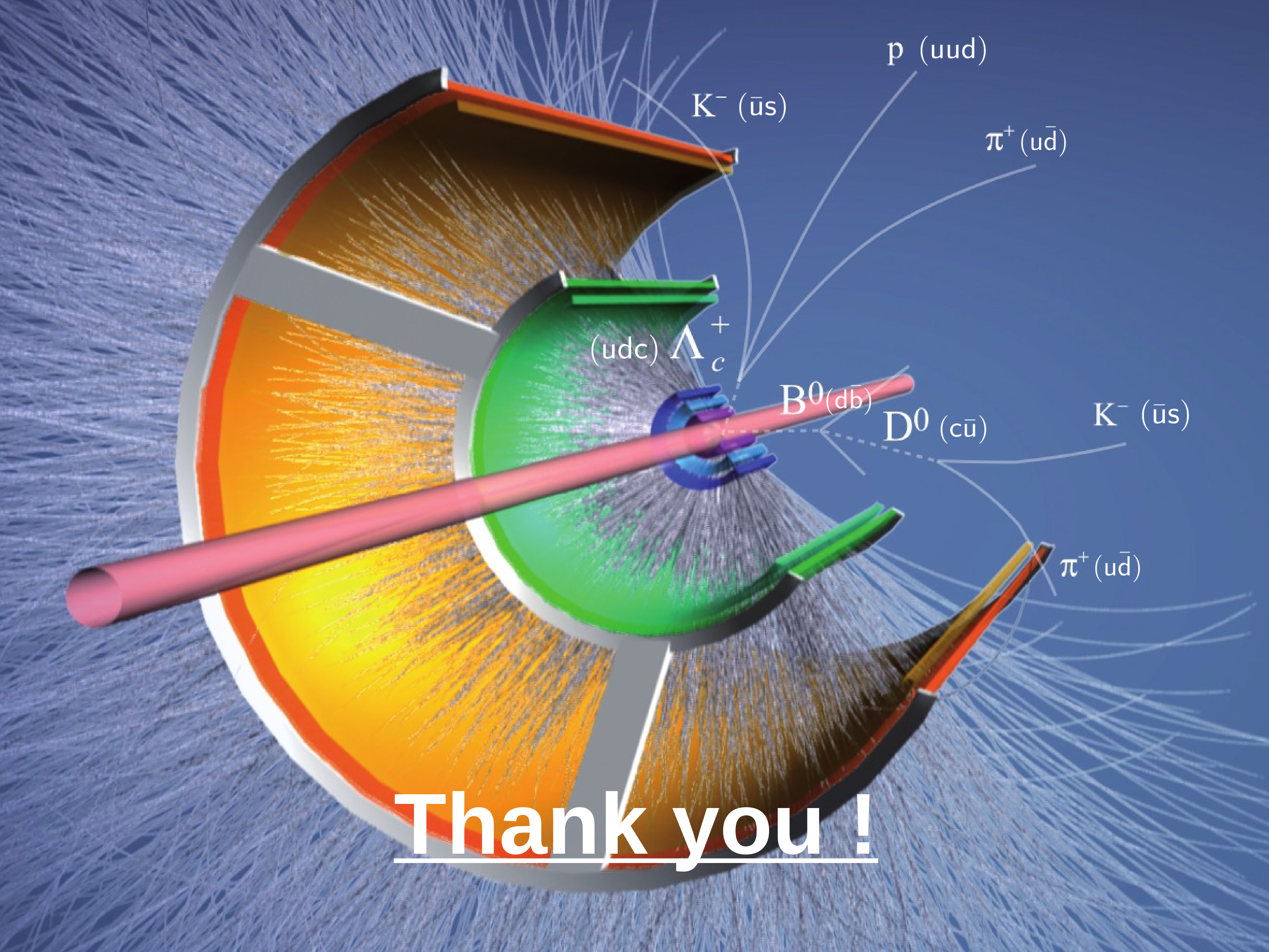
p (uud)
K^- ($\bar{u}s$)
π^+ ($u\bar{d}$)
(udc) Λ_c^+
B^0($d\bar{b}$)
D^0 ($c\bar{u}$)
K^- ($\bar{u}s$)
π^+ ($u\bar{d}$)
Thank you !

Backup
Stage Master 2

Elongation due to pixels geometry

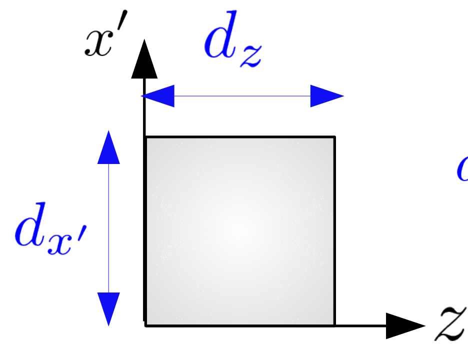

$d_z = 29,24\ \mu\text{m}$

$d_{x'} = 26,88\ \mu\text{m}$

$$\frac{d_{x'}}{d_z} \sim 90\% \quad \overset{?}{\Rightarrow} \quad (\lambda = \psi \simeq 0^\circ)$$

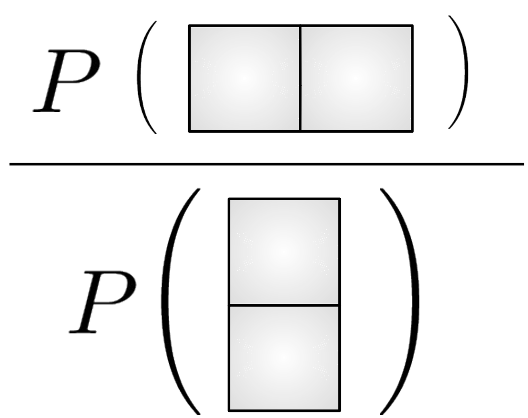

$\sim 0,9$

Backup for I)

Some figures

- ITS:
  - Active surface ~10 m² (75% on the last 2 layers)
  - ~12G pixels
  - up to ~200 kHz

→ gigantic camera
(up to 200 000 photographs per second)

- Commissioning of the ITS (Nov.2019-Dec.2020):
  - ~1 day for the Outer Barrel (@11 kHz) → ~1G triggers
  - ~7 days for the Inner Barrel (@44 kHz) → ~25G triggers

Some figures

Table 1.1: Geometrical parameters of the upgraded ITS.

	Inner Barrel			Outer Barrel			
	Inner Layers			Middle Layers		Outer Layers	
	Layer 0	Layer 1	Layer 2	Layer 3	Layer 4	Layer 5	Layer 6
Radial position (min.) (mm)	22.4	30.1	37.8	194.4	243.9	342.3	391.8
Radial position (max.) (mm)	26.7	34.6	42.1	197.7	247.0	345.4	394.9
Length (sensitive area) (mm)	271	271	271	843	843	1475	1475
Pseudo-rapidity coverage[a]	± 2.5	± 2.3	± 2.0	± 1.5	± 1.4	± 1.4	± 1.3
Active area (cm^2)	421	562	702	10 483	13 104	32 105	36 691
Pixel Chip dimensions (mm^2)	15×30						
Nr. Pixel Chips	108	144	180	2688	3360	8232	9408
Nr. Staves	12	16	20	24	30	42	48
Staves overlap in $r\phi$ (mm)	2.23	2.22	2.30	4.3	4.3	4.3	4.3
Gap between chips in z (µm)	100						
Chip dead area in $r\phi$ (mm)	2						
Pixel size (μm^2)	$(20-30) \times (20-30)$			$(20-50) \times (20-50)$			

[a] The pseudorapidity coverage of the detector layers refers to tracks originating from a collision at the nominal interaction point ($z = 0$).

Photo of a half barrel (during ITS commissioning)

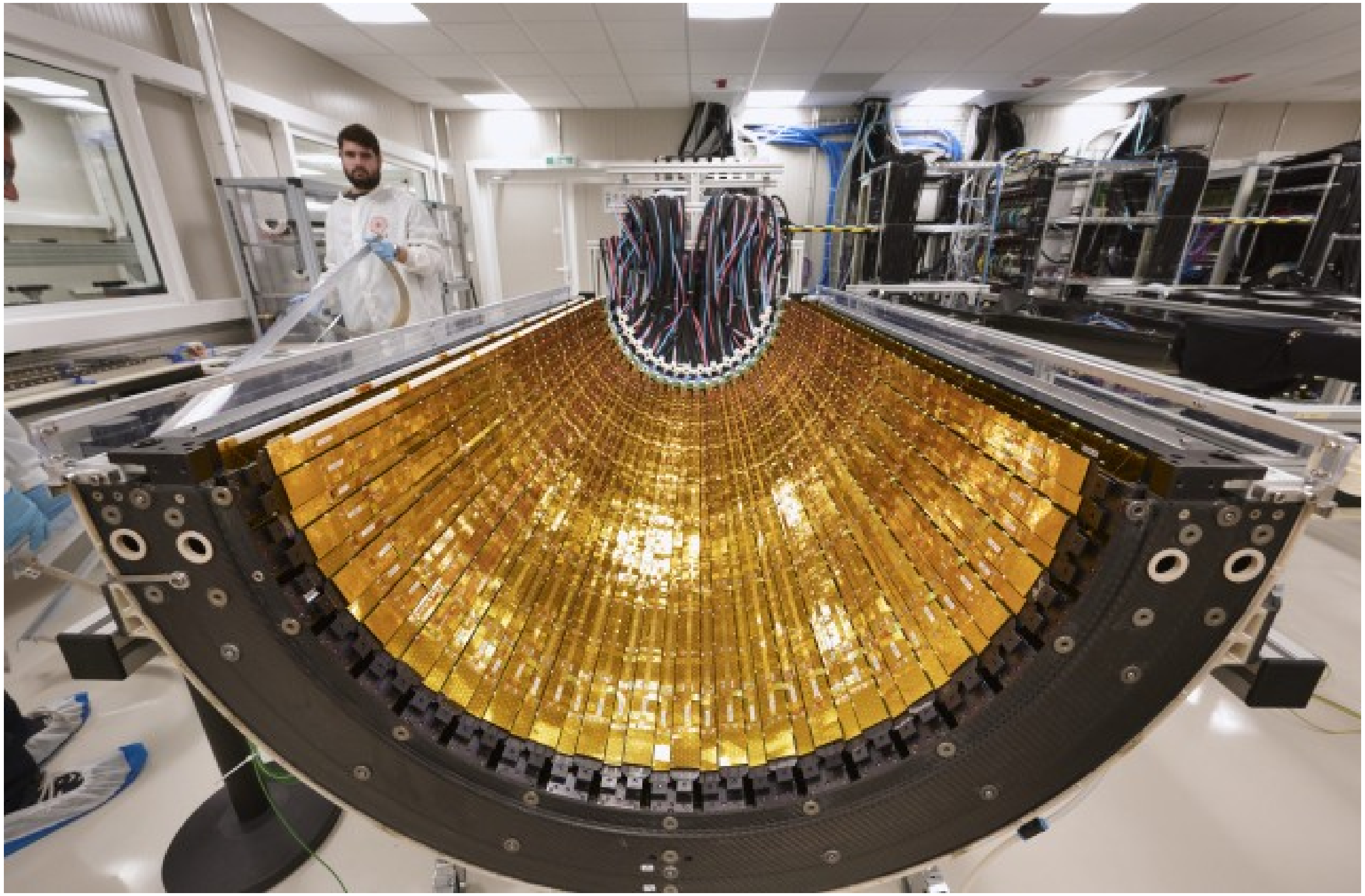

Cross section of a pixel

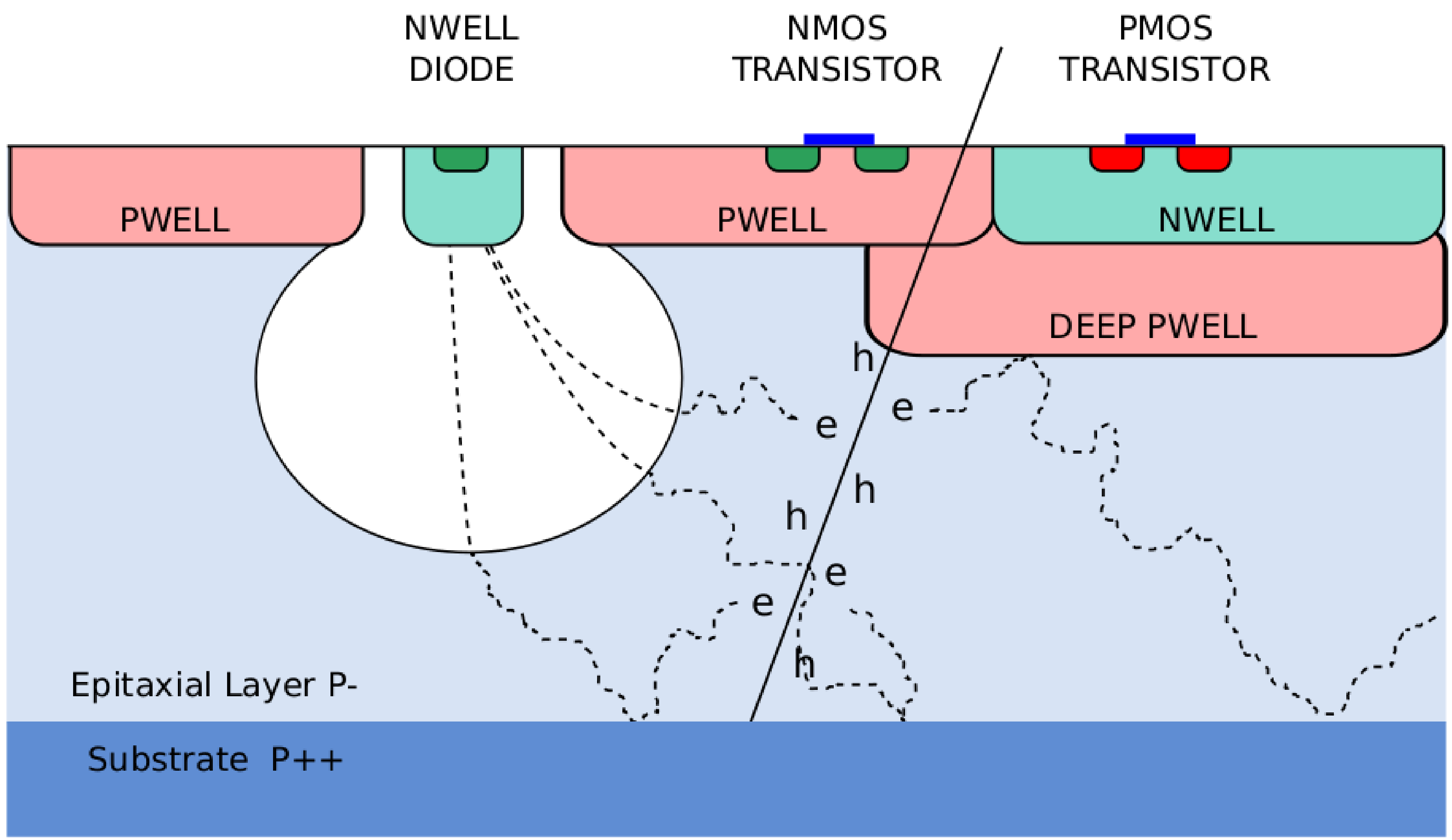

Why calibrating ?

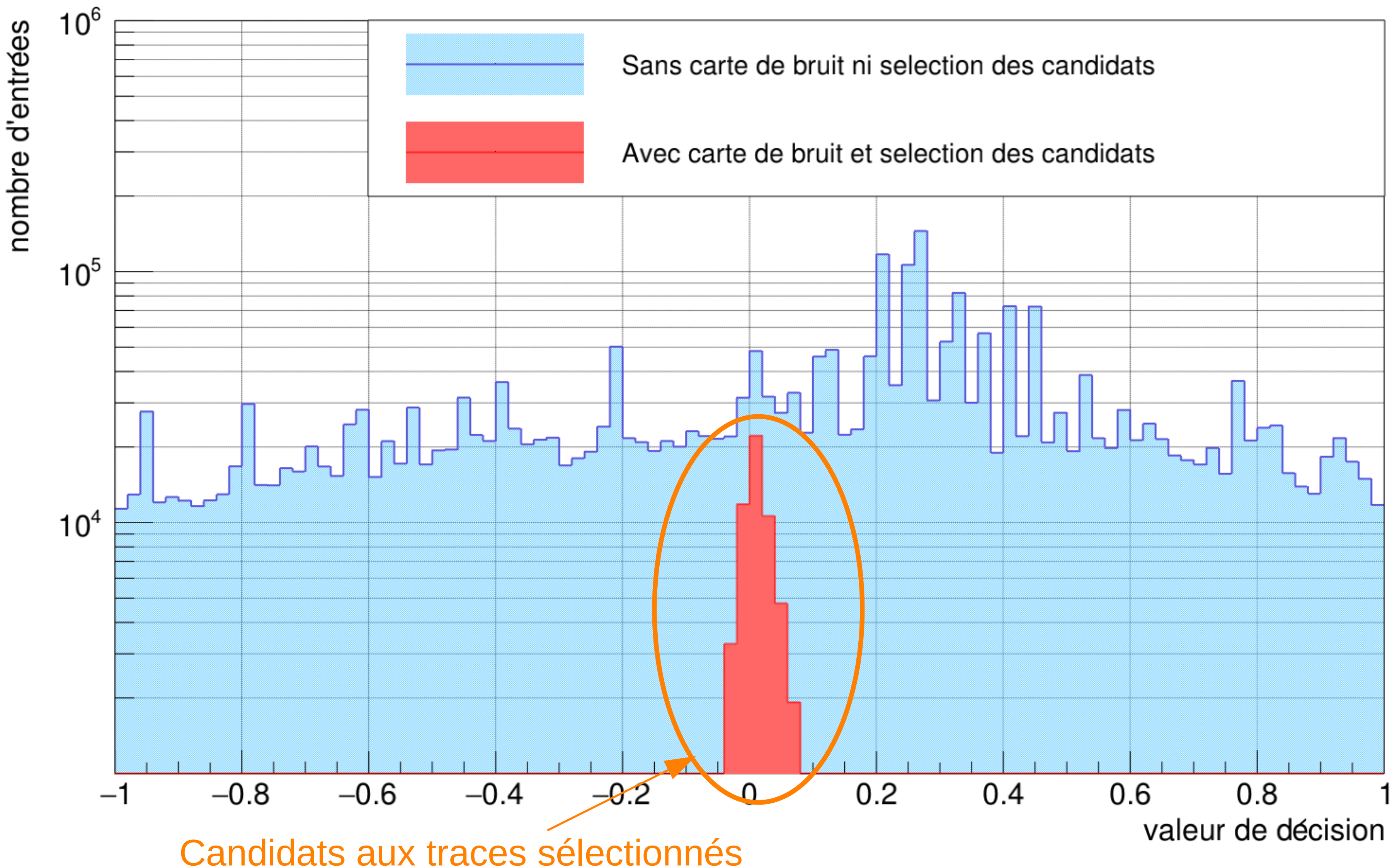

Simple calibration ?

Amas de 1 pixel

Au moins 10³ plus de bruit que de candidats

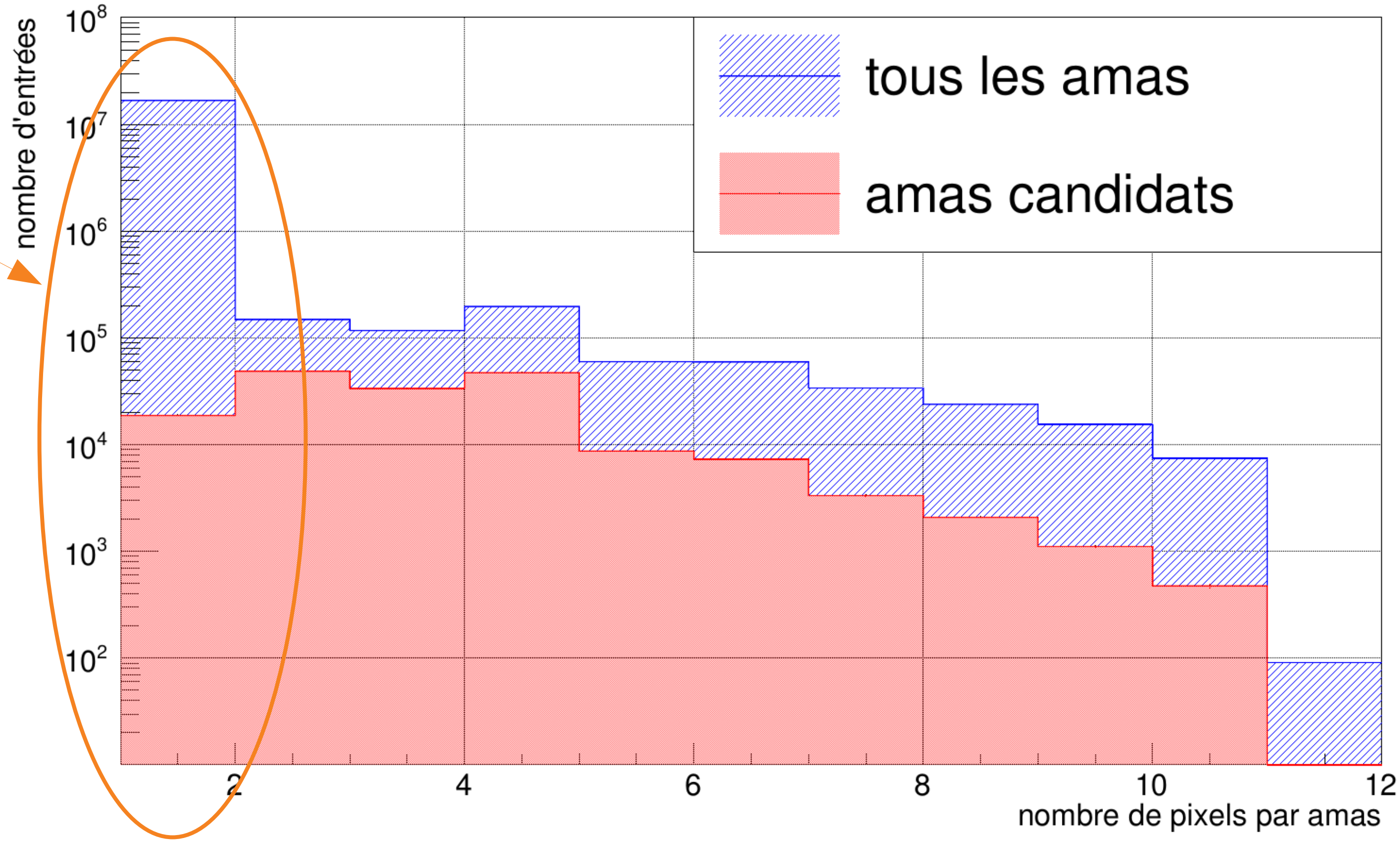

Simple étalonnage: “simplement” **rejeter** les amas unipixel

Simple calibration ?

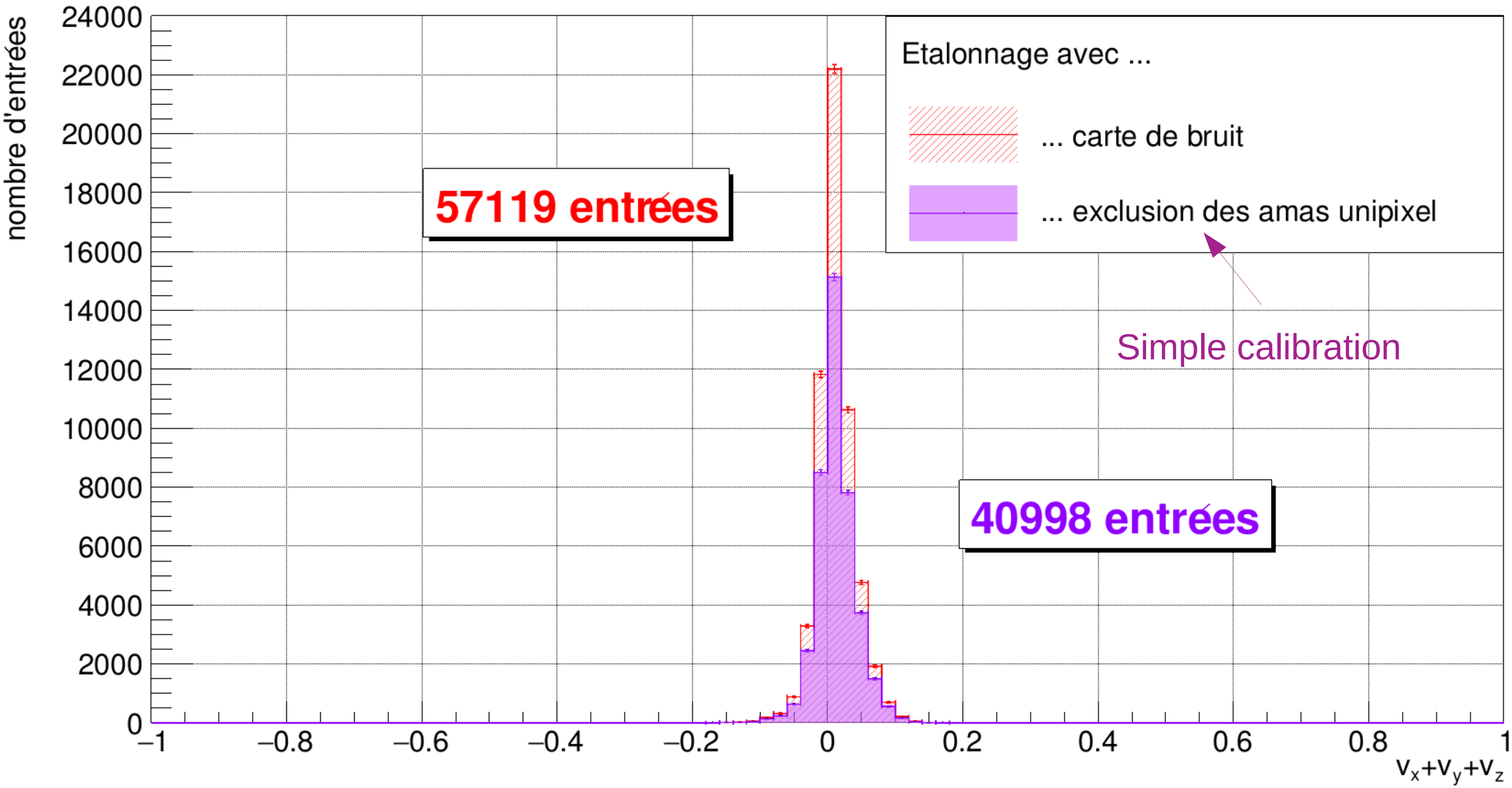

Simple calibration ?

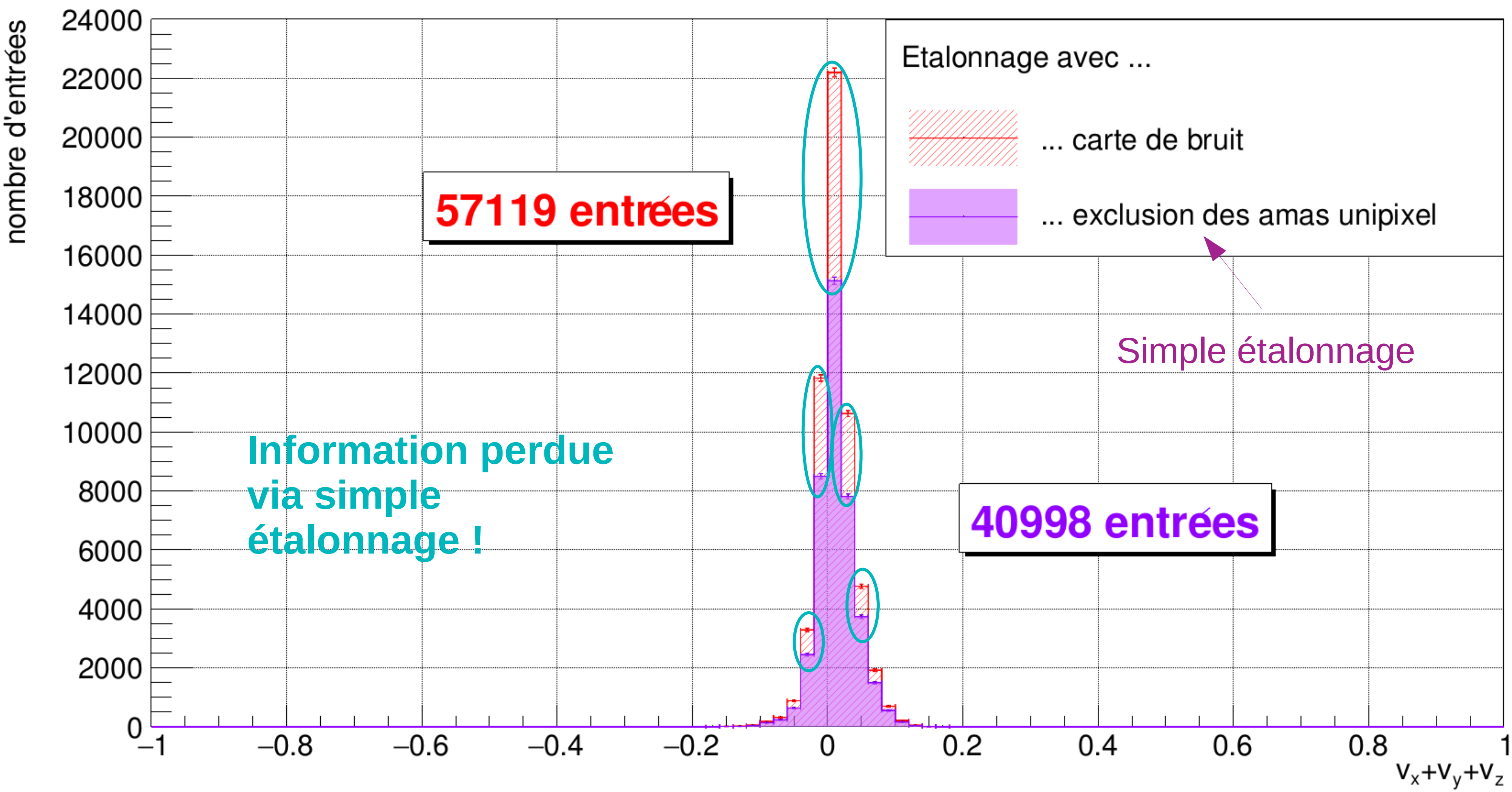

Simple calibration ?

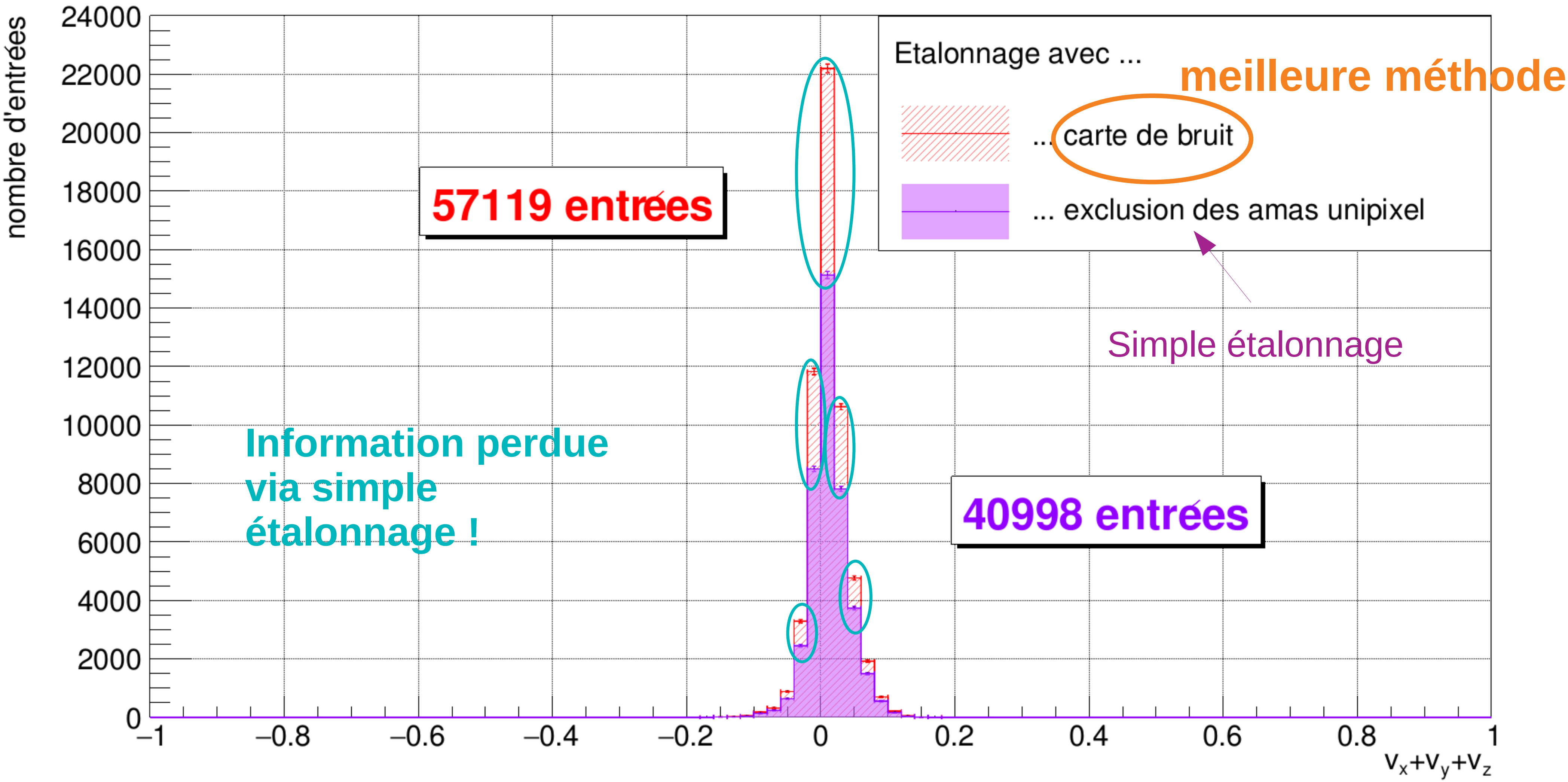

Noise map

(on more than 12 billions pixels for each measurements series)

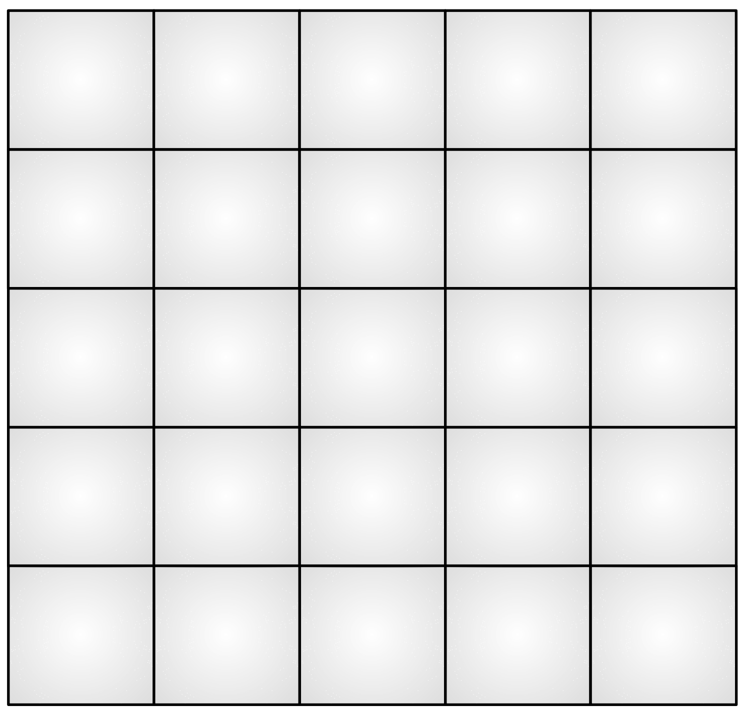

Map of pixels

Noise map

(on more than 12 billions pixels for each measurements series)

Noisy pixel = pixel **activated more than once** during a measure

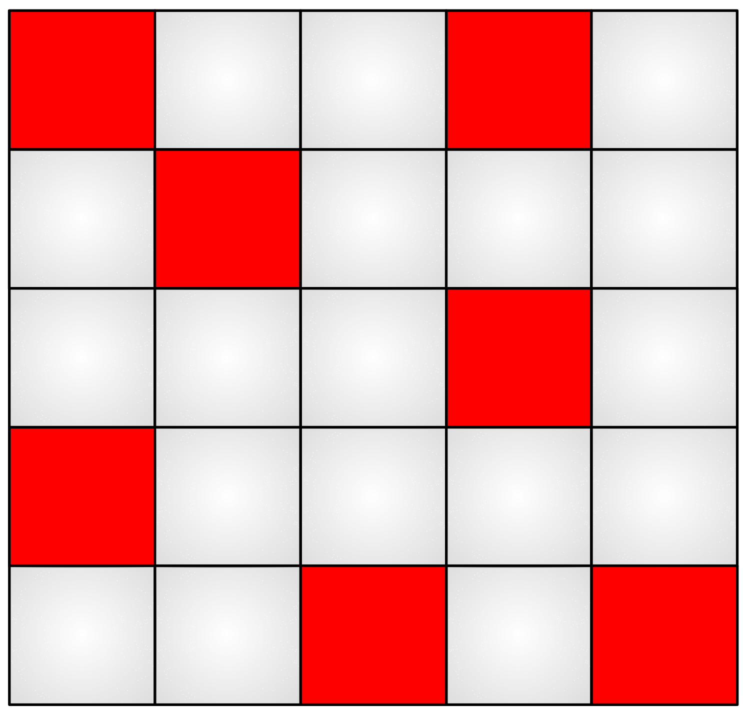

Map of pixels

Noise map

(on more than 12 billions pixels for each measurements series)

Noisy pixel = pixel **activated more than once** during a measure

Pixel **activated once or not activated**

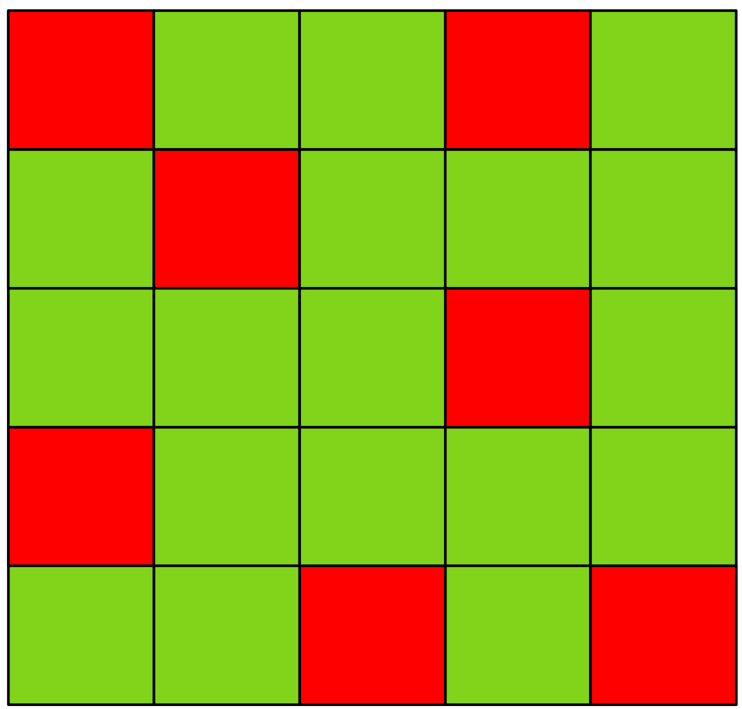

Map of pixels

Noise map

(on more than 12 billions pixels for each measurements series)

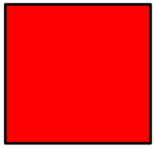

Noisy pixel = pixel **activated more than once** during a measure

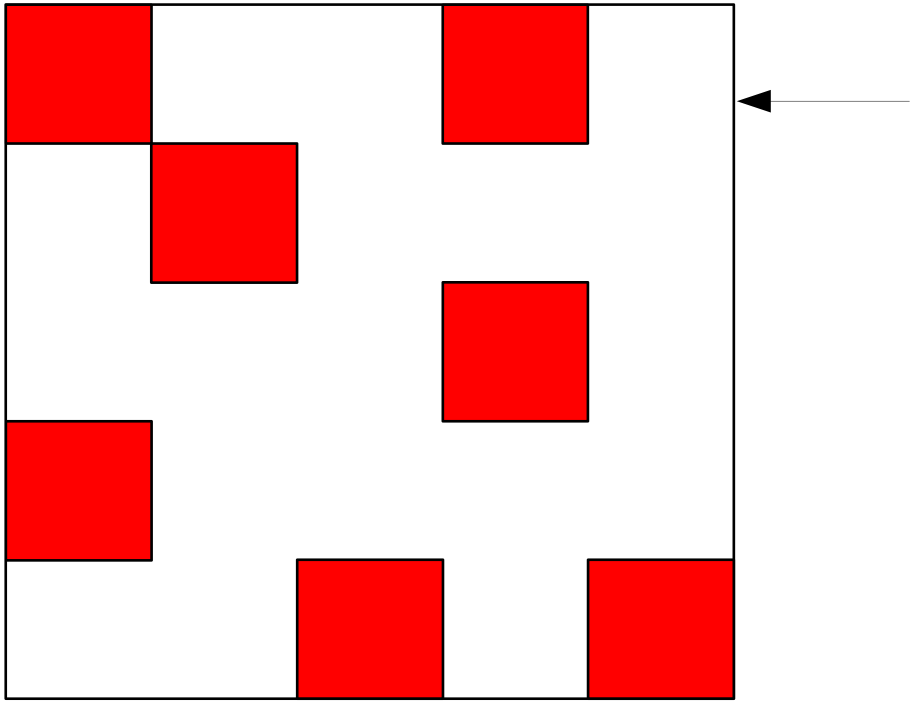

Noise map

(pixels identity)
(pixels position)

Selection on candidates' rate

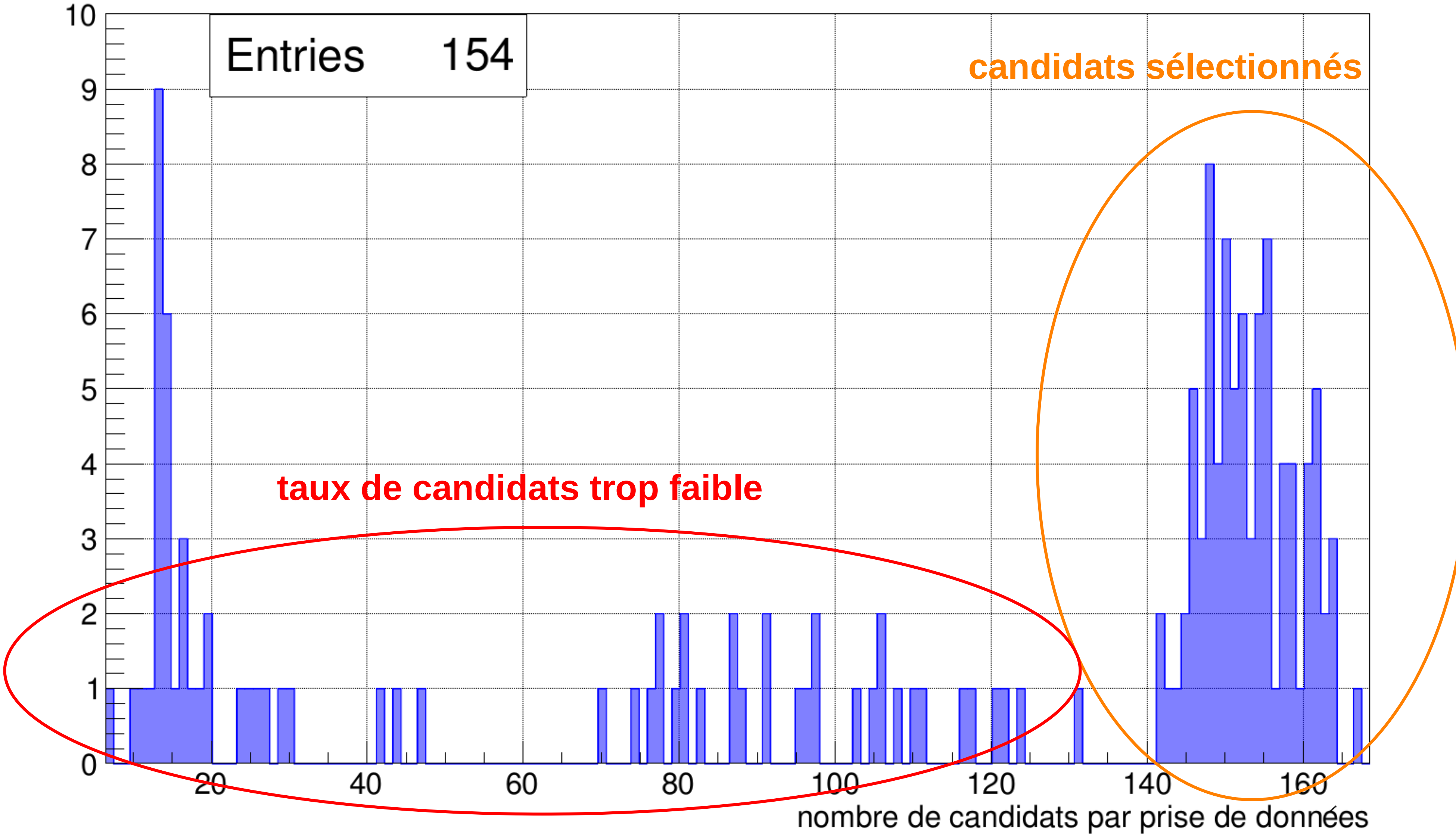

Correlation peak

- Noise map
- Candidates selection

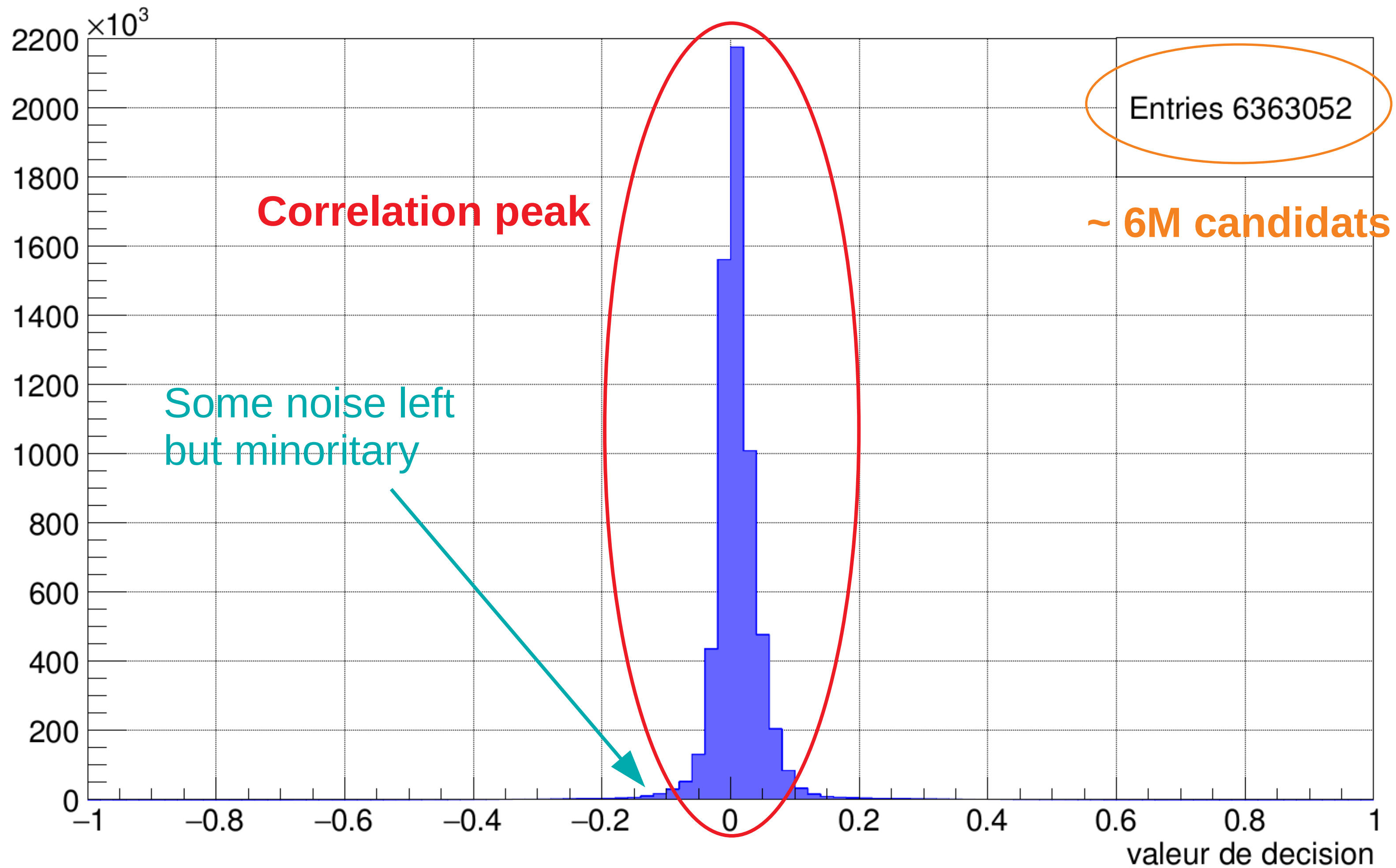

Pour toutes les mesures du Tonneau Externe

Inclination angles

λ défini globalement

ψ défini localement

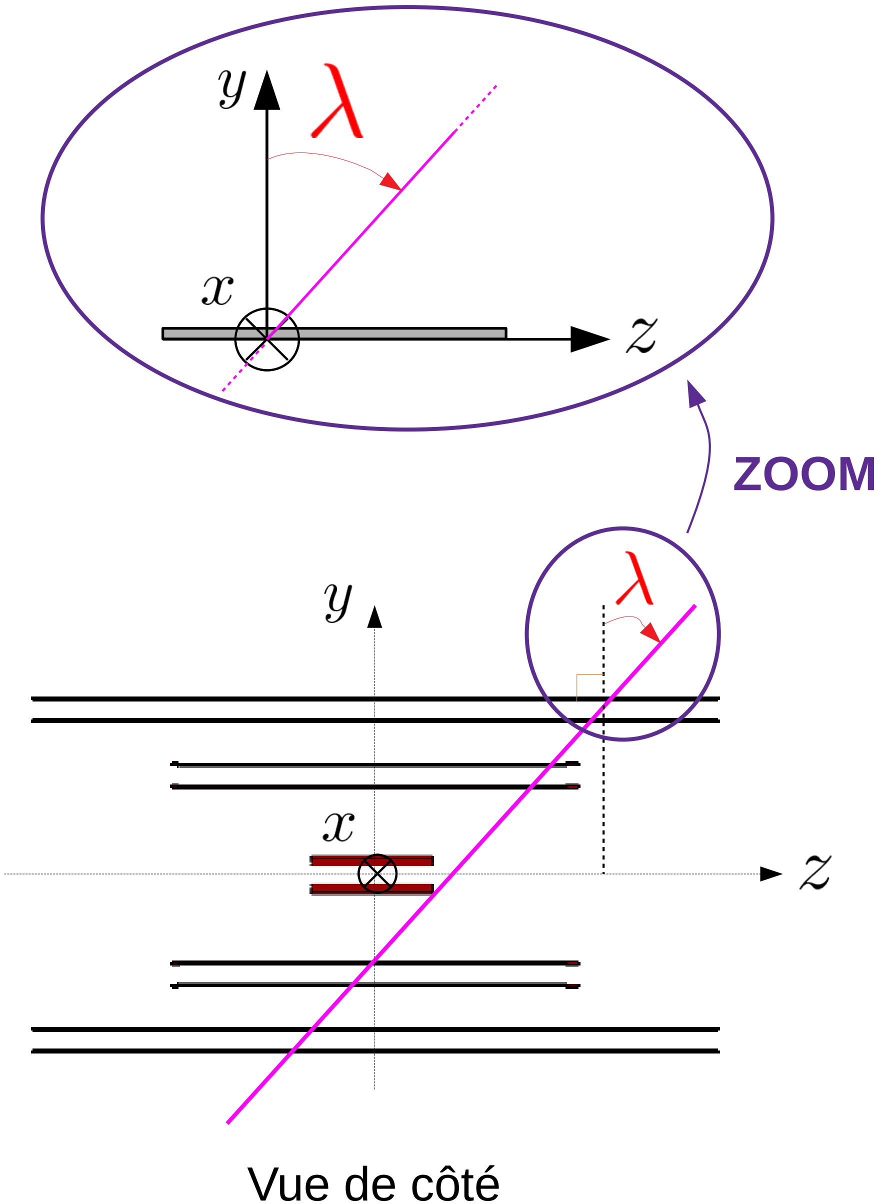

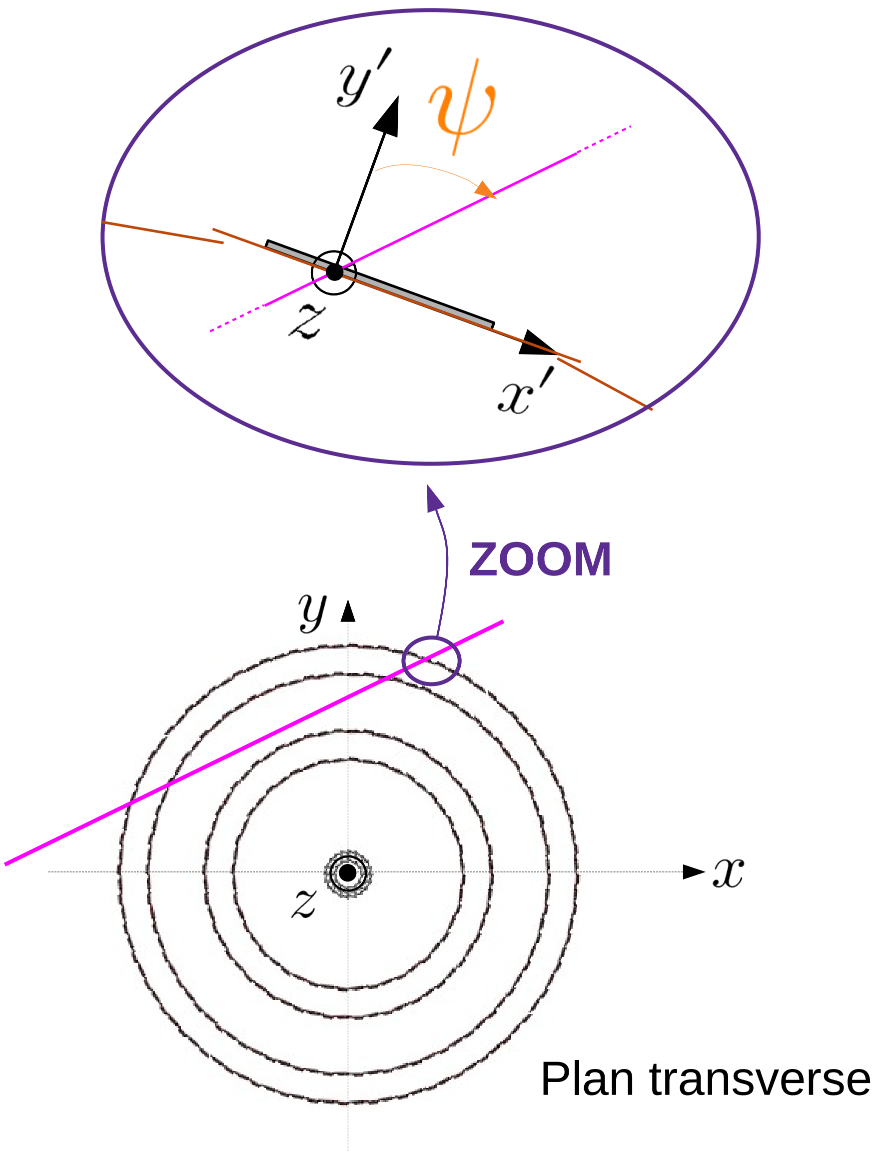

Construction of the angle ψ

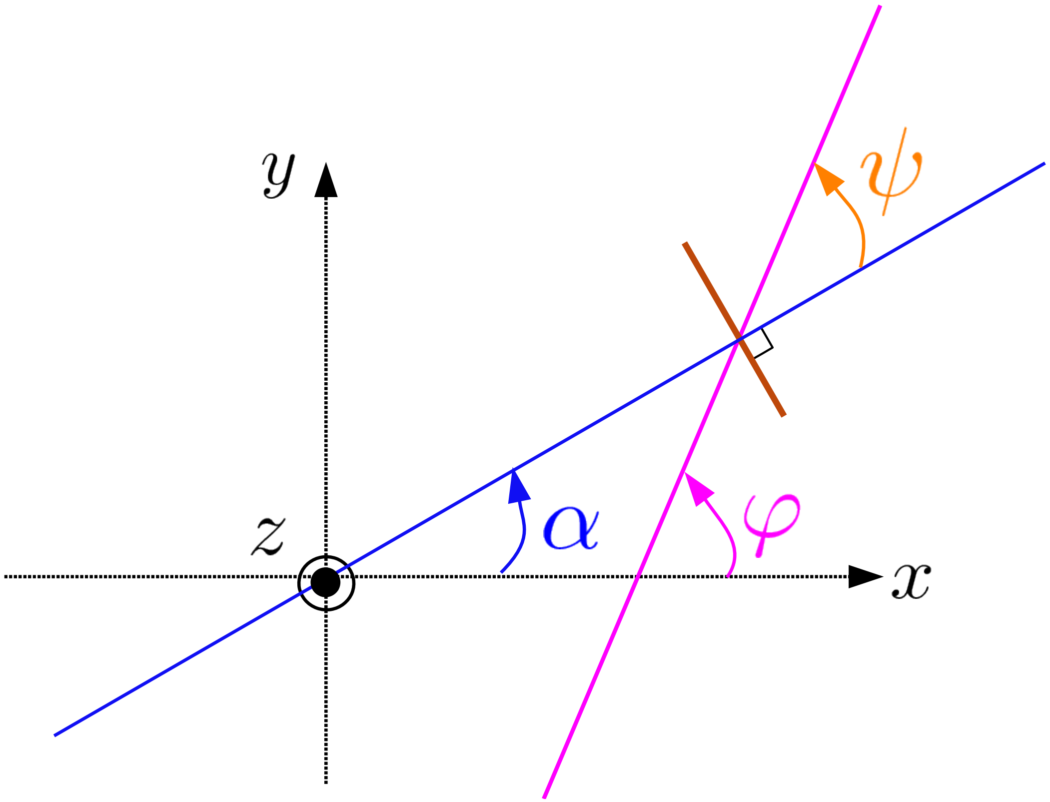

$$\psi = \varphi - \alpha$$

Backup for II)

Backup
CERN Summer Student Programme

Efficiency

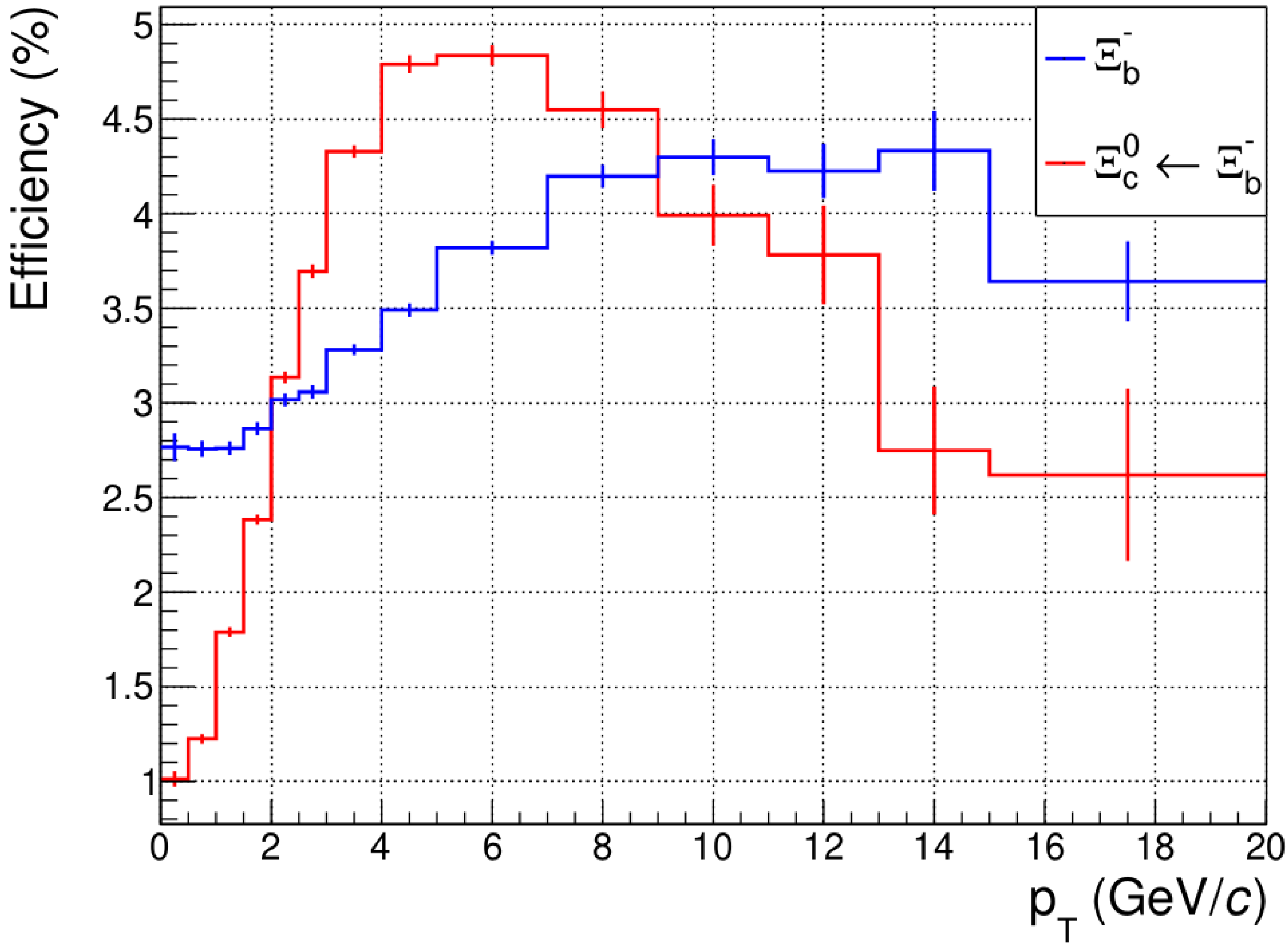
Efficiency (%)
5
4.5
4
3.5
3
2.5
2
1.5
1
0
2
4
6
8
10
12
14
16
18
20
p_T (GeV/c)
Ξ_b^-
$\Xi_c^0 \leftarrow \Xi_b^-$

DCA between daughters

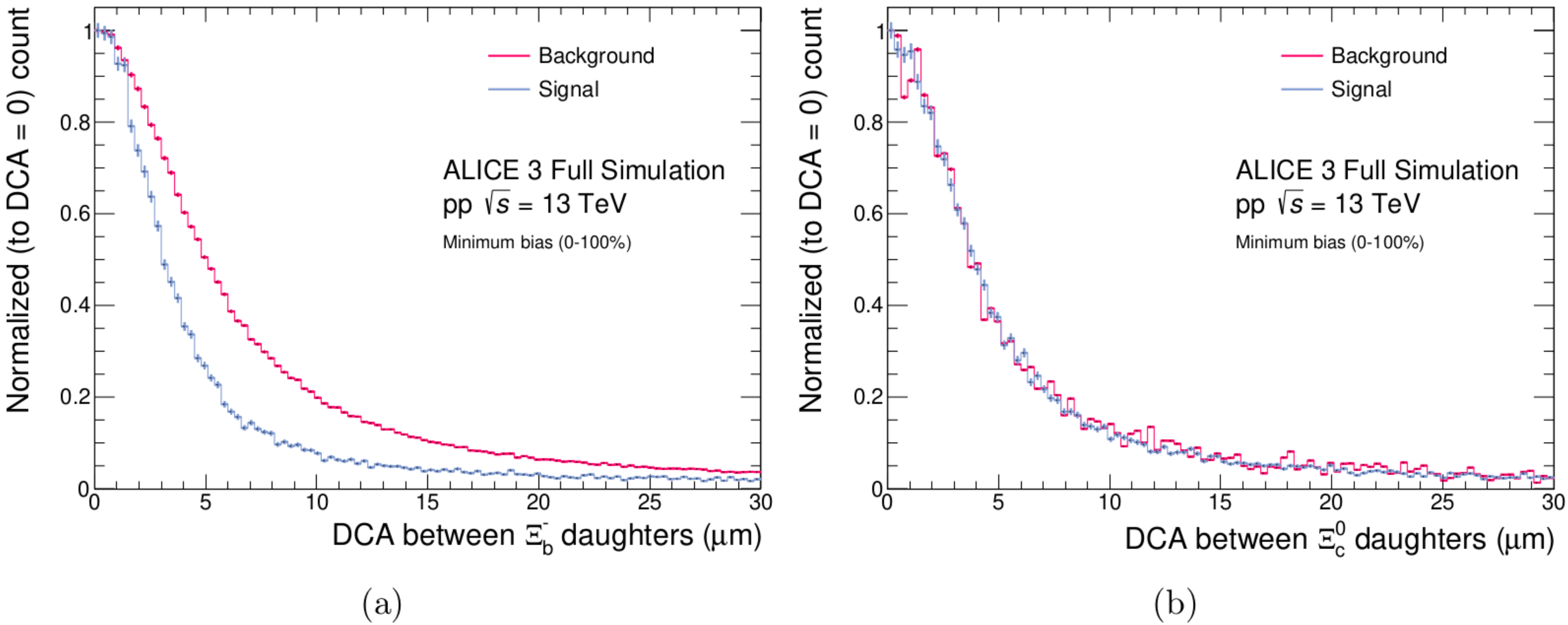

FIGURE 6 – DCA between the daughters of Ξ_b^- (6a) and Ξ_c^0 (6b) for the signal (in blue) and the background (in red).

DCA to primary vertex

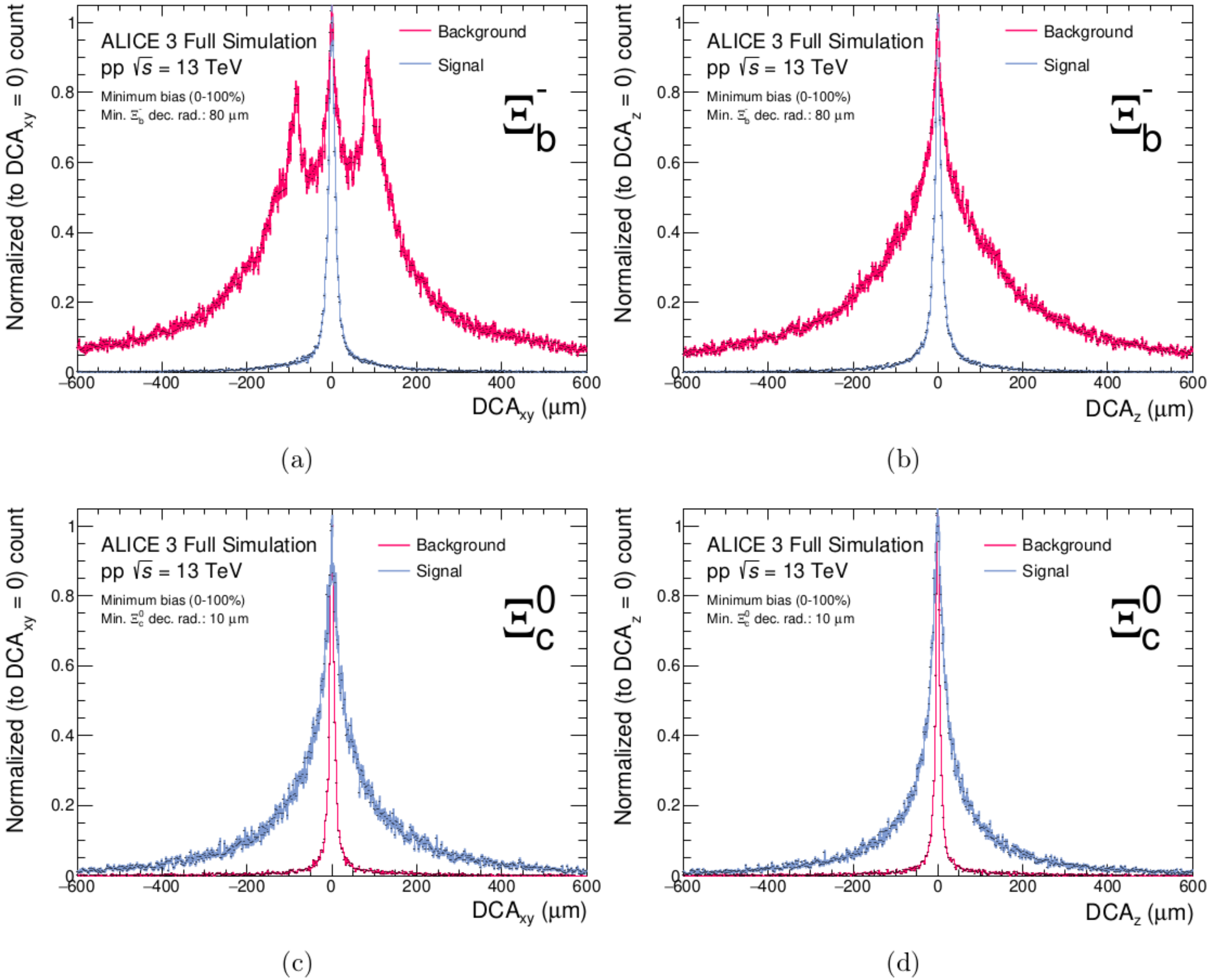

FIGURE 7 – DCA to the primary vertex of Ξ_b^- (7a and 7b) and Ξ_c^0 (7c and 7d) for the signal (in blue) and the background (in red).

Main results

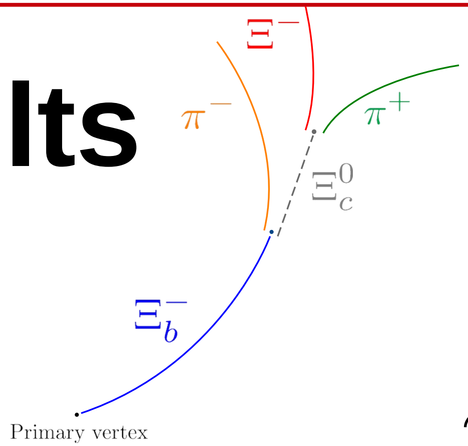

Majority of Ξ_c^0 peak loss comes from primary Ξ_c^0 (79%) and not from $\Xi_c^0 \leftarrow \Xi_b^-$ (34%)

Some signal is lost but significantly more background is suppressed

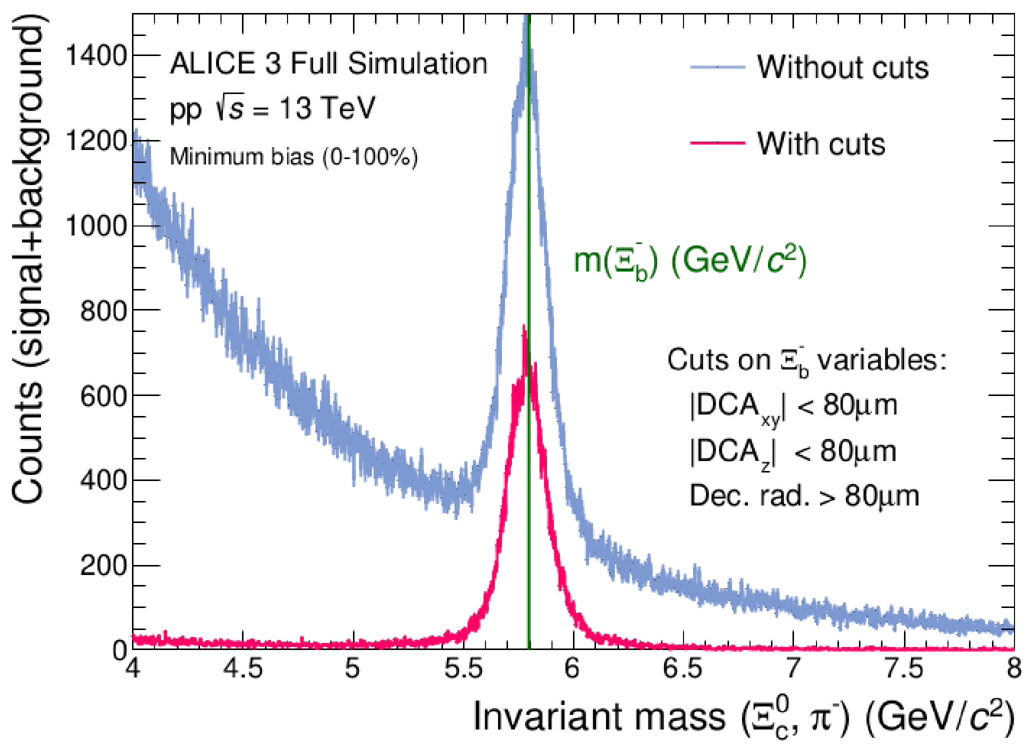

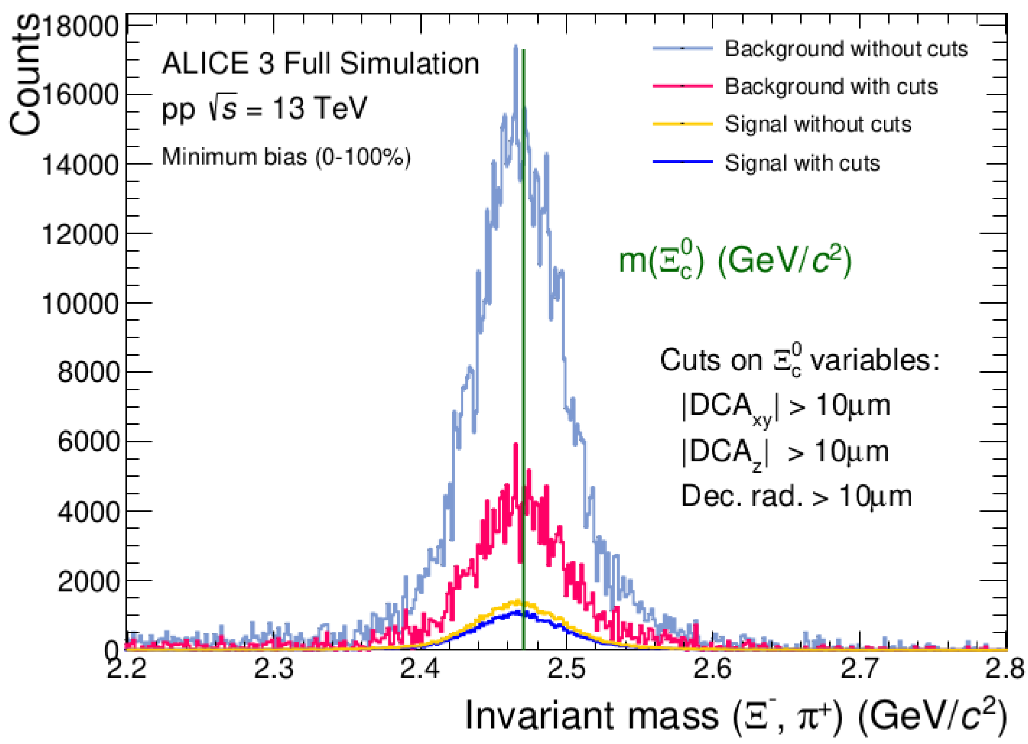

Majority of background noise is reduced → nice peak → **functional analysis prototype**